SCUOLA DI DOTTORATO

UNIVERSITÀ DEGLI STUDI DI MILANO-BICOCCA

Department of Material Science

PhD Program in Material Science and Nanotechnology
XXXIII Cycle - Industrial curriculum

LIGHT WEIGHT POLYSACCHARIDES AS BIOFILLERS FOR ELASTOMERIC COMPOUNDS

Imiete Ikpoemugh Elo
Reg. No. 834560

Supervisor: Prof. Marco Emilio Orlandi
Co-supervisor: Prof. Luca Zoia
Industrial Tutor: Dr. Luca Giannini
PhD Coordinator: Prof. Marco Bernasconi

April 2021

Acknowledgement

I have faith in God and the consciousness of my belief makes me rely on Him to guide me in the journey of my life. In this regard, the prayer of the Psalmist '' *Teach us to realize the brevity of life, so that we may grow in wisdom* (Psalm 90:12)'' is my daily prayer and I am always grateful to God who leads me through the pursuit of my life.

The doctoral program started with Prof. Marco Emilio Orlandi accepting me into his research group. I am most grateful for the support and leadership he provided me to enable me to finish my program. During the research, Prof. Luca Zoia was simply the catalyst and source of encouragement. I stood on his suggestions, advice, and scholarly support to make resounding academic progress. Ignoring his counsel was equal to courting scientific failures. He made my program fun with wonderful memories, and I am indebted to him for all his support. I would like to thank Danish, Eeva Liisa, Anika, Francesco and all the research group members who were always available to assist me.

To learn about cellulose chemistry, I was opportune to collaborate with the Renewable Materials and Nanotechnology research group of KU Leuven, Belgium as a visiting scholar. Prof. Wim Thielemans hosted me for several months, giving me access to his labs and facilities. I learnt several characterization techniques during my visit, and I appreciate him and his group: Reeta Salminen, Samuel Eyley, and other group members for the support I received. I want to use this medium to also appreciate my previous supervisors Viacheslav Nabatov and Nadezhda Alekseeva for their innumerable support.

This research was done under the consortium for the development of advance materials (CORIMAV) project between the University of Milano-Bicocca and Pirelli tires S.p.A. Luca Castellani, Luca Giannini and Luciano Tadiello were instrumental to guiding me in the industrial aspect of the project. Their support and the cooperation of Pirelli staffs were instrumental to the success of all my experiments within Pirelli research and development facilities and I am grateful for their support.

Lastly, I would like to appreciate my Mother, Boomni, my maternal family, bosom friends that have turned family to me and all the people that have prayed and wished me the best. This page is an indication that the prayers offered on my behalf were answered and I am deeply grateful to everyone.

TABLE OF CONTENTS

Synopsis

1.1 Research background

The preparation of composites has been in existence for decades as humans try to satisfy their material needs. This is dependent on the fact that a single material may not provide the desired properties. Combining several materials to prepare a composite could result in a material having interesting properties distinct from each component. In the tire industry, a typical tire composite comprises of polymers, fillers, curatives, metals etc. Polymers are mixed with fillers to give reinforcement, and then other additives are added to actualize the preparation of the entire product. Besides the polymer that acts as the continuous phase, the filler is another large component, gulping close to 30% of the tire. This volume is large and has attracted a lot of attention on different types of fillers, preparation techniques, and functionalization methods. The conventional fillers in the tire industry are silica and carbon black. In fact, carbon black has been the dominant filler for decades since it was discovered. Its excellent properties and reinforcements are almost unmatched. As a product derived from petroleum, it is certainly not sustainable. Various legislations are presently promoting the reduction of petroleum-based products because of toxicity and environmental concerns. On silica, it is a product that is abundant in nature, but it has a high density and can result to tires having higher weight. More so, the production process of the reinforcing silica filler results to large chemical waste, which is also not desirable to the environment. Presently, highly dispersible silica filler has been in the market and there is a gradual shift from carbon black to silica as reinforcing filler. In most instances, there are combinations of carbon black and silica fillers in the tire compound. These fillers are not biomaterials and the end life of the product could be a rather deferred problem. This is part of the current drive to find alternative fillers from biomaterials that would replace these conventional fillers. Although other inorganic materials are explored, biomaterials such as cellulose nanocrystals, engineered polysaccharides, fibres, etc are extensively researched as possible replacements. Biofillers have drawn attention because of their numerous advantages. They are abundant in nature, sustainable, lightweight, and biodegradable. When used in tires, they can give good reinforcements and help reduce the weight of the tire. This in turn leads to low rolling resistance and high fuels savings, among others. Besides the plausible advantages, they have their drawbacks that would need to be overcome. They have abundant surface hydroxyl groups, which makes them aggregates and tends

to agglomerate into larger particles that are difficult to disperse in polymer matrixes. Their hydrophilicity in a hydrophobic matrix results in poor filler-polymer interaction that affects the composite. Overcoming these drawbacks is the focus of this work. The biofillers that are explored in this research were lightweight polysaccharides: alpha-1,3-glucan and cellulose nanocrystals. Cellulose is the most abundant polymer on earth and has been used for decades to satisfy human material needs. Several industries have been tailoring cellulose to meet specific applications. More recently, cellulose nanocrystals having dimensions in the nanometre range and high aspect ratio have been found to possess interesting properties. Their reinforcing properties are fascinating with good filler-filler networking in a matrix. Their drawback is the high agglomerations leading to poor filler dispersion and poor filler-polymer interactions, which often requires surface modification for compatibilization. Alpha-1,3-glucan is another new entrant as potential reinforcing filler. It is produced by microorganisms and is found mainly in cell walls of fungi. Its abundance in nature is not profound and several researches have been devoted to alternative synthesis in large scales. One of its existence as a dental plaque in humans has been a result of extracellular synthesis by glucansucrase enzymes. Researchers are therefore using same enzymes and suitable substrate to synthesize alpha-1,3-glucan in commercial quantity and to find possible use as a biofiller in tire compounds. Besides the interesting properties of biofillers, the method of compound preparation contributes immensely to the properties of the composites. Most often, dispersion of the filler in the polymer matrix, good filler-filler network and filler-polymer interaction are task that need to be achieved to have a good composite and the preparation method plays a crucial role. Preparation of biofiller composites takes different forms depending on the physical state of the components. For example, composites made with cellulose nanocrystals (CNCs) in suspension, may requires the co-coagulation method of mixing the CNC suspension and latex rubber then applying an acid to coagulate. In situ polymerization is another method or a physical blending and drying. However, when components are in dry form, melt mixing and compounding are employed. Several preparation techniques have been successful in the laboratory scale but are tedious and complicated in commercial scale. In most instance, during scale up, the properties are poor and far unmatched with properties obtained at the laboratory scale. To overcome some of the outlined problems, this work employs the use of co-coagulation methods for nanofillers in suspension and compounding using a brabender internal mixer for fillers in dried form. The CNC, alpha-1,3-glucan and silica compounds were prepared with natural rubber and the resulting composites were characterized to understand their unique properties. More so, different functionalization methods

requiring the use of both aliphatic and cyclic silanes and enzymatic modifications have been employed to overcome the compatibility drawback. Details of results are presented below in the various chapters.

1.2 Thesis outline

This thesis is structured into six chapters with CNC related compounds drawing a much larger attention.

- **Chapter 1:** In this chapter is described the research background and the concept necessitating the research. An overview of the thesis outline has also been detailed consequently.
- **Chapter 2:** An overview of the composites, processing techniques as well as the fillers used in this study has been explained in detail. The characterization methods and conditions the experiments were carried out as well as the various parameters that were studied have been elucidated.
- **Chapter 3:** This chapter proceeded by the establishment of a compounding procedure using different silanes. APS and TESPD silanes were used for this study and results were always compared with silica compounds. Subsequently, reactive cyclic silanes were explored and extended to understand the properties it will confer on CNC/silica hybrid compounds.
- **Chapter 4:** The CNC used in this study were prepared by sulphuric acid, which results into CNC having sulphates half esters on the surface. The influences of these sulphate groups on composite properties as well as the impact they have on the filler have been studied.
- **Chapter 5:** Processing methods for CNC fillers especially the acid treatment was also applied for the treatment of alpha-1,3-glucan before preparing alpha-1,3-glucan composites. The composites from this treatment were characterized and properties were compared with silica as a reference.
- **Chapter 6:** The previous chapters employed the use of silanes for compatibilization. Here, lipase enzymes were used to graft different functionalities on the CNC surface. The functionalization was done before co-precipitation and the functionalized CNC in natural rubber compounds were characterized to understand their properties without silanes.
- **Chapter 7:** The research project was concluded in this chapter with important highlights of results and possible applications.

Chapter 2

Lightweight filler compounds for tire applications

2.1 Tire components and structure

The tire compounds are complex materials due to the many ingredients added to achieve their desired properties. Generally, up to twenty components could be used to make a tire compound and at least 12 compounds are used in a tyre, comprising of rubber (both natural and synthetic), fillers, chemicals and oils, textiles, steels etc. A typical tire structure is shown in figure 2.1. The role played by each component is unique and varies in composition according to the type of tire. For example, a passenger tire may have more synthetic rubber part compared to off-road, agricultural, and other industrial tires. The composition is tailored to meet either performance characteristic such as good wear, low rolling resistance, improved skid resistance etc. or meeting high load bearing and longer distance tires [1].

The tread part of the tire often contains reasonable amount of rubber and additives that are patterned to have sufficient contact with the road. The formulations must have good wear resistance properties, wet skid, provide traction and the depth of the tread varies with tires. During the service life of the tire, the tread is expected to wear away and it is one of the means used to determine tire replacement. At the base of the tread are steel or woven textiles overlaid to serve as cushion and stiffening which tunes overall tyre mechanics and helps to reduce damage. The plies also run from end to end, primarily serving as a support to the tire casing.

The amount of materials used for tire manufacturing is shown in table 2.1 [2-4]. This varies according to the applications. Fillers comprising of carbon black and silica are added to primarily give reinforcement and are some of the largest constituents, followed by synthetic or natural rubber. The amount of these components consumed in the manufacturing process is a source of concern both for the environment and sustainability. Most researches are therefore directed at improving the properties of the materials, production process, reducing the consumption of environmentally unfriendly materials or eventual replacement.

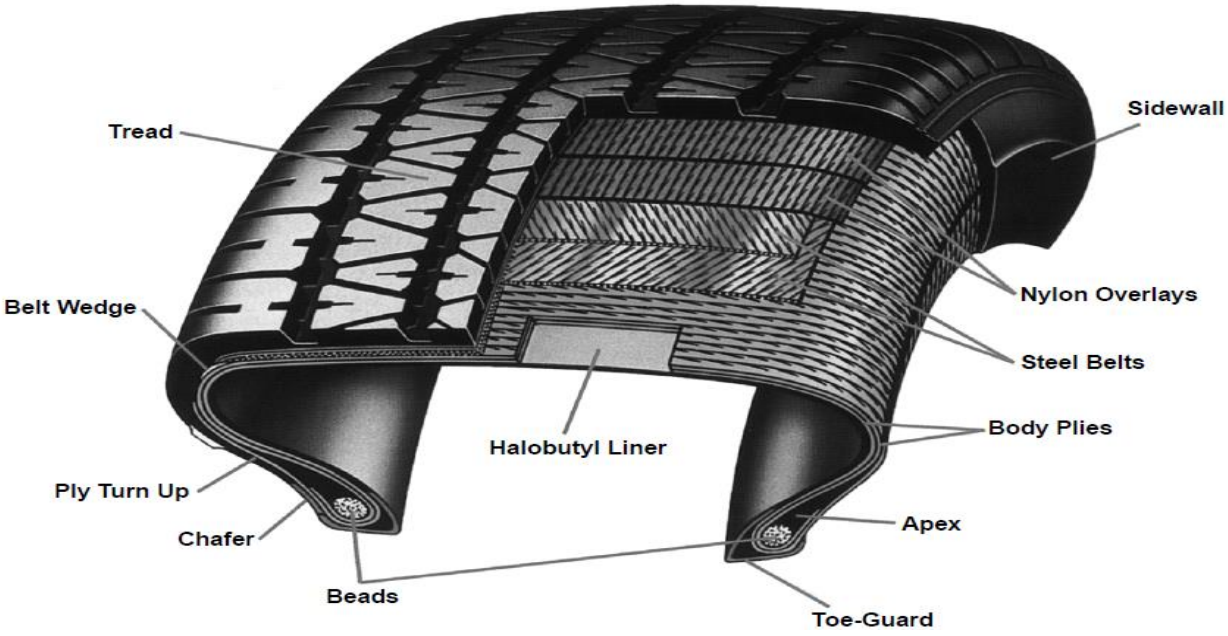

Figure 2.1 Cross-section of a high-performance passenger tire [2]

Material	Car Tyre (%)	Truck Tyre (%)
Natural rubber	14	27
Synthetic rubber	27	14
Fillers (carbon black, silica)	26–28	26–28
Plasticizers (oil and resin)	5–6	5–6
Chemical additives (sulfur, etc.)	5–6	5–6
Metal for reinforcement	16.5	25
Textile for reinforcement	5.5	-

Table 2.1 Composition of passenger and truck tires.

The manufacturing process requires numerous steps. At the first stage, the polymers are homogenised by mixing to form a uniform matrix. Thereafter the fillers and perhaps some oil are added to aid dispersion and homogeneity. The temperature of the process is vital to reduce viscosity while avoiding the decomposition of the rubber component. Internal mixers or roll mills are used to form the rubber compounds. When it is formed, the compound is used to generate semifinished components by extrusion or calendaring, and to coat processed textiles and steel cords. Other components are added and assembled on the tire-building machine and cured under heat and pressure. Inspections and testing to meet quality standards come at the last stage.

2.2 Polymer matrix system

Rubber compounds have unique elastomeric properties and are majorly used in the tire industry. These polymers serve as the continuous phase where fillers and additives are dispersed to achieve desired properties. The rubber chains are long, flexible and can undergo large deformations even up to 1000% strains [5] with the ability to return to its original state after strain removal. This unique property is essential, varies according to the type of rubbers, and is dependent on the nature of polymeric backbone, the functionalities, degree of polymerization and the networking of the polymeric chains.

Since the discovery of natural rubber and its unique properties, researchers have continued to synthesize rubber compounds with wide range of properties for industrial applications. In the tire industry, a blend of both synthetic and natural rubber is used, and formulations are made for specific applications.

2.2.1 Natural rubber

Natural rubber is a cis 1,4-polyisoprene and exist as aqueous colloidal suspension of rubber particles. There are several sources of natural rubber but of most commercial significant is the rubber latex derived from *Hevea Brasilienses* tree with production reaching 14 million metric tons in 2018 [6]. It contains high rubber content up to 40wt % dry rubber [7]. Other sources of latex rubber have not gained commercial significant, as the amount of rubber content are relatively low with the presence of large amount of water and non-rubber constituents. Although natural rubber from Guayule has been extensively researched [8-10] as another potential source of latex rubber, results that show effective use or replacement of rubber from *Heavea Brasilienses* are lacking. Therefore, subsequent discussions on natural rubber are devoted to natural rubber derived from *Hevea brazilienses*.

The rubber tree grows in the tropics having sizable amount of rainfalls, bright sunshine, moderate wind, and humidity not extending to the extreme. These conditions are typical of few countries of the world although researches have been devoted to modifying and adapting the tree to other parts of the world. Typically, the latex is contained on the bark of the tree and it requires scraping (tapping) the surface up to the necessary depth to make the tree exude the latex into cups or containers sustained on the collection point. The latex rubber particle has a typical size of about

0.02 to 3 microns and is spherical in shape [5]. Studies on the stability of the suspension allude to the encapsulation of rubber particles by proteins and phospholipids [11, 12]. The colloidal stability could be removed either by use of coagulants or exposure to media where the proteins or lipids are degraded. The range of constituents of freshly produced natural rubber latex is shown below [5].

Components	Percentage
Rubber	30-40
Proteins	1-1.5
Resins	1.5-3.0
Minerals	0.7-0.9
Carbohydrates	0.8-1.0
Water	55-60

Table 2.2 Composition of fresh latex rubber.

Transportation and sales of rubber latex are uneconomical if it is not concentrated or coagulated. The field latex is evaporated to reduced considerable amount of water, creamed, and centrifuged to have concentrated latex up to 60wt % dry rubber content. Preservation of the concentrated latex is done with ammonia. Subsequently, several preservation systems have reduced the amount of ammonia alongside the incorporation of several additives to maintain stability of the suspension and to avoid degradation. Besides the latex, there is the coagulated processed rubber with different technical specifications and market grades. In this regard, attention is given to the processing methods and the various additives used which influences the end use.

The demands for natural rubber increased when its unique properties were continuously explored. It has been known with high tensile strength, low hysteresis, resistance to crack propagation etc. [13-15]. Some of these properties are quite unique that synthesized polymers may be difficult to replace. The superior qualities have been attributed to the stereoregularity or tacticity of natural rubber, which makes it easier for the chains to align along the direction of an induced stress leading to strain induced crystallization [16-19]. The crystallites from the alignment of the natural rubber chains under strain act like fillers or crosslinks with a resulting increase in tensile strength. This behaviour helps in promoting crack resistance [20, 21]. This singular feature has also impacted on the rheological properties of natural rubber. Processability of natural rubber in the tire industry is a

huge advantage as it has good ability of holding its compounds together (tack) up to the stage of moulding. Also, the green strength, which is needed to avoid distortions of the uncured compound before moulding or expansions after moulding is well connected to the strain induced crystallization [5].

Despite the many interesting properties of natural rubber, it is highly susceptible to oxygen and ozone [22] because of the unsaturation of the polymeric chain. Radiation, heat, and chemicals also initiate degradation. Ordinarily, there are few amounts of antioxidants that protect it from degradation. This amount is mostly used up during processing and is not sufficient to protect the processed natural rubber. Addition of antioxidants or blends with synthetic rubber having strong resistance to degradation is employed. These drawbacks from natural rubber are the major drive leading to the synthesis of rubber with introduced functionalities to overcome them. The increase demand for natural rubber is not likely to be met, as the rubber tree grows better only in the tropics, frequent spread of plant diseases and rise of other profitable crops [23-25]. It was also reported [6] that a 57,000 metric tons of natural rubber demand was unmet in 2017 with other incessant loses in production. Some of these reasons have continued to promote the use of synthetic rubber as alternative.

2.2.2 Synthetic rubber

The synthetic rubber industry was developed as alternative to the several drawbacks of natural rubber. They are prepared by polymerizations from petroleum-based derivatives and have been grouped into general-purpose synthetic rubbers, special and specialty purpose rubbers [26]. The general-purpose rubbers comprise mainly of styrene butadiene rubbers (SBR), polybutadiene rubbers (PBR) and polyisoprene rubbers (IP) which are heavily consumed in the tire industry [7]. In general, some of these rubbers are used to blend with natural rubber during tire manufacturing and are discussed below.

Styrene-butadiene rubber (SBR): SBR is a copolymer of styrene and butadiene made by either emulsion or solution polymerization. The structure is shown in figure 2.2. Due to the polymerization route, there are variations in the properties of SBR resulting from the rearrangement of the monomers, molecular weight distribution. The styrene content ranges from about 20% to about 40% [27] both for the emulsion and solution polymerization process.

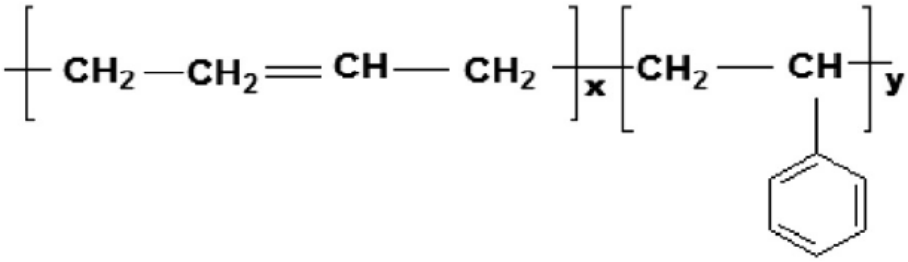

Figure 2.2 Monomers of styrene-butadiene rubber.

SBR is relatively low cost compared to natural rubber. It is also unsaturated with attendant susceptibility to degradation in the presence of ozone, oxygen, UV light and oils. Irrespective of the inferior mechanical properties in its neat form, it has better resistance to abrasion, flex fatigue, and high heat resistance [28]. The higher hysteresis loss is a major advantage for tire formulations directed at achieving a better wet-grip [27]. This singular benefit has made SBR find better use in tire treads. However, because of the low tensile strength, it requires large amount of reinforcing fillers to prepare SBR compounds.

Polybutadiene rubber (PBR): PBR is a homopolymer containing only butadiene monomers with the structural formula shown in figure 2.3. It is the second largest produced polymer and finds use in tire and shoes because of the good abrasion resistance properties.

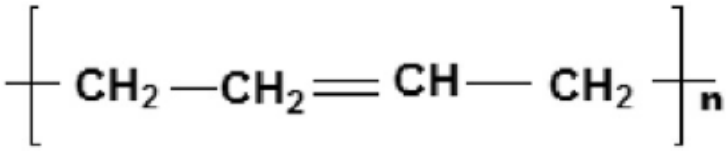

Figure 2.3 Monomer unit of polybutadiene polymer.

Polybutadiene is produced by solution polymerization. Three possible microstructures can be formed during the polymerization process. They are cis-1,4, trans-1,2 and 1,2 vinyl and the properties of the PBR are governed by their amount. The ability of the polymer to crystalize is also depended on the amount of cis or trans present [29]. A high cis-1,4 in the polymer decreases the glass transition temperature to about -90 C leading to low temperature flexibility. Other notable properties are high flex resistance, high abrasion resistance, low heat build-up, high resilience. It is used in blend with NR or SBR in tread and other part of the tire compounds. The narrow molecular weight distribution also makes some PBR grades difficult to process. Similarly, to natural rubber and styrene butadiene, PBR is unsaturated and highly susceptible to degradation in the presence of oil,

UV light, ozone, oxygen etc. and requires additives that would protect the compounds during processing.

Polyisoprene (IP): Polyisoprene rubber is the synthesized form of natural rubber. It has the same empirical formula and cis structure. The properties are also similar such as good tensile strength, good uncured tack, better mastication, and less processing time. The monomer unit is shown in figure 2.4.

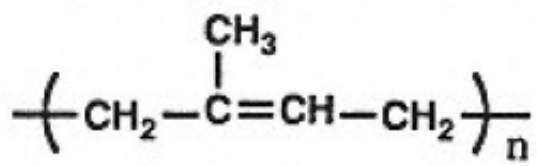

Figure 2.4 Monomer unit of isoprene

Synthetic polyisoprene is produced by solution polymerization using different catalyst systems with possible microstructures as cis-1,4, trans-1,4, 1,2-addition, and 3,4-addition. It has a narrow molecular weight distribution, which reduces its tendency to crystallize under strain. The use of polyisoprene in tire compounds has increased especially when blended with other rubbers to promote some properties. Although similar with natural rubber, it could be considered as having inferior mechanical properties, which is difficult to out rightly replace natural rubber in tire compounds.

2.3 Conventional filler system

Rubber materials are known with interesting properties especially their ability at recovering their original shape after some level of deformations. In their unfilled state, their use is limited. Subsequently, upon the discovery that carbon black, when added to rubber materials can confer considerable reinforcement, a new phase of elastomeric composites became actively researched. Carbon black has continued to serve as reinforcing filler for the tire industry for decades and its presence alongside the useful properties may not be phased out soon. Owing to the environmental concerns as carbon black is fossil derived, nano silica alongside its useful properties is having a considerable share of the filler market in the tire industry presently. Both the carbon black and silica are the conventional fillers used in the tire industry. Not only these, other fillers such as carbon nanotubes, clay, graphene etc. are being explored for use as reinforcing agents.

When fillers are used in composites, their inherent properties such as surface area, crystallinity, morphology, surface chemistry and aggregate sizes are major contributing factors to the final properties of the composite. The preparation process dictates these properties. While carbon black is majorly produced by the pyrolysis of oil at certain conditions [30] amorphous silica is produced from vitreous silicates by dissolving in water and subjecting to acidification in a reactor. Under constant agitation, the nano silica is precipitated out [30, 31].

When these fillers are produced, the inherent primary nanoparticles are in the range of few tens of nano metres. Subsequently they fuse together to form aggregates in the range of hundreds of nanometres. The aggregates can also fuse together to form agglomerates sizes extending to the micrometre range. Eventually, the micron size agglomerates are weaker compared to the aggregates structures that are formed by covalent bonding. The aggregates structures are the main determinant of the reinforcement mechanism in the polymer matrix. During compounding, the agglomerates are broken down and the fillers are dispersed in the polymer matrix in their aggregate form. The size range and the necessary reinforcement it confers on the composite is shown in figure 2.5. Therefore, it is necessary to have fillers with smaller particle sizes so that the effective surface area will increase with increasing filler-polymer interactions.

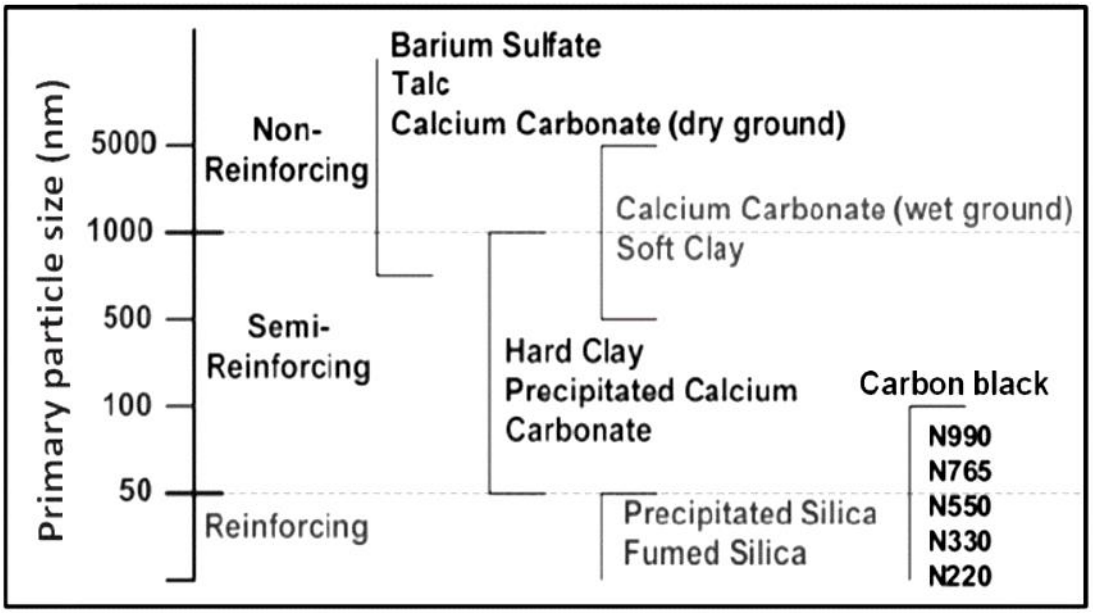

Figure 2.5 Filler sizes and their reinforcements [32].

Within the matrix, the aggregates form structures that network among each other to confer reinforcements. For effective network where the aggregates are connected to each other and

extending to all regions of the polymer matrix, they must reach a threshold (percolation threshold). This percolation amount is depending on the morphology. The idea of the percolation phenomenon suggest in essence that the fillers are essentially the continuous phase with rubber chains winding round the filler networks or trapped in some filler regions especially for three-dimensional fillers. To determine the amount of filler required to reach the percolation threshold, stress strain studies could be conducted to understand the viscous nature of the composite. This is predicated on the fact that fillers are rigid, and the viscoelastic behaviour of the composite should tend more towards the elastic character at some filler volume. In addition, for conductive fillers, various amounts of fillers could be used, and the conductivity is measured to know the threshold where the composite becomes conductive. An illustration of percolation threshold relative to filler is shown in figure 2.6.

Silica and carbon black are still being studied for tire formulations. The art of compounding these fillers is so vital that when it is done wrongly, characterizations can infer that the fillers have poor properties. For example, when fillers are poorly dispersed in polymer matrixes, some regions of the polymer would not have contact with filler. During characterization, results may infer that filler volume fraction was not sufficient and posit that the filler amount be increased to reach percolation threshold.

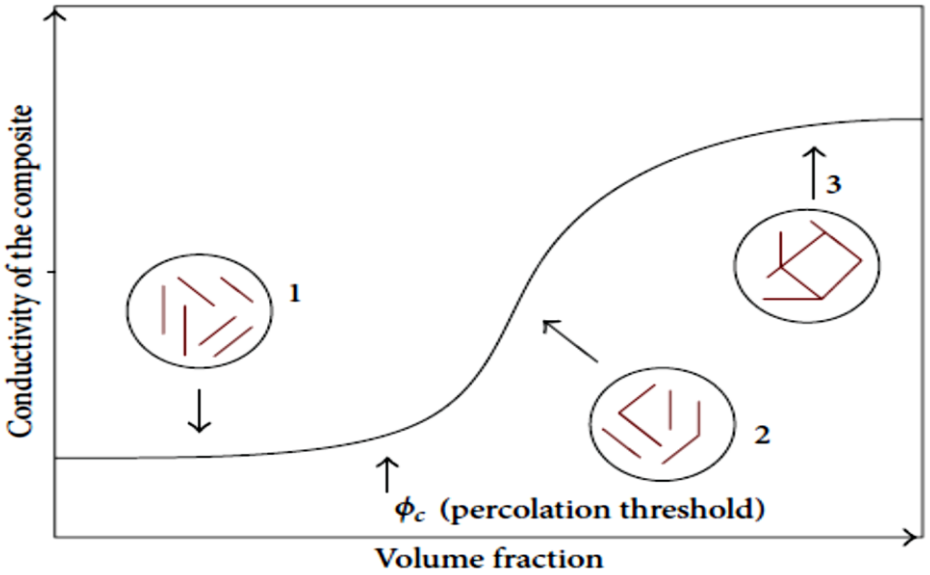

Figure 2.6 Percolation thresholds for conducting composites [33].

Most often, beyond the percolation threshold, it would be necessary to explore filler structures that do not aggressively promote aggregations. Some filler with very high surface energy could end up interacting among itself beyond the threshold and it could create difficulties in dispersion.

Besides the networking of fillers in the composites also comes the importance of filler-polymer interaction. This would be one of major property when the composite is subjected to periodic deformations. The surface chemistry of carbon black and silica are different and they have different mechanism to interact with polymer chains. Carbon black contains few amounts of functional groups on the surface such as carboxyl, hydroxyls, phenols, quinone, etc. and their role in promoting interaction with polymer chains is not overtly remarkable. In this case, physical adsorption and chain-filler entanglements prevail for carbon black-polymer interactions. That of silica on the contrary proceeds by the coupling of the silanol groups on the surface with silane coupling agents to form bridges with polymer chains. This approach therefore achieves silica-based compounds with improved properties such as lower rolling resistance, better wet-traction and ranking in the same performance with carbon black in abrasion resistance [34].

2.4 Lightweight polysaccharides as potential fillers

The rewarding properties of the conventional fillers such as carbon black and silica have been elucidated. Their dominance in the tire industry in terms of properties may not have rivals that would immediately outstrip them. However, considering carbon black that is derived from fossil fuels, environmental concerns are part of major drives to find alternative replacements. Regulations have also made consumers to plan for tire manufacturing without carbon black in the future. That of silica is from nature (sand or ore). The production process is intensive, both mechanically and thermally and requiring considerable amount of acids that generates chemical waste [35, 36]. Silica and carbon black have higher density, which does not favour fuel efficiency [37]. Going back to nature to find abundant materials that are lighter in weight, inexpensive and renewable have led to considering the two fillers: Cellulose derivatives and alpha-1,3-glucan for use as a replacement of the conventional fillers for natural rubber compounds.

2.4.1 Cellulose nanocrystals

2.4.1.1 Sources and production

Cellulose is the most abundant renewable polymer and has been in use for decades with annual production estimated at 7.5 x 10^{10} tons [38]. There are several cellulosic sources such as higher plants, algae, fungi, marine animals, invertebrates etc. The typical cellulose unit consist of a glucose

molecule with a repeating unit comprising of anhydroglucose ring (AGU) $(C_6H_{12}O_5)_n$. A 1-4 linkage requiring a flip of the glucose units links these units together. A pair of the linked glucose molecule is known as cellobiose measuring about 1 nanometre and is shown in figure 2.7. Depending on the source of the cellulose, the repeating units can reach tens of thousands, constituting themselves into fibres. These fibres owing to the surface chemistry of the glucose molecules having abundant hydroxyl groups promotes inter and intra hydrogen bonding that leads to subsequent alignment of cellulosic chains. Several interesting reviews have been published on cellulose and the cellulose nanocrystals [39-42]. The alignment of these fibrils leads to regions with high crystallinity and this is the main source of reinforcement in plants. The structures it forms are of prime interest as it confers on the cellulose unique properties spanning several applications.

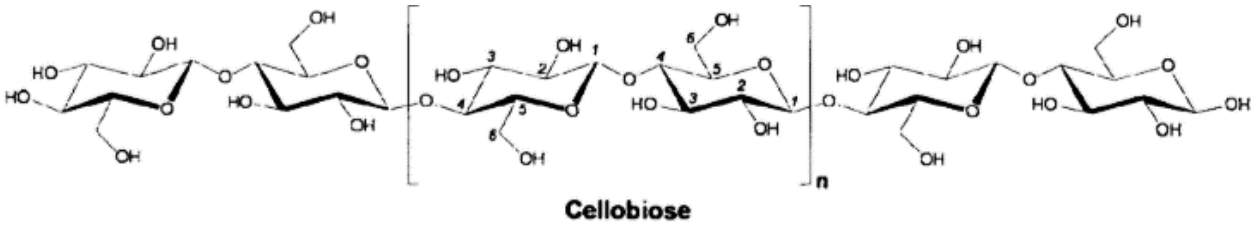

Figure 2.7 Scheme of cellulose chain.

The successive controlled delamination of the fibre bundles and reduction in the chain length leads to obtaining cellulose in the nanometre range. Their morphology is three-dimensional rod-like structure (figure 2.8) with an aspect ratio that is dependent on the cellulose source and production process.

The production of cellulose nanocrystals has come with different terminologies. Notably the micro fibrillated cellulose (MFC) or microcrystalline cellulose (MCC) have dimensions spanning into the micron meter range. This type of cellulose majorly is produced by mechanical means where cellulose fibre bundles are subjected to high shear forces leading to detachments of the cellulose fibres.

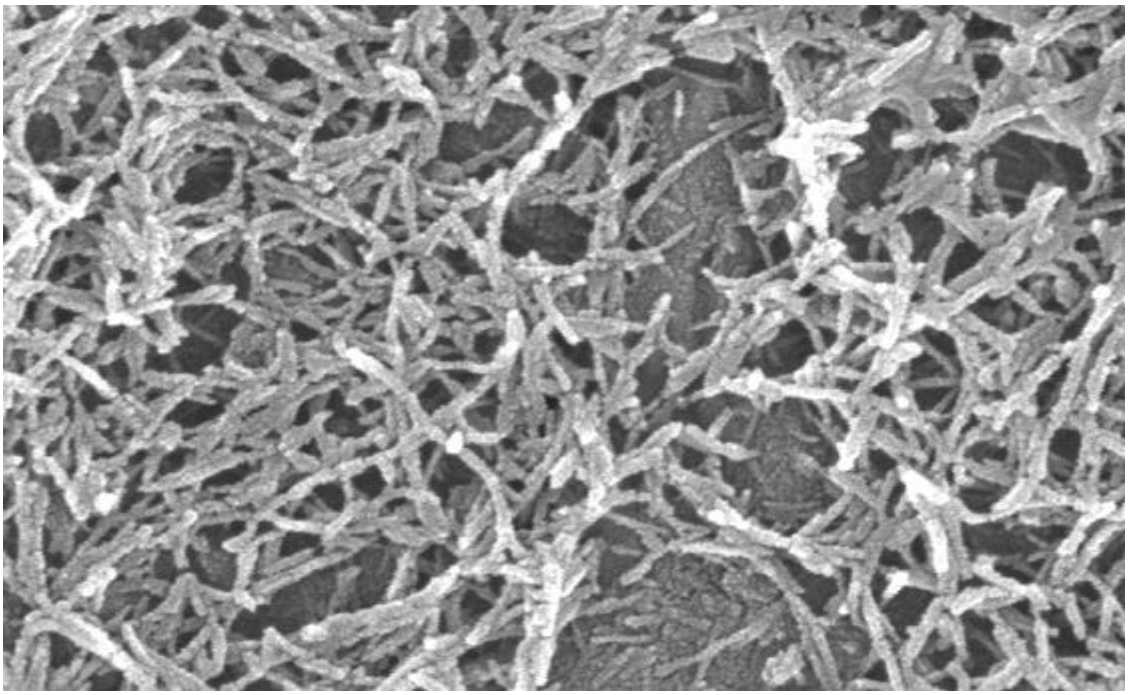

Figure 2.8 SEM image of cellulose morphology.

That of cellulose nanocrystals (CNC), cellulose nano fibre (NF) or nano cellulose (NC) comes from chemical or enzymatic degradations with high crystallinity.

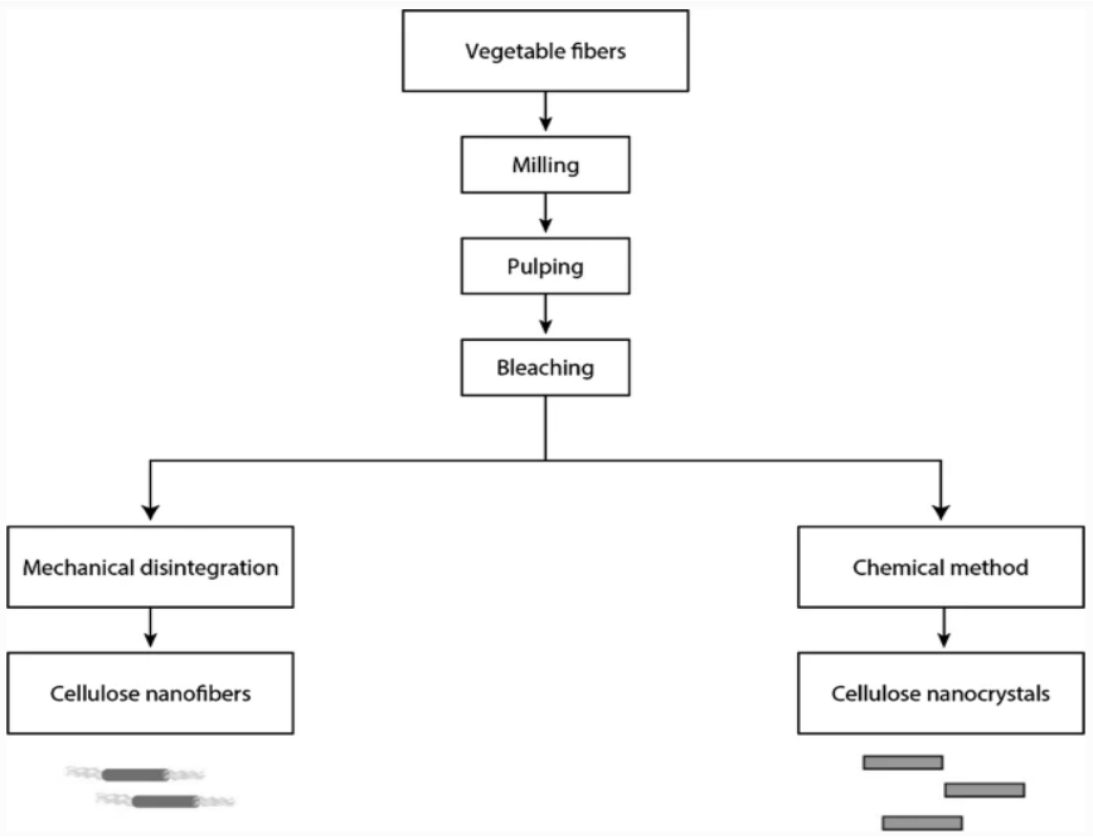

Figure 2.9 Cellulose nanomaterials production process [43].

The chemical means uses several acids. By far, the use of sulphuric acid to selectively hydrolyse the amorphous regions to obtain the nanocrystals is the most widely used method [44]. The use of sulphuric acid confers on the CNC surface a sulphate half-ester groups, which gives rise to colloidal stability. This is vital as it gives the opportunity for further processing. The amount of sulphate half esters is dependent on the preparation conditions and is a major contributor to specific properties of CNC. The CNC used in this project were made from sulphuric acid hydrolysis and chapter 4 has been dedicated to exploring the role of these sulphate esters.

2.4.1.2 Properties and applications

Cellulose has constituted several industries for decades. The unique properties majorly stem from the resilient crystalline fibres, which contributes to good thermal stability and huge mechanical properties. The cellulose nanocrystals when compared with other widely used fibres, shows that the mechanical properties are leading in several aspects coupled with the fact that it is a fibre that is derived from nature, renewable and biodegradable. In table 2.3 is shown comparative mechanical properties of CNC.

Material	Tensile strength (MPa)	Elasticity modulus (GPa)	Density (g/cc)
Cellulose nanocrystals	7500	120-143	1.50
Glass fiber	4800	86	2.50
Steel wire	4100	207	7.85
Graphite whisker	21	410	1.80
Carbon nanotubes	11-63	270-970	1.33
Kevlar	3.5	124	1.40

Table 2.3 Properties of cellulose nanocrystals relative to other materials [45]

These properties coupled with the low density of CNC are a good replacement for so many materials used in composite manufacturing. To improve the properties of cellulose nanocrystals, several modifications are carried out, taking advantage of the abundant hydroxyl groups available on the surface. For example, the hydrophilic nature of the CNC makes them good candidates for applications requiring modifications in rheology of suspensions or use in health care products. However, for composites, CNC is widely considered as reinforcing filler. In a hydrophobic matrix, it would require the functionalization of CNC surface for compatibility. Due to this factor, the tailoring of CNC by means of chemical or enzymatic functionalization is heavily researched. Contributions

exploring the use of CNC in composites [46, 47], packaging [48, 49], and medicine [50] among others are continuously published. The chart in figure 2.10 describes potential applications of cellulose nanocrystals.

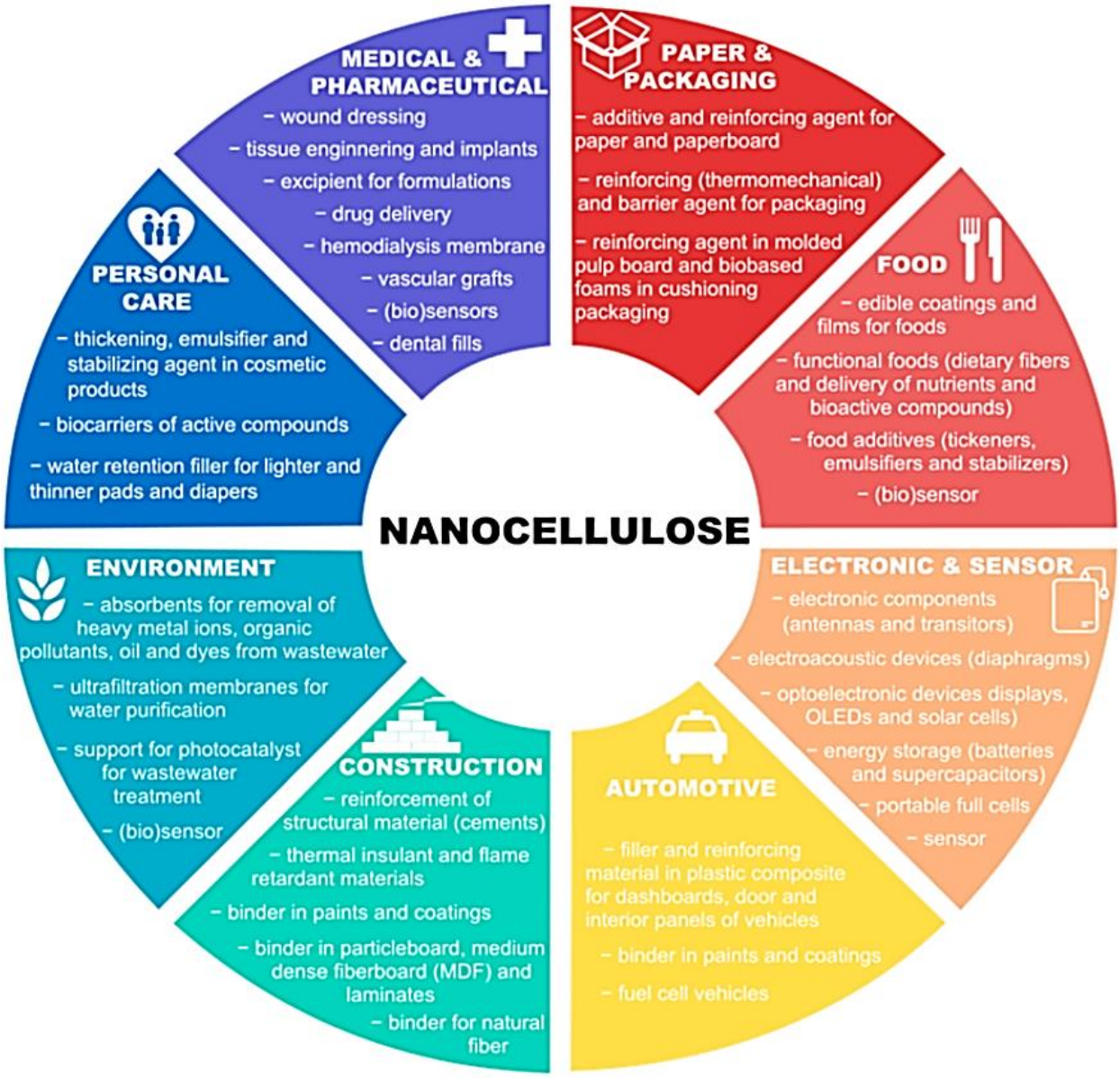

Figure 2.10 Applications of cellulose nanocrystals in different industries [51].

The use of cellulose nanocrystals for composite preparation is the centrepiece of this work. Their use as reinforcing filler could only be realized by surface functionalization for compatibility with polymer matrixes. The tire industries use mostly hydrophobic polymers as matrixes such as natural rubber, polyisoprene, polybutadiene etc. For filler-polymer compatibility in composites, silanes are mostly used to functionalize the surface and there have been recorded success with nano silica as reinforcing filler. Silica has similar surface chemistry with CNC with their abundant surface hydroxyl

groups available as active sites for functionalization. The functionalization process employing the use of silanes as a compatibilizing agent, could be carried out *in situ* during filler-polymer compounding. Several silanes containing different functionalities are used for compatibility and dispersion within the matrix. Silanes are bi-functional and for the fact that they are not a naturally derived resource, it also cast doubts on the green life of CNC in some of the process. There are also the possible considerations of the biodegradation of cellulose nanocrystals after it has been modified. Without modifications, the properties of cellulose nanocrystals are few and its uses are very limited. Apart from chemical modifications, enzymatic catalysed modifications are other possibilities, which have been considered in a later part of this work in chapter 6.

2.4.2 Alpha-1,3-glucan

Alpha-1,3-glucans are water insoluble polysaccharides found in the cell wall of many fungi [52-54] which have been explored for decades for medicinal use. In human occurrence, it is one of the main components of dental plaque resulting from enzymatic activity of sucrose residue with little amount of 1,6 linkages at the side chain. In the cell wall of fungi, they form structures with 1,3-beta glucan, 1,6-beta glucan, chitin, and glycoproteins [55] which serves as a rigid protective means while flexible enough to support growth.

Beta-1,3-glucans are more studied and published owing to their prevalent occurrence in many species. The specie that has been adjudged to have the highest amount of alpha-1,3-glucan is the *Laetiporus sulphureus* specie with amount reaching 57% in dry fungal mass [56]. Many other species have little or no presence of the alpha glucans. This is what has led to reduced studies compared to the other components within the fungi cell wall. Being an insoluble polysaccharide, derivatization such as carboxylation and sulfation renders it soluble to widen its applications [57, 58].

The exploitation of this material is shifting from the medicinal benefits to other aspects of industrial applications. This stemmed from subsequent studies to understand the properties of alpha glucan and its biosynthetic pathway. Most importantly is the understanding of the contributions of alpha glucan to the structure and resilience of the cell wall. Also, the role it plays that makes dental plaques rigid shows that alpha 1,3 glucan has good properties that can support rigidity or reinforcement in several media. In this regard, it is expected that using alpha 1, 3 glucan as bio filler could give considerable reinforcement in polymeric composites.

The extra cellular synthesis of alpha-1,3-glucan resulting in dental plaque is a process that could be replicated to reach huge amount for industrial applications. It has been known that alpha-1,3-glucan is produced by *Streptococcus spp.* found in oral cavity which leads to the formation of dental plaque and deposition of oral caries [59]. In the synthesis, glucosyltransferase (Gtfs) enzymes that are secreted by lactic bacteria found in the mouth were reported to catalyse the reaction [60]. The produced glucan could be insoluble if it contains dominantly the 1,3 glucan linear chains and soluble if there is the presence of alpha 1,6 chains. Recently, Puanglek *et al*. (2016) [61] succeeded in synthesizing the glucan that can selectively produce either alpha-1,3-glucan or 1,6-glucans. After producing the Gtfs enzymes from *Streptococcus salivarius*, sucrose was used as a starting material. The reaction is presumed to proceed from the Gtfs cleavage of the sucrose to glucose up to growing chains of alpha-1,3-glucans [62] as shown in figure 2.11.

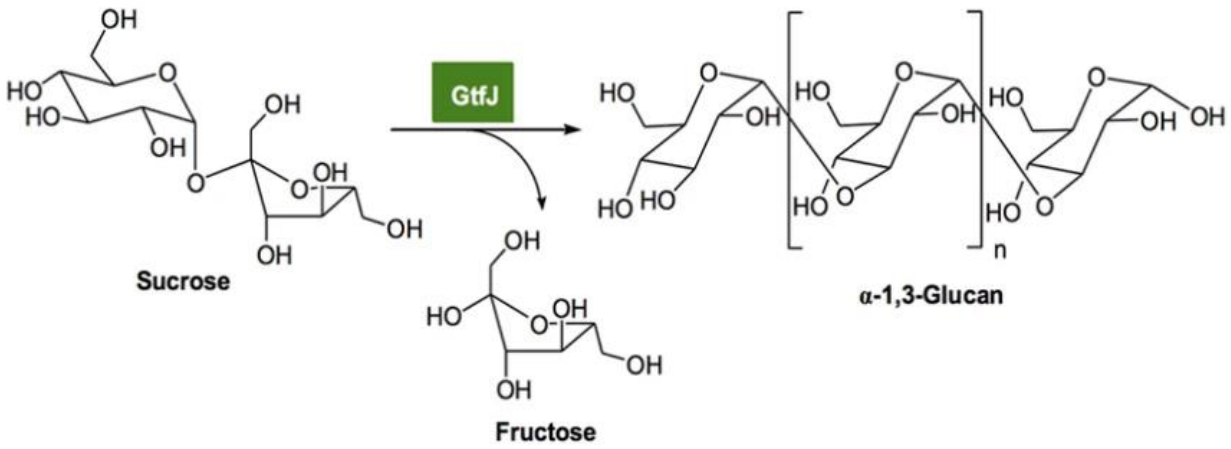

Figure 2.11 Enzymatic polymerization of alpha-1,3-glucan [61].

The obtained alpha-1,3-glucans were also modified and there were remarkable improvements in thermal properties especially alpha-1,3-glucan propionate, and acetate. This is advantageous especially for composite processing requiring higher temperatures. More so, the ease of functionalization by the authors [61] alludes to the possibility of using alpha-1,3-glucan as fillers which could be compatibilized without constraints in polymeric matrixes.

The structures of the alpha glucan chains have abundant hydroxyl groups, which helps in maintaining a high degree of crystallinity. This property which enhances the mechanical value of many fillers used in the tire industry would present alpha-1,3-glucan as another entrant into the filler market. Although these studies are ongoing, there are differences in crystalline form when hydrated, anhydrous and when derivatized [63, 64] alongside their potential applications.

The possible use of alpha-1,3-glucan as substitutes in many applications is evident in the success recorded in the preparation of alpha-1,3-glucan esters, and films [65] and would be studied. Subsequently, alpha 1,3 glucan has been used as a filler in chapter 5 to understand the reinforcing properties.

2.5 Composite preparation

Since the advent of reinforcing rubber compounds with fillers, various techniques have been developed to add fillers into rubber matrixes. The preparation methods are also dependent on the nature of the filler and if the filler is in the wet or dry form. The aim is to create efficient dispersion that can enhance good filler-polymer interactions. Some preparation methods are discussed below which are mostly applicable to cellulose nanocrystals but by extension, it could be applied to alpha-1,3-glucan.

2.5.1 Dry compounding

The various forms of CNC preparation leads to nanocrystals in suspension. When cellulose nanocrystal is dried especially oven drying, it can result to irreversible aggregations. Other method of drying such as spray drying, air drying, and lyophilisation are various means to avoid leaving CNC in the form of suspension. To add these fillers into the matrix, it may require milling the dried CNC to obtain smaller particle sizes resulting from the aggregations. Britinis *et al*. [66] pulverized microcrystalline cellulose to obtain nanocellulose and thereafter extruded the lyophilized CNC with natural rubber. For lyophilisation when the percentage of CNC in the suspension is low, the CNC could be fluffy with reduced aggregation compared to oven drying.

Fillers and rubber materials are easily handled when dried. Therefore, processing from the dry form would be less expensive. A generally employed method is melt mixing the filler and rubber materials in internal mixers (such as the Brabender®) at higher temperature to reduce the viscosity of the mix to promote dispersion. From observations, the obtained composites may not be compared with the composites prepared from the wet form in terms of dispersion and good properties. Albeit the procedures employing these dry forms are simple to scale up in commercial quantity. Unlike the biofillers with processing difficulties in the dry form, carbon black is easily dispersible in polymer matrix. Highly dispersible silica is also in the market. It is therefore needful to develop these biofillers

in a highly dispersible form in the dry state to bridge the gap between scientific challenges and industrial stakes [67].

2.5.2 Wet preparation

Biofillers are processed and obtained in suspension, paste or slurry, likewise the matrix materials obtained in the form of latex or suspension. It is easier to blend both materials in their wet form and process from there. This could be achieved by blending the latex with the filler suspension and drying, coagulating, or adding the filler and initiating polymerization therefrom etc. By far, processing from the wet form has been the dominantly published techniques for cnc composites. The blending can come in different form. Some researchers alternatively solubilize the elastomer in a solvent before adding the filler [68]. After which, the solvent is evaporated under vacuum. The filler can also be dispersed in a solvent. In the case of CNC, solvents that disperse the cellulose nanocrystals are few and when used, it is difficult to remove from the system. More so, when some biofillers are dispersed, the hydrogen bond networking is affected. This in turn can affect the crystallinity of the material, which can result in lower composite properties. The method of mixing the filler and latex before evaporation has been used to produce CNC films [69, 70]. In most cases, if additives are not added, they could be added in later stage and further processed to achieve the desired properties or shape. However, one of the challenges mostly encountered in this step is the possibility of the filler sedimenting or self-aggregating during the evaporation stage. This can result to a non-homogeneous composite where filler particles tend to form localized aggregates in some regions of the composite.

The solution blending with coagulation is another method that has been used to make CNC composites. Chen *et al.* [71] prepared CNC composites by mixing CNC with various blends of rubber. This method often referred to as co-precipitation, or co-coagulation uses different acids. The procedure adopted in this work requires the mixing of a water-based filler suspension with a latex rubber suspension with a magnetic stirrer until homogeneity. The mixtures are thereafter coagulated with glacial acetic acid in dropwise addition. After the coagulation, the samples are pressed, soaked in water to remove unwanted materials, and dried till constant weight. This process enhances good dispersion within the polymer matrix, support good filler-filler networking and filler-polymer interaction. A major challenge in this process as observed with CNC is the concentration of CNC suspension. Commercial CNC suspension is mostly produced in the concentration range of 5wt % to 15wt %. Lower than 6wt %, the mixtures can be difficult to coagulate with substantial amount

of the filler or elastomer leached out of the coagulated material. In this case, it is important to weigh the material after drying to ascertain the actual amount that was lost during the coagulation process. However, at high concentrations, the rheological properties of CNC changes and blending become difficult which would require addition of water for easy homogeneity. At the subsequent stages of the composite preparation, silanes, vulcanization agents and anti-degradants are added, mixed by melt blending and vulcanized to obtain the composite. At the coagulation step, it is necessary to reduce the use of large amount of acid and to control the addition especially if more water was added to the mixtures for homogeneity. From practical point of view, as experienced with CNC and alpha-1,3-glucan, their coagulation requires the dropwise addition of concentrated acetic acid that is 10% of the entire volume of filler and latex suspension. Large amount of acid in the material has the potential of interfering with the vulcanization step and must be washed away.

2.5.3 Compatibilization

The mechanism of carbon black reinforcement is different from other fillers such as silica. This is because, carbon black is easily dispersible within elastomeric matrixes and interaction is achieved by carbon black adsorption on the polymer chains. At the advent of silica having a different surface chemistry, the need for a compatibilizing agent was necessary. Silica has numerous surface hydroxyl groups, making it hydrophilic as against a majority hydrophobic polymer matrix. To create compatibility, silanes are heavily consumed as a simple means of surface functionalization.

Silanes are organo-functional compounds and have been used in the tire industry since the introduction of silica fillers. Cellulose nanocrystals and alpha-1,3-glucan have similar surface chemistry with abundant surface hydroxyl groups and the use of silanes for coupling proceeds in the same manner. In figure 2.12 [72] is shown the coupling mechanism that takes place on the surface hydroxyl groups of fillers.

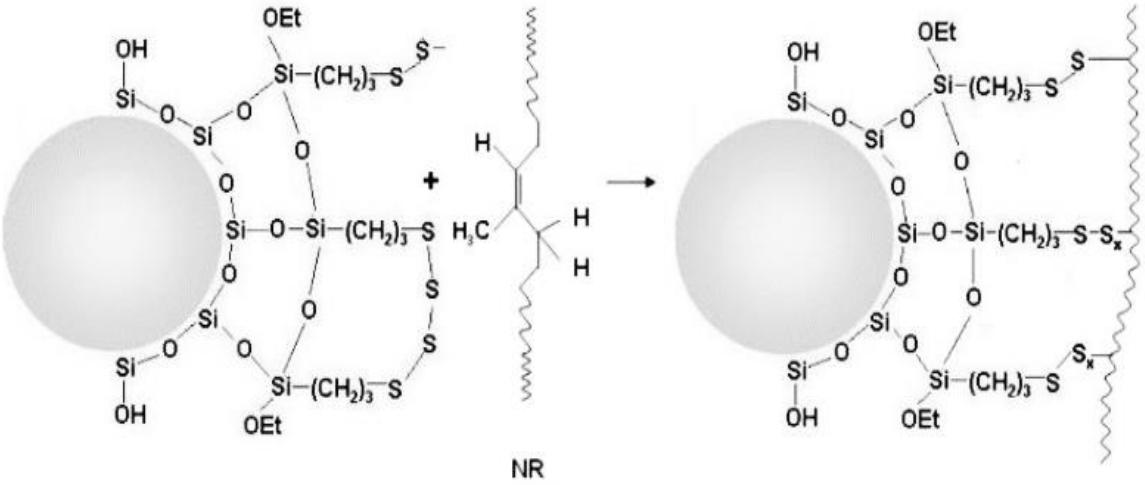

Figure 2.12 Silane coupling bridges.

In this work, the bis(triethoxysilylpropyl)disulfide (TESPD) and (3-aminopropyl)triethoxysilane (APS) were used as aliphatic silanes while cyclic silanes such as 2,2-dimethoxy-1-thia-2-silacyclopentane (SID), and n-n-butyl-aza-2,2-dimethoxysilacyclopentane (SIB) were also used.

The reaction process of the aliphatic silanes proceeds by hydrolysis, condensation and coupling of the silanes. Therefore, the silanes are capable of structural formation, which are typical of their molecular nature and the prevailing condensation reaction. That of cyclic silanes proceeds by ring opening due to loss of ring strain energy [73] and does not need hydrolysis. Therefore, they seem more reactive and are susceptible to hydroxyl containing molecules. It is important to keep the materials dry to avoid the cyclic silane reaction with the moisture content in the material instead of the hydroxyl groups available on the surface.

It is simple to add these silanes *in situ* when compounding in brabender internal mixer instead of pre functionalization. When pre-functionalized and dried, the biofillers still faces challenge of dispersion despite the surface hydrophobization. Unlike CNC, *in situ* functionalization of silica compound with APS silanes is feasible but the functionalization does not promote a direct matrix-filler bonding. Albeit majority of silica functionalized with APS is conducted prior to addition into the rubber matrix. The APS is one of interesting silanes that provide structures, which can facilitate vulcanization. The amine functionality is touted to be a silanization booster [74]. This is predicated on the ability of amine functionality to present basic conditions that would lead to the ease of hydrolysis of the alkoxy groups enabling it to form reactive hydroxyl species before condensation.

Majority of the functionalization intended to compatibilize biofillers such as CNC are targeted to hydrophobize the surfaces and reduce the surface energy for easy dispersion. CNC have been functionalized by other methods apart from the widely used silanization in composites such as esterification, amidation, etherification, oxidation etc. [75]. Subsequently, in the later part of this work, enzymes were used to transesterify cellulose nanocrystals using vinyl esters as ester donors. While modifying the biofillers for compatibility within polymer matrixes, the green character of the modified biofiller is another subject that requires detail studies. Most importantly if the advantage of biofiller degradability could be maintained after functionalization. However, modifying cnc or alpha 1,3 glucan fillers with other method other than silanes, may require pre-modification before introduction into the polymer matrix and may be tedious compared to the silanization during in situ compounding.

2.5.4 Additives

It is difficult to have a material that provides all the properties required for applications. When composites are prepared, additives are added to compensate the vulnerability of the material in certain operating conditions. For example, natural rubber mostly used as matrix is unsaturated. The presence of the double bond makes it susceptible to degradations. Natural rubber has low resistance to UV, ozone, oil, fuel, and high temperatures. To remedy these drawbacks, additives are added during composite preparation to improve the materials resilience to these degradations. When additives are added, it becomes critical to study the possible influence on other interesting properties of the composite.

Antidegradants are classed as antioxidants or antiozonants, which are based on amines or phenolic derived compounds [7]. The amine type impact colour on the compound and are generally considered as staining antidegradants. The recipe adopted in this work uses 2,2,4-trimethyl-1,2-dihydroquinoline (TMQ) and N-(1,3-dimethylbutyl)-N’-phenyl-p-phenylenediamine (6PPD) as antioxidant and antiozonants.

2.5.5 Vulcanization system

A rubber material is generally inferior in properties when uncured. The properties at this point especially the mechanical worth could come from the nature of the polymeric backbone, functionalities, or the chain entanglements. When rubber is cured, sulphur is added to create

bridges to increase the elasticity of the material and improve the general properties. There are other types of curing such as: peroxide curing, UV, phenolics etc. but the sulphur curing system constitutes the most utilized in the tire industry.

The sulphur system form bridges as shown in figure 2.13.

When sulphur vulcanization was discovered by Goodyear, it achieved its aim of making rubber compounds stiff through the crosslinking. However, it took a long period of time to achieve vulcanization with only sulphur in the curing system. The emergence of accelerators in the sulphur cure system reduced the vulcanization time to a large extent. In the vulcanization package, stearic acid (or similar fatty acids) and zinc oxide acts as activators while widely used compound such as N-cyclohexylbenzothiazole-2-sulfenamide (CBS) accelerates the vulcanization process.

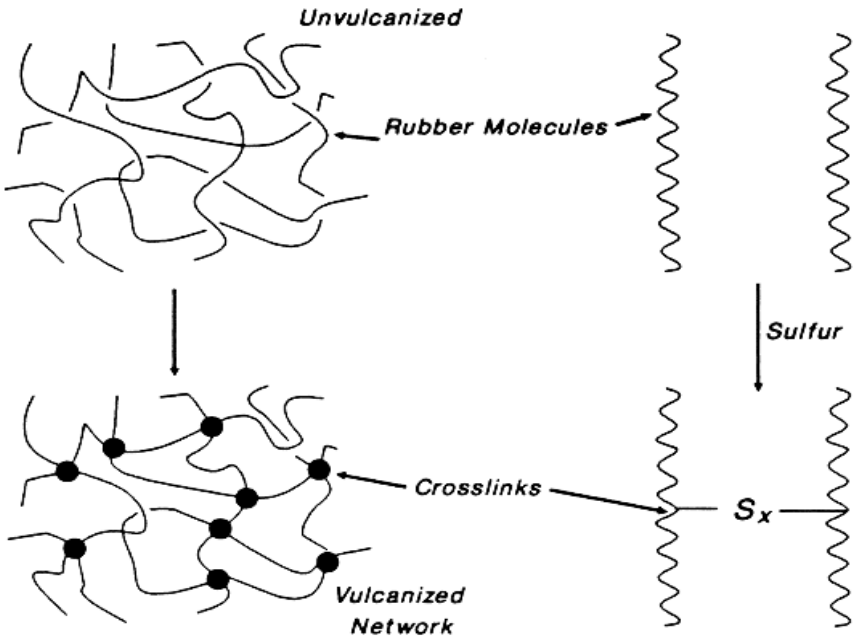

Figure 2.13 Sulphur bridges in rubber chains.

The zinc oxide and fatty acids reacts to form complexes with accelerators. This complex further reacts with sulphur to form sulfurating agents [76] and subsequently interacts with polymer chains to form sulphur bridges.

The progress of the reaction is expected to be monitored to know when to end the vulcanization reaction. The moving die rheometer is one of the reliable tools to study the progress of the vulcanization reaction. Samples are placed in a moving die, which measures the torque required to

rotate the die as the vulcanization proceeds. The torque therefore translates to the extent of crosslinking achieved in the vulcanization.

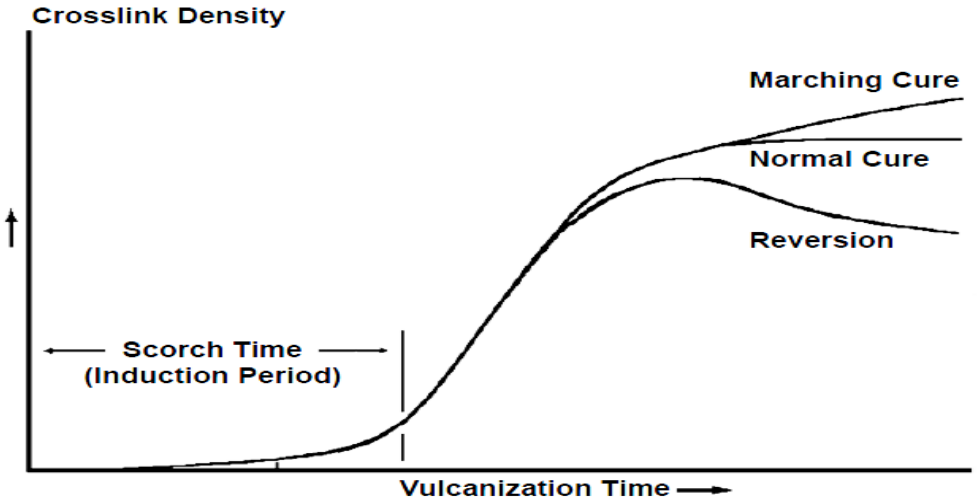

Figure 2.14 Vulcanization curve

A typical vulcanization curve is shown in figure 2.14. At the onset, of the vulcanization, the activators and accelerators play a huge role in forming the material for the start of vulcanization. It is necessary to know the optimum time of the vulcanization T_{90} when about 90% of the crosslinks has been achieved. For most samples when a reversion sets in, a part of the crosslinking is lost which affects the properties of the material. The conventional approach to determining curing time is to make an array of curing temperatures and time, which will serve as a guide to determine the actual temperature and time to end the curing process. The evolution of the vulcanization process is monitored by some parameters as outlined below.

- **T_S2 (min):** During the vulcanization process, the induction time spanning from the beginning of the process to the time where there is an increase in torque is the scorch time. When there is a rise of 2 unit, which is evidenced in the increase in torque, the vulcanization is considered to have started. The Ts2 is when 2% of the crosslinking have been achieved and is therefore seen as the time crosslinking starts and is vital to understand the required induction time for each compound.
- **T_{90} (min):** The curing kinetics differ across compounds. Most often, it can result to reversion, normal cure, or marching. For a normal cure, the curing continues to almost a constant after the highest torque has been achieved. To avoid curing close to the point where the

vulcanization properties would change, a 90% curing is sometimes considered optimum and is deduced as

$$90/100\ (M_H - M_L) + M_L \qquad (2.1)$$

Where M_H and M_L are the maximum and minimum torque. At the T_{90}, the crosslinking achieved is sufficient to end the vulcanization at this stage. Sometimes, curing is also done up to T_{95} to attain a 95% crosslinking. Curing to reach the highest torque before ending the vulcanization may not be ideal.

- **M_L (dNm):** This is the minimum torque which indicates the base point at the start of vulcanization. The viscosity of the compound at this point is lowest and starts to increase when the crosslinking starts. It is used alongside the maximum torque to determine the crosslinking density.
- **M_H (dNm):** This is the maximum torque achieved during the vulcanization and is used to understand the moment vulcanization properties may be compromised or no longer becoming desirable. At this point when the maximum torque is achieved, curing beyond this point becomes undesirable as it could result to reversion. The M_H is therefore used to monitor and understand the time needed to end the vulcanization.
- **CRI (min^{-1}):** The cure rate index is a measure of the efficiency of the curing process. Considering the scorch time and the optimum curing, the CRI is deduced as below.

$$100/(t_s 2 - t_{90}) \qquad (2.2)$$

When the scorch time is short (without premature vulcanization), an optimum curing time is achieved early which is an indication of higher curing rate. However, at delayed scorch time, the curing rate is often impacted leading to lower curing rate index.

2.5.6 Characterizations

2.5.6.1 Dynamic light scattering (DLS)/ Zeta potential (ZP)

The dynamic light scattering method has been a useful tool for the analysis of nano particle sizes alongside the zeta potential to understand the surface charge corresponding to its colloidal stability. For composite preparation, particle sizes and surface area of the fillers are important as it gives an

idea of the effective contact available for interaction in the composite. Particles scatter light when illuminated and the DLS uses the scattering to determine the particle sizes. In a colloidal suspension, particles undergo a Brownian motion and interaction among particles creates an absorbed layer on the interfaces. The DLS and zeta potentials make use of the interactions within the colloidal suspension to estimate the hydrodynamic radius of the particles [77].

CNC particle morphology is rod-like in shape while the dynamic light scattering method estimates the hydrodynamic diameter from the translational diffusion coefficient of spherical particles undergoing Brownian motion. The hydrodynamic diameter estimated from the Stokes-Einstein equation does not effectively correlate to the length or width of CNC rod-like particles. This is due to the geometry of CNC particle with unequal dimensions and undergoing uneven motion from both axes. The size estimate for cellulose nanocrystals with different morphology is therefore considered to serve for relative comparison [78]. Other methods such as AFM, SEM, and TEM are some of dominant methods used to effectively estimate the sizes of CNC particles and substantial difference exist when compared with DLS particle sizes. The average particle sizes estimated from DLS are in most cases approximately half of the length obtained from electron microscopy [79]. CNC suspension is polydisperse and the particle size distribution is essential in the estimation of the average particle sizes.

Sample preparation method is a crucial step in achieving accurate estimation. Samples must not be sedimenting or aggregating and must be prepared at defined concentrations to have a good comparison among samples.

2.5.6.2 Elemental analysis

The presence of some chemical components could be measured using the elemental analyser. In subsequent chapters, the use of the instrument was necessary to determine the elemental composition of the various samples. For example, when CNC is produced, the sulphate half esters on the surface of the CNC promotes stability of the colloidal suspension. The contributions of these sulphate groups in the CNC composites are worthy of studies. The amount of these sulphate groups could be assessed corresponding to the amount of sulphur content using the elemental analyser.

The amount of sulphur present in CNC estimated from elemental analyser often represents the total amount compared to titrimetric method that may have limitations accessing some amount of sulphur [80].

In addition, for modification reactions involving the grafting of some functionality on the surface of CNC, the increment in the values of the elemental content is an indication of the success of the reaction if there are no contributions from impurities. Estimations of the elemental content such as carbon, hydrogen, nitrogen, and sulphur (CHNS) alongside some calibrations have been made possible and simple by some vendors. Elemental analyser was therefore one of the indispensable means to access the success of some of the reaction.

2.5.6.3 X-Ray Diffraction

CNC and alpha-1,3-glucan have abundant hydroxyl groups on the surface which results in strong hydrogen bond interactions. These interactions help in maintaining fibre alignments, which results in well-organized crystalline regions. The crystallinity of the filler particle contributes immensely to the behaviour, which can remarkably affect the properties of the composites. X-ray diffractometer are used to study the crystallinity of materials.

A crystallite has minimal defects and can diffract rays when directed at it at a particular angle. The diffractions are therefore analysed to understand the crystallinity and atomic structure of the materials. Subsequently, the information is used to estimate the crystallinity index of materials. Analysis to estimate the crystallinity index (CI) especially for cellulose has been met with large discrepancies among results depending on the process employed. The simplest method is finding the ratio of the largest crystalline peaks to the total crystalline and amorphous regions [81, 82]. This method is fast and convenient, but it does not consider contributions from other crystalline peaks. Rather, the deconvolutional method using Gaussian distribution considers the ratio of all the crystalline peaks to the crystalline and amorphous regions [83-85]. This approach comes with the challenge of constructing a base line with good precision of selecting the peaks base when the peaks are broad at the base as is obtainable for CNC and alpha-1,3-glucan. The deconvolutional method was employed in estimating the various crystallinity indexes of the used fillers.

2.5.6.4 Thermogravimetric analysis (TGA)

The thermogravimetric analysis has been a useful means to study the thermal properties of materials. During composite processing, especially for thermoplastics where high processing temperatures are required, the fillers are expected to be thermally stable to withstand the processing temperatures. The TGA method is suitable which heats the material at wide range of

temperatures and at specific heating rates. The response of the material is indicative of its thermal resilience.

Samples are added to crucibles and heated in inert atmospheres especially for materials that are susceptible to oxidation or other reactions that can influence the results. In this work, alpha-1,3-glucan and cellulose nanocrystals were analysed under nitrogen flow with heating temperatures ranging from 30 to 600^0C.

2.5.6.5 Scanning Electron Microscope (SEM)

The reinforcement of composites by fillers in part has contributions from the particle morphology. Cellulose nanocrystals, alpha-1,3-glucan and silica have their specific morphologies. During synthesis, the morphology could be impacted. The scanning electron microscope is a reliable method of studying the morphological characteristics of filler particles. This method is easier to study the filler before the addition into the composites.

The process uses electron beam to bombard a surface containing the sample. The signals from the secondary electrons resulting from the bombardment are analysed to understand the surface topology of the materials. In this case, it is required of the sample to be conductive. However, polymeric materials such as the fillers under study are not conductive. To overcome this drawback, a conductive coating such as gold or carbon is used. For practical purpose, a coating in the range of 5-10 nanometre was found adequate to aid image acquisition for cellulose nanocrystals and glucan materials. More so, the conductive coating should be deposited in a manner that it does not form a film layer on the sample and thereby preventing image acquisitions.

2.5.6.6 Dynamic mechanical analysis

When a polymer is filled by particulate material, the properties improve considerably. The behaviour of the composites is majorly dependent on the filler-filler interaction resulting from the dispersion and aggregate structures as well as the filler polymer interaction. Dynamic mechanical analysis of the materials therefore gives an understanding of these properties by providing information of the material response when subjected to deformations.

To study the reinforcement mechanism, the oscillating disk rheometer has been a useful tool in the industry for this purpose. The measurement principle involves applying a certain stress or strain on the material and measuring the response of the material. When a sinusoidal force is applied on the

material, a phase lag results which is due to the deviation of the material from an ideal elastic medium. In this case, considering a hydrodynamic model, the compound is typical of a viscous media filled with particulate materials. These particulate materials cannot be deformed unlike the viscous phase. Hence it acquires a hydrodynamic behaviour when subjected to deformation. A derivation accounting for this hydrodynamic behaviour in a viscous phase alongside other considerations is used to estimate the reinforcement of filler particles. An in-phase response corresponding to the storage modulus and out of phase detected sinusoidal wave corresponding to the loss modulus are important parameters to understand the reinforcement of the filler particles. The ratio of the loss modulus to storage modulus is known as the tangent delta, which is the damping ability of the material. Detailed derivations of these parameters have been presented elsewhere [86-87].

The test conditions are critical in the measurement. Mostly used in this work is taking measurements at 70^0C and at a frequency of 1 Hz. In these conditions, the oscillating disk makes an angular sweep corresponding from 1 to 100% elongation.

The storage modulus at low strain is always higher and depicts the stiffness of the material. However, when the strain increases from 1 to 100%, the material undergoes cyclic deformations thereby loosing part of its networking structure. The difference from the highest to the lowest storage modulus is considered the Payne effect. This is the filler network breakdown, which can lead to hysteresis. In tire testing, these parameters are crucial to give an idea about the service life of the tire compound. It is difficult sometimes to have a pegged value on the parameters because when tires are designed, the applications may place a preference on a specific property. For example, tires that are expected to provide a better grip might require a lower tangent delta. For each compound, some of these parameters were determined as outlined below.

- **Storage modulus (G', kPa):** When polymers are filled with particulate materials, they contribute to the reinforcement of the compounds, thereby making them stiff. The storage modulus G' could therefore be loosely translated as the ability of the material to elastically resist deformations. Although, there are several postulations to the exact contributions to the storage modulus, the filler-filler networking contributes immensely to the storage modulus. Fillers such as cellulose nanocrystals and micro fibrillated cellulose with higher aspect ratio have a strong filler-filler networking and compounds prepared therefrom possess high storage modulus at low strain. Besides the contributions of the filler, the crosslinking created during vulcanization and possible contributions of crystallization

properties of polymers add to increase in storage modulus. Comparatively, the green uncured compounds have a lower storage modulus with possible contribution from the filler networking alone. While the vulcanized compounds have crosslinks, which increases the storage modulus. For each compound, this parameter was estimated.

- **Payne effect:** During cyclic deformations, the filler network is broken down and the successive deformations leads to non-recoverability of the filler networks. At 100% deformations, the filler networking is totally broken down and the extent of breakdown from deformations at low strain up to 100% strain is known as the Payne effect. At high Payne effect, the compounds possibly demonstrate a poor dispersion and poor filler-polymer interaction. When filler and polymer networks are broken down during the deformations process, the energy loss creates heat which is related to **hysteresis**. For the service life of a tire, the Payne effect is a vital parameter used to understand the ability of the compound to cope at certain extreme conditions.
- **Tangent Delta:** Polymeric materials have increased applications when filled with particulate materials. The properties obtained from this combination is a mixture of viscous and elastic portions and the tangent delta gives the ratio of both properties. At low tangent delta, the elastic properties of the material tend to increase and at high tangent delta, the compounds show a more viscous character. For most compounds, low tangent delta is desired at 70°C, although specialised uses might require higher values.

2.5.6.7 Tensile measurements

It is important to study the static and dynamic conditions of the composite material. The tensile measurement provides this opportunity to subject the material to different types of stresses and measure its response to it. Most importantly is the response of the material at different percent elongations, up to elongation at break. It shows the maximum strain and stress the material can bear. This also gives an idea about the interaction between the filler and polymer chains. The Mullins effect is a clear description.

When a filler-polymer material is subjected to stress, a debonding tends to occur between the filler and the polymer chains. In fact, when a polymer is filled with particulate fillers, besides the interactions that takes place, there are high restrictions to the mobility of the chains, and it will depend at what level of strain a total detachment leading to easy mobility will occur. When the

material is strained, its response will also indicate the ability of the material to strain crystalize to resist the effect of the strain. It is therefore necessary not just to understand the dynamic mechanical analysis, which gives a better understanding of the filler networking and energy dissipations but also the strength it possesses and the maximum stress it can bear.

References

1. Dunn, J.R., Jones, R.H. (1991) Automobile and Truck Tires Adapt to Increasingly Stringent Requirements. Elastomerics, pp 11-18.
2. Rodgers, B., Waddell, W. (2005) Tire engineering. In Mark, J.E., Erman, B., Eirich, F.R. (Eds.), Science and technology of rubber (3rd ed.). Elsevier.
3. Danon, B., Gorgens, J. (2015) Determining rubber composition of waste tyres using devolatilisation kinetics. Thermochim. Acta, 621, 56-60.
4. Pehlken, A., Essadiqi, E. (2005) Scrap tire recycling in Canada. Technical Report, · November, DOI: 10.13140/2.1.1941.8400
5. White, J.R., De, S.K. (Eds.) (2001) Rubber technologist's handbook. Rapra Technology Limited, UK
6. Bich, N.N., (2019) ANRPC releases natural rubber trends & statistics, December 2018. News from Secr.http://www.anrpc.org/html/news-secretariat-details.aspx?ID¼9&PID¼39&NID¼2271. Accessed 08.10.20.
7. Sisanth, K.S., Thomas, M.G., Abraham, J., Thomas, S. (2017) General introduction to rubber compounding. In Thomas, S., Maria, H.J. (Eds), Progress in rubber nanocomposites. Elsevier Ltd.
8. Ren, X., Barrera, C.S., Tardiff, J.L., Gil, A., Cornish, K. (2020) Liquid guayule natural rubber, a renewable and crosslinkable processing aid in natural and synthetic rubber compounds. Journal of Cleaner Production, 276, 122933.
9. Hamilton, R.G., Cornish, K., (2010) Immunogenicity studies of guayule and guayule latex in occupationally exposed workers. Ind. Crop. Prod. 31, 197-201.
10. Ikeda, Y., Junkong, P., Ohashi, T., Phakkeeree, T., Sakaki, Y., Tohsan, A., Kohjiya, S., Cornish, K. (2016) Strain-induced crystallization behavior of natural rubbers from guayule and rubber dandelion revealed by simultaneous time-resolved WAXD/tensile measurements: indispensable function for sustainable re-sources. RSC Adv. 6, 95601-95610.
11. Archer, B.L., Barnard, D., Cockbain, E.G., Dickenson, P.B., McMullen, A.I. (1963) Composition of Hevea latex. In Bateman, L. (Ed.) The Chemistry and Physics of Rubber-Like Substances. Maclaren and Sons Ltd., London.

12. Low, F.C. (1978) Distribution and concentration of major soluble carbohydrates in latex. The effect of ethephon stimulation and the possible role of these carbohydrates in latex flow. Journal of the Rubber Research Institute of Malaysia, 26, 1-21.
13. Morton, M. (2013) Rubber Technology. Springer Science & Business Media, Boston, Mass, USA,
14. H. Ismail, H., Ahmad, Z., Mohd Ishak, Z.A. (2001) Comparison of cetyltrimethylammonium maleate and sulphenamide as an accelerator in carbon black filled natural rubber compounds. Polymer Testing, 6, 607-614.
15. Tanaka, Y. (2001) Structural characterization of natural polyisoprenes: solve the mystery of natural rubber based on structural study. Rubber Chemistry and Technology, 74 (3), 355-375.
16. Liu, J., Tang, Z., Huang, J., Guo, B., Huang, G. (2016) Promoted strain-induced-crystallization in synthetic cis-1,4-polyisoprene via constructing sacrificial bonds. Polymer 97, 580-588.
17. Che, J., Burger, C., Toki, S., Rong, L., Hsiao, B.S., Amnuaypornsri, S., Sakdapipanich, J. (2013) Crystal and crystallites structure of natural rubber and synthetic cis1,4-polyisoprene by a new two dimensional wide angle x-ray diffraction simulation method. I. strain-induced crystallization. Macromolecules, 46, 4520−4528.
18. Tosaka, M., Murakami, S., Poompradub, S., Kohjiya, S., Ikeda, Y., Toki, S., Sics, I., Hsiao, B.S. (2004) Orientation and crystallization of natural rubber network as revealed by WAXD using synchrotron radiation. Macromolecules, 37, 3299-3309.
19. Toki, S., Sics, I., Hsiao, B.S., Tosaka, M., Poompradub, S., Ikeda, Y., Kohjiya, S. (2005) Probing the nature of strain-induced crystallization in polyisoprene rubber by combined thermomechanical and in situ x-ray diffraction techniques. Macromolecules, 38, 7064-7073.
20. Trabelsi, S., Albouy, P.A., Rault, J. (2004) Stress-induced crystallization properties of natural and synthetic cis-polyisoprene. Rubber Chem Technol, 77, 303-316.
21. Le Cam, J-B., Toussaint, E. (2010) Volume Variation in Stretched Natural Rubber: Competition between Cavitation and Stress-Induced Crystallization. Macromolecules, 43, 4708-4714.
22. Morton, M., (1987) Rubber Technology, Van Nonstrand Reinhold Co. New York.
23. Salvucci, M.E., Coffelt, T.A., Cornish, K., (2009) Improved methods for extraction and quantification of resin and rubber from guayule. Ind. Crop. Prod. 30, 9-16.
24. Priyadarshan, P., (2011) Biology of hevea rubber. https://doi.org/10.1079/9781845936662.0001.

25. Soratana, K., Rasutis, D., Azarabadi, H., Eranki, P.L., Landis, A.E., (2017) Guayule as an alternative source of natural rubber: a comparative life cycle assessment with Hevea and synthetic rubber. J. Clean. Prod. 159, 271-280.
26. Dick, J.S., Annicelli, R.A. (2009) Rubber technology: compounding and testing for performance. Munich: Hanser Publishers, Hanser Gardner Publications.
27. Thorn, A.D., Robinson, R.A. (1994) Compound design. In Bhowmick, A.K., Hall, M.M., Benarey, H.A. (Eds.) Rubber products manufacturing technology. Marcel Dekker, Inc., New York.
28. Guntur, N.P.R., Yadav, S.G, Gopalan, S. (2020) Effect of titanium carbide as a filler on the mechanical properties of styrene butadiene rubber. Materials Today: Proceedings, 24, 1552-1560.
29. Blow, C.M. (1971) Rubber Technology and Manufacture. Butterworths.
30. Integrated Pollution Prevention and Control, Reference Document on Best Available Techniques for the Manufacture of Large Volume Inorganic Chemicals- Solids and Other Industry (2006). European Commission.
31. Schaefer, D.W., Rieker, T., Agamalian, M., Lin, J.S., Fischer, D., Sukumaran, S., Chen, C., Beaucage, G., Herd, C., Ivie, J. (2000) Multilevel structure of reinforcing silica and carbon. J. Appl. Crys., 33, 587-591.
32. Engels, H.-W., Weidenhaupt, H.-J., Pieroth, M., Hofmann, W.; Menting, K.-H.; Mergenhagen, T.; Schmoll, R.; Uhrlandt, S. (2011) Rubber, 9. Chemicals and additives. In Ullmann's Encyclopedia of Industrial Chemistry, Wiley-VCH Verlag GmbH & Co. KGaA: Weinheim.
33. Vargas-Bernal, R., Herrera-Pérez, G., Calixto-Olalde, M., Tecpoyotl-Torres, M. (2013) Analysis of DC electrical conductivity models of carbon nanotube-polymer composites with potential application to nanometric electronic devices. J. Electr. Comput. Eng., 1-14.
34. Luginsland, H.-D., Niedermeier, W. (2003) Rubber World, 228, 34.
35. Fernandes, I.J., Santos, R.V., Santos, E.C.A., Rocha, T.L.A.C., Junior, N.S.D, Moraes, C.A.M. (2018) Replacement of commercial silica by rice husk as in epoxy composites: a comparative analysis. Material Research, 21, 1-10.
36. Haus, R., Prinz, S., Priess, C. (2012) Assessment of High Purity Quartz Resources. In: Götze J, Möckel R, eds. Quartz: Deposits, Mineralogy and Analytics. Berlin: Springer Geology. p. 29-51.

37. Bai, W., Li, K. (2009) Partial replacement of silica with microcrystalline cellulose in rubber composites. Composites: Part A, 40, 1597-1605.
38. French, A. D., Bertoniere, N. R., Brown, R. M., Chanzy, H., Gray, D., Hattori, K., Glasser, W. In Kirk-Othmer Encyclopedia of Chemical Technology 5th ed., Seidel, A., Ed., John Wiley & Sons, Inc.: New York, 2004, Vol. 5.
39. Moon, R.J., Martini, A., Nairn, J., Simonsen, J., Youngblood, J. (2011) Cellulose nanomaterials review: structure, properties and nanocomposites. Chem. Soc. Rev., 40, 3941-3994.
40. Ummartyotin, S., Manuspiya, H. (2015) A critical review on cellulose: from fundamental to an approach on sensor technology. Renewable and sustainable energy reviews, 41, 402-415.
41. Habibi, Y., Lucia, L.A., Rojas, O.J. (2010) Cellulose nanocrystals: chemistry, self-assembly and applications. Chem. Rev., 110, 3479-3500.
42. Kim, J.-H., Shim, B.S., Kim, H.S., Lee, Y.-J., Min, S.-K., Jang, D., Abas, Z., Kim, J. (2015) Review of nanocellulose for sustainable future materials. Int. J. Precision Eng., and Manufacturing-green Tech., 2, 197-213.
43. Amorim, J.D.P., Souza, K.C., Duarte, C.R., Duarte, I.S., Ribeiro, F.A.S., Silva, G.S., Farias, P.M.A., Stingl, A., Costa, A.F.S., Vinhas, G.M., Sarubbo, L.A. (2020) Plant and bacterial cellulose: production, properties and applications in medicine, food, cosmetics, electronics and engineering. A review. Env. Chem. Letters, 18, 851-869.
44. Rajinipriya, M., Nagalakshmaiah, M., Robert, M., Elkoun, S. (2018) Importance of agricultural and industrial waste in the field of nanocellulose and recent industrial developments of wood based nanocellulose: A review. ACS Sustainable Chem. Eng., 6, 2807-2828.
45. Chauhan, V.S., Chakrabarti, S.K. (2012) Use of nanotechnology for high performance cellulosic and papermaking products. Cellulose Chem. Tech., 46, 389-400.
46. Oksman, K., Aitomaki, Y., Mathew, A.P., Siqueira, G., Zhou, Q., Butylina, S., Tanpichai, S., Zhou, X., Hooshmand, S. (2016) Review of the recent developments in cellulose nanocomposite processing. Composites: Part A, 83, 2-18.
47. Mariano, M., El-Kissi, N., Dufresne, A. (2014) Cellulose nanocrystals and related nanocomposites: review of some properties and challenges. J. Polym Sci Part B: Polym Phys, 52, 791-806.
48. Lavoine, N., Desloges, I., Dufresne, A., Bras, J. (2012) Microfibrillated cellulose - its barrier properties and applications in cellulosic materials: a review. Carbohydrate polymer, 90, 735-764.

49. Klemm, D., Kramer, F., Moritz, S., Lindström, T., Ankerfors, M., Gray, D., Doris, A. (2011) Nanocelluloses: a new family of nature-based materials. Angew Chem Int Ed., 50, 5438-5466.
50. Jorfi, M., Foster, E.J. (2015) Recent advances in nanocellulose for biomedical applications. J Appl Polym Sci., 132, 41719/1-19.
51. Michelin, M., Gomes, D.G., Romani, A., Polizeli, M.L.T.M., Teixeira, J.A. (2020) Nanocellulose production: Exploring the enzymatic route and residues of pulp and paper industry. Molecules, 25, 3411.
52. Wang, T., Deng, L., Li, S., Tan, T. (2007) Structural characterization of a water-insoluble (1,3)-α-D-glucan isolated from the Penicillium chrysogenum. Carbohydrate Polymers, 67, 133-137.
53. Choma, A., Wiater, A., Komaniecka, I., Paduch, R., Pleszczyńska, M., & Szczodrak, J. (2013) Chemical characterization of a water insoluble (1 →3)-α-D-glucan from an alkaline extract of Aspergillus wentii. Carbohydrate Polymers, 91, 603-608.
54. Leal, J. A., Guerrero, C., Gómez-Miranda, B., Prieto, A., & Bernabé, M. (1992) Chemical and structural similarities in wall polysaccharides of some Penicillium, Eupenicillium and Aspergillus species. FEMS Microbiology Letters, 90, 165-168.
55. Grün, C.H. (2003) Structure and Biosynthesis of Fungal α-Glucans. Ph.D. Thesis, University of Utrecht, Utrecht, The Netherlands.
56. Wiater, A., Paduch, R., Pleszczynska, M., Próchniak, K., Choma, A., Kandefer-Szersze ´n, M., Szczodrak, J. (2011) α-(1→3)-d-Glucans from fruiting bodies of selected macromycetes fungi and the biological activity of their carboxymethylated products. Biotechnol. Lett., 33, 787-795.
57. Kiho, T., Yoshida, I., Nagai, K., Ukai, S., Hara, C. (1989) (1→3)-α-d-glucan from an alkaline extract of Agrocybe cylindracea, and antitumor activity of its O-(carboxymethylated) derivatives. Carbohydr. Res., 189, 273-279.
58. Zhang, L., Zhang, M., Chen, J., Zhang, F. (2001) Solution properties of antitumor carboxymethylated derivatives of α-(1→ 3)-d-Glucan from Ganoderma lucidum. J. Polym. Sci., 19, 283-289.
59. Loesche, W. J. (1986) Role of *Streptococcus mutans* in Human Dental Decay. J. Microbiol. Rev., 50, 353-380.
60. Monchois, V., Willemot, R. M., Monsan, P. (1999) Glucansucrases: mechanism of action and structure function relationships. FEMS Microbiol. Rev., 23, 131-151.

61. Puanglek, S., Kinura, S., Enomoto-Rogers, Y., Kabe, T., Yoshida, M., Wada, M., Iwata, T. (2016) *In vitro* synthesis of linear α-1,3-glucan and chemical modification to ester derivatives exhibiting outstanding thermal properties. Scientific report, 6, 30479.
62. Leemhuis, H., Pijning, T., Dobruchowska, J.M., Leeuwen, S.S., Kralj, S., Dijkstra, B.W., Dijkhuizen, L. (2013) Glucansucrases: Three-dimensional structures, reactions, mechanism, α-glucan analysis and their implications in biotechnology and food applications. J. Biotechnol., 163, 250-272.
63. Kobayashi, K., Hasegawa, T., Kusumi, R., Kimura, S., Yoshida, M., Sugiyama, J., Wada, M. (2017) Characterization of crystalline linear (1 → 3)-α-D-glucan synthesized in vitro. Carbohydrate Polymers, 177, 341-346.
64. Złotko, K., Wiater, A., Wasko, A., Pleszczynska, M., Paduch, R., Jaroszuk-Scisel, J., Bieganowski, A. (2019) A Report on Fungal (1→3)-α-d-Glucans: Properties, Functions and Application. Molecules, 24, 3972.
65. Kasat, R.B., Paullin, J.L. (2014) Preparation of poly alpha-1,3-glucan esters and films therefrom. WO Patent 2014/105698 A1.
66. Bitinis, B., Verdejo, R., Cassagnau, P., Lopez-Manchado, M.A. (2011) Structure and properties of polylactide/natural rubber blends. Mater Chem Phys., 129, 823-831.
67. Nunes, R.C.R (2017) Rubber nanocomposites with nanocellulose: in Thomas, S., Maria, H.J. (Eds.) Progress in rubber nanocomposites. Woodhead publishing, UK.
68. Pramanik, M., Srivastava, S.K., Samantaray, B., Bhowmick, A.K. (2003) Rubber_clay nanocomposite by solution blending. J. Appl. Polym. Sci., 87, 2216-20.
69. Abraham, E., Elbi, P.A., Deepa, B., Jyotishkumar, P., Pothen, L.A., Narine, S.S. (2012) X-ray diffraction and biodegradation analysis of green composites of natural rubber/nanocomposites. Polym. Degrad. Stab., 97, 2378-2387.
70. Thomas, S., Stephen, R. (2010) Rubber nanocomposites: preparation, properties and applications. John Wiley & Sons, Singapore.
71. Chen WJ, Gu J, Xu SH. (2014) Exploring nanocrystalline cellulose as a green alternative of carbon black in natural rubber/butadiene rubber/styrene-butadiene rubber blends. Express Polym. Lett., 8, 659-668.
72. Sarkawi, S. (2013) Nano-Reinforcement of Tire Rubbers: Silica-Technology for Natural Rubber. PhD. Thesis, Dept. of Elastomer Technology and Engineering, Univ. of Twente, Enschede, the Netherlands.

73. Arkles, B., Pan, Y., Larson, G.L., Berry, D.H. (2004) Cyclic azasilanes: volatile coupling agents for nanotechnology, In, Mittal, K.L. (Ed.) Silanes and other coupling agents. Vol 3, 179-191.
74. Hayichelaeh, C. (2018) Silica-reinforced natural rubber tire compounds with safe compounding ingredients. PhD thesis, University of Twente.
75. Eyley, S. Thielemans, W. (2014) Surface modification of cellulose nanocrystals. | Nanoscale, 6, 7764-7779.
76. Mostoni, S., Milana, P., Credico, D.B., D'Arienzo, M., Scotti, R. (2019) Zinc-based curing activators: new trends for reducing zinc content in rubber vulcanization process. Catalyst, 9, 664.
77. Lim, J., Yeap, S.P., Che, H.X., Low, S.C. (2013) Characterization of magnetic nanoparticle by dynamic light scattering. Nanoscale Res. Lett., 8, 381.
78. Beyene, D., Chae, M., Dai, J., Danumah, C., Tosto, F., Demesa, A.B., Bressler, D.C. (2018) Characterization of cellulase-treated fibers and resulting cellulose nanocrystals generated through acid hydrolysis. Materials, 11, 1272.
79. Boluk, Y., Danumah, C. (2014). Analysis of cellulose nanocrystals rod lengths by dynamic light scattering and electron microscopy. J. Nanopart Res, 16:2174.
80. Araki, J., Wada, M., Kuga, S., & Okano, T. (1998). Flow properties of microcrystalline cellulose suspension prepared by acid treatment of native cellulose. Colloids and Surfaces A: Physicochemical and Engineering Aspects, 142(1), 75-82.
81. Segal, L., Creely, J.J., Martin, A.E. Jr, Conrad, C.M. (1959). An empirical method for estimating the degree of crystallinity of native cellulose using the X-ray diffractometer. Text Res. J., 29,786-794.
82. Nam, S., French, A.D., Condon, B.D., Concha, M. (2016) Segal crystallinity index revisited by the simulation of X-ray diffraction patterns of cotton cellulose Iβ and cellulose II. Carbohydrate Polym., 135, 1-9.
83. Rongpipi, S., Ye, D., Gomez, E.D, Gomez, E.W. (2019) Progress and opportunities in the characterization of cellulose - An important regulator of cell wall growth and mechanics. Front. Plant Sci., 9, 1894.
84. Rambo, M.K.D., Ferreira, M.M.C. (2015) Determination of cellulose crystallinity of banana residues using near infrared spectroscopy and multivariate analysis. J. Braz. Chem. Soc., 26, 1491-1499.

85. Park, S., Baker, J.O., Himmel, M.E., Parilla, P.A., Johnson, D.K. (2010) Cellulose crystallinity index: measurement techniques and their impact on interpreting cellulase performance. Biotechnology for Biofuels, 3, 10.
86. Donnet, J.-H., Custodero, E. (2005) Reinforcement of elastomers by particulate fillers. In Mark, J.E., Erman, B., Eirich, F.R. (Eds.) The science and technology of rubber, 3rd ed. Elsevier academic press, UK.
87. Ouyang, G.B. (2006) Modulus, hysteresis and the Payne effect. J. construction and simulation, 332-343.

Chapter 3

CNC as a biofiller: optimizations of compounding conditions.

3.1 Introduction

There is a rise in discovery of more interesting properties of cellulose and it have continued to generate enormous research and reviews [1-3]. Some of these researches are targeted at tailoring CNC to different applications. It is obvious that the use of CNC is limited because of their hydrophilic nature. The presence of hydroxyl groups on the surface cast a hydrophilic character which makes it incompatible with widely used hydrophobic polymer matrixes. A possible solution is to functionalize the surface of the CNC (or the matrix) to promote compatibility. Besides the modification of cnc to extend its use, the cnc synthesis as well as composite preparation techniques are vital areas that contributes immensely to the applications of cellulose nanocrystals.

For the tire industry, silanes are heavily consumed as a simple and reliable means of functionalizing fillers for compatibility with polymers matrixes [4-6]. Silica is one of the dominant fillers for tire composite and has a similar surface chemistry with cellulose hence the attempt to use silanes to prepare CNC-natural rubber composites.

Previous work has been done by Danish *et al.* [7] on the preparation of CNC-natural rubber composites using silanes. A 30 phr of CNC co-precipitated with latex rubber was studied with different silanes and properties were compared to silica as a reference. This plausible work and others did not explore the optimization of the CNC-natural rubber preparation process such as the effect of compounding temperature, silanization time, amount of loaded silanes and stages for the addition of zinc oxide and other additives. The variation of these conditions could result in remarkable changes in the properties of the prepared compound. This chapter is therefore devoted to understanding the resulting properties from the variations in the processing conditions and to establish a mixing procedure that would be used subsequently.

To achieve this target, aliphatic and cyclic silanes were used as shown in figure 3.1. The aliphatic silanes are bifunctional, and their coupling reaction is different from the cyclic silanes. The cyclic aza

silanes are rather reactive and proceed by ring opening reaction by the cleavage of Si-N and Si-S bond within the silane structure. Subsequently, a hybrid material was prepared by varying the amount of silica and CNC in the NR composite using cyclic silane as the compatibilizing agent.

(a)

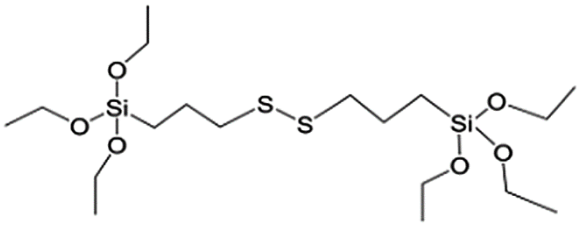

(b)

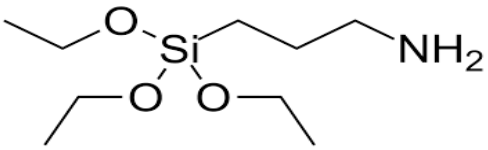

(c)

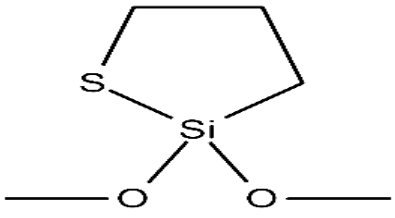

(d)

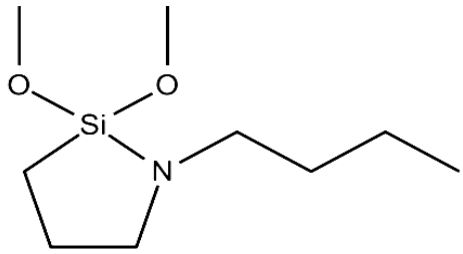

Figure 3.1 Aliphatic and cyclic silanes (a) bis(triethoxysilylpropyl)disulfide (TESPD), (b) (3-aminopropyl) triethoxysilane (APS), (c) 2,2-dimethoxy-1-thia-2-silacyclopentane (SID), (d) n-n-butyl-aza-2,2-dimethoxysilacyclopentane (SIB).

3.2 Experimental method

3.2.1 Materials

Cellulose nanocrystals suspension was purchased from Celluforce, Canada. Acetic acid, bis(triethoxysilylpropyl)tetrasulfide, (3-aminopropyl)triethoxysilane, were purchased from Sigma Aldrich. 2,2-dimethoxy-1-thia-2-silacyclopentane, N-n-butyl-aza-2,2-dimethoxysilacyclopentane were purchased from Geelest. Sulphur, stearic acid, zinc oxide, N-(1,3-dimethylbutyl)-N'-phenyl-p-phenylenediamine (6PPD), N-cyclohexyl-2-benzothiazylsulfenamide (CBS), 2,2,4-trimethyl-1,2-dihydroquinoline (TMQ) and natural rubber latex were provided by Pirelli. All materials were used as received.

3.2.2 Composites preparation

A masterbatch containing 30 phr of cellulose nanocrystals was prepared by weighing an appropriate amount of CNC suspension and mixed with latex rubber for 20 minutes until homogeneity. Acetic acid amounting up to 10 % v/v of the mixtures was measured and used to co-precipitate the mixtures by adding dropwise thereto with continuous stirring. The coagulated CNC-rubber was pressed, washed, and chopped in smaller pieces. Thereafter, it was soaked overnight and dried at 40^0C in a convection oven till constant weight (approximately 7 days). The dried CNC-NR compound was mixed with other ingredients in a brabender mixer and later characterized to understand the properties.

3.2.3 Characterization

The prepared composites were characterized by the following:

Dynamic mechanical properties: The dynamic mechanical properties of both cured and uncured CNC-NR compounds were performed using a Rubber Process Analyzer (RPA 2000, Alpha Technologies). Measurements of the strain sweep extending from 1 to 100% were conducted at 70^0C, 1Hz.

Tensile measurement: Tensile measurements were performed using a Zwick/Roell tensile testing machine. The test was performed according to ISO 37 and UNI 6065 standards. Green samples were vulcanized and cut into a dumbbell shaped specimens and tensile strength, stress at elongation of 10, 50, 100, 300 % and elongation at break properties were measured.

Vulcanization properties: The vulcanization kinetics of samples was studied using a moving die rheometer (RPA 2000, Alpha Technologies). The vulcanization of the samples was carried out at 150^0C, 30 minutes and rotor frequency of 1Hz. From the measurement, the minimum (M_H) and maximum torque (M_L), scorch time (T_S2) and optimum cure time (T_{90}) were determined.

3.3 Discussions and results

3.3.1 Aliphatic silanes

TESPD and APS were used as compatibilizing agents in CNC-NR composite, while silica reinforced compounds were prepared with TESPD and used as a reference. Silica-NR compound could be prepared with APS silanes but the functionalization does not promote filler-polymer compatibility during *in situ* functionalization in brabender internal mixers. Modifications of silica nanoparticles with APS are majorly successful when they are pre functionalized with APS before addition into polymer matrixes [8-10]. The CNC-NR compound was prepared by co-precipitation while silica-NR compound was prepared by melt mixing dry silica with coagulated rubber in brabender internal mixer and the effect of silanization time, temperature and amount of silanes are discussed below. The mixing recipe is shown in table 1.2 while the procedure was adopted [7] with addition of silanes amounting to 8% of the filler content.

Mixing stage	Time (min)	Temperature (0C)	Activity
Step 1	0	60	Load rubber and filler
	3		Add silanes
	8		Add stearic acid, zinc oxide
	10		Unload
Step 2	0	60	Load masterbatch from Step1
	1		Add sulfur, CBS, TMQ, 6PPD
	3		Unload

Table 3.1 Mixing procedure for silica and CNC compounds.

Ingredients	S-TESPD	CNC-TESPD	CNC-APS
Polymer/filler system			
Natural rubber	100		
Silica	30		
100PHR NR + 30PHR CNC		130	130
Compatibilizer			
TESPD	2.4	2.4	
APS			2.4
Vulcanization system			
Soluble sulfur	2	2	2
Zinc oxide	5	5	5
Stearic acid	2	2	2
CBS	2	2	2
Antioxidants/antiozonants			
TMQ	1	1	1
6PPD	1.5	1.5	1.5

Table 3.2 Mixing formulation for silica and CNC compounds

3.3.1.1 Silanization time

The various compounds were prepared and allowed to silanize from two to four minutes at 60^0C (Brabender temperature setting) and the effect on the vulcanization and dynamic mechanical properties were studied. From table 3.3, it is evident about the changes from two minutes to four minutes silanization time. There were moderate changes from the time increment, and it was more remarkable for APS functionalized compounds. The cnc compounds prepared with TESPD and APS showed better curing kinetics compared to the reference compounds (Silica-TESPD). The difference in the torque ΔM which corresponds to the crosslinking density was higher in CNC-APS and CNC-TESPD silanized compounds. For example, at 2 minutes silanization, cnc compounds prepared with TESPD and APS had 13.1 dNm and 16.73 dNm respectively compared with silica compound having a ΔM = 11.01 dNm. When the silanization time was increased to 4 minutes, the crosslinking density also increased as reflected in the increased values of ΔM. This is an indication that allowing more time for silanization could increase the crosslinking density.

Silica compounds are known to absorb curatives [11] and part of the curatives may be excluded or delayed from contributing to the curing process which is evident in the delayed curing and lower torque compared to CNC-NR compounds. TESPD silanized compounds also showed a delayed curing with optimum curing T_{90} both for silica and CNC having closely related values. The slow curing could

also be attributed to the size of TESPD molecule being large with networks providing steric hindrances. However, APS silanized compounds achieved an early optimum curing (T90). The increase in silanization time from two to four also promoted the ability of amine functionality to enhance the cure rate [12]. More so, the high crystallinity of CNC does not promote absorption of curatives hence curing kinetic were dictated by the structure of the silanes and other interactions within the polymer composites. The marginal improvement in the curing properties for four minutes silanization supports the adoption of four minutes as the silanization time.

Parameters		S-TESPD	CNC-TESPD	CNC-APS	S-TESPD	CNC-TESPD	CNC-APS
		2 min			4 min		
		Dynamic mechanical properties					
G'0 (kPa)	Unvulcanized	231.16	287.16	542.32	194.74	238.57	541.95
G'∞ (kPa)		117.71	82.40	117.59	88.84	77.48	105.45
Payne effect		**113.45**	**204.76**	**424.73**	**105.9**	**161.09**	**436.5**
G'0 (kPa)	Vulcanized	940.99	1111.33	1326.46	917.45	1175.17	1387.89
G'∞ (kPa)		657.98	707.82	891.52	629.81	717.70	910.75
Payne effect		**283.01**	**403.51**	**434.94**	**287.64**	**447.47**	**477.14**
Tan δ0		0.033	0.052	0.030	0.040	0.045	0.034
Tan δ∞		0.048	0.058	0.062	0.057	0.068	0.070
		Vulcanization characterisics					
Parameter		S-TESPD	CNC-TESPD	CNC-APS	S-TESPD	CNC-TESPD	CNC-APS
		2 min			4 min		
TS2 (min)		11.19	8.48	3.06	10.23	8.67	3.15
T90 (min)		17.51	14.33	5.58	15.84	14.39	5.93
CRI (min-1)		15.82	17.09	39.68	17.83	17.48	35.97
ML (dNm)		1.59	1.07	2.33	0.98	1.02	1.83
MH (dNm)		12.60	14.38	19.06	12.74	15.23	20.11
ΔM (dNm)		11.01	13.31	16.73	11.76	14.21	18.28

Table 3.3 Vulcanization and dynamic mechanical properties of silica and CNC compounds from 2 to 4 minutes silanization time at 60^0C.

The dynamic mechanical properties of both vulcanized and unvulcanized compounds showed a mixed trend. Most importantly are the values of the storage modulus G' which is a measure of the stored energy in the form of reinforcement. Contributions from the crystallinity and morphology of CNC coupled with the strain induced crystalline properties of natural rubber are considered vital in promoting reinforcements under dynamic deformations. In the green compounds (unvulcanized), there is a reduction in the storage modulus of all the compounds when the silanization time was increased from two minutes to four minutes. The possible explanation to this occurrence especially for cnc compounds is the fact that cnc particles are hydrophilic and have the tendency to aggregate even during compounding in matrixes. Therefore, increasing the silanization time during compounding could possibly allow some dispersed particle to form localised aggregates that will affect the storage modulus. When the compounds were vulcanized, there was no remarkable improvement in the storage modulus from two to four minutes. The APS compatibilized compounds were shown to have higher storage modulus compared to TESPD compatibilized compounds. The trends in APS compatibilized compounds showed that the silane structure promotes dispersion but compatibility between the filler and polymer was poor. During higher deformations it was easy to break down the filler networking alongside debonding the weak interaction of the filler and polymer within the matrix hence the higher Payne effect. From the vulcanization kinetics, there were higher crosslinking densities when silanization was increased to four, which resulted in a reduced chain mobility contributing to higher reinforcement at low strain. Accordingly, the increase in Payne effect shows that the dispersion and filler networking was good. However, the compatibility was not sufficient to create a resilient filler-polymer interaction that can withstand high deformations. The earlier postulation of localized aggregates when the silanization time is increased from two to four minutes could be connected to the high Payne effect as seen in the four minutes silanized compounds. The tangent delta as a measure of the damping properties of the compounds also increased marginally for all samples when the silanization time was increased. This could also be attributed to possible aggregates of fillers during longer processing that would create viscous regions without the presence of strong polymer-filler interactions. Also, the reduction of polymer molecular weight during mixing can be another factor. Although the concept of dispersion, filler-filler network, filler-polymer networking relating to the filler structure and chemistry need to be revisited for each filler type [13].

3.3.1.2 Compounding temperature/zinc oxide addition

From the section above, it was evident that a four minutes silanization time and processing at 60^0C (as Brabender setting) had an aspect of improved properties and gave sufficient time for compound preparation. However, it was observed that compounding at lower temperature could result in unreproducible compounds. The friction from the compounding process increases the real compound temperature with a temperature profile different from successive compounds, which could affect compound properties. After comparisons of compounds made at 60^0C and 130^0C, results (not presented) were relatively the same at both temperatures. The compounds made at 130^0C maintained a relatively the same temperature profile up to the end of the mixing process because of reduction and near constant viscosity. More so, the role of zinc oxide as a sulphur vulcanization activator was considered. It was understood that the complex it forms alongside stearic acid has the possibility of masking the surface of CNC when added with silanes. This led to formulation of a different mixing procedure by adding the zinc oxide in the second mixing stage to avoid interruption of the silanization process. Below is presented a new mixing procedure.

Mixing stage	Time (min)	Temperature (0C)	Activity
Step 1	0	130	Load rubber and filler
	2		Add silanes
	6		Add stearic acid
	7		Unload
Step 2	0	60	Load masterbatch from Step1
	1		Add sulfur, CBS, TMQ, 6PPD, zinc oxide
	3		Unload

Table 3.4 Mixing procedure for compounds at 4 minutes silanization and at 130^0C.

The vulcanizations as well as the dynamic mechanical properties were studied with compounds made from this procedure and presented in Table 3.5. The vulcanization characteristics showed a similar trend from the previously presented results (table 3.3). The cure rate index (CRI) and optimum curing time (T_{90}) increased remarkably for all compounds. The vulcanization also started early. APS silanized compounds were outstanding as all the vulcanization parameters showed a very fast curing, which could be critical for processability. It appears that the amine functionality in the silane structure contributed actively to the vulcanization process. This could be an indication for considering CNC compounds that would be functionalized with the incorporation of NH_2 groups to aid fast vulcanization. In general, the CNC structure and morphology also, do not self-assemble in a manner that would impede on the vulcanization process. Therefore, the vulcanization of CNC compounds is faster than silica compounds. There are suggestions that sulphuric acid derived CNC

(which are used in this work) with the available sulphate half esters could form a chemical network with zinc oxide that would facilitate the vulcanization process [14]. It also shows that processing the composites at higher temperature reduces the viscosity of the compound, which can facilitate an easy dispersion of filler particles. This has the tendency to reduce localised aggregations of CNC particles that could have negatively impacted on the crosslinking.

Parameters		S-TESPD	CNC-TESPD	CNC-APS
Dynamic mechanical properties				
G'0 (kPa)	Unvulcanized	201.72	357.67	629.3
G'∞ (kPa)		97.04	99.45	117.59
Paygne effect		**104.68**	**258.22**	**511.71**
G'0 (kPa)	Vulcanized	1075.58	1330.14	1230.46
G'∞ (kPa)		704.47	815.84	869.69
Paygne effect		**371.11**	**514.3**	**360.77**
Tan δ0		0.033	0.052	0.03
Tan δ∞		0.048	0.058	0.062
Vulcanization characterisics				
Parameter		**S-TESPD**	**CNC-TESPD**	**CNC-APS**
TS2 (min)		11.19	8.48	3.06
T90 (min)		17.51	14.33	5.58
CRI (min-1)		15.82	17.09	39.68
ML (dNm)		1.59	1.07	2.33
MH (dNm)		12.60	14.38	19.06
ΔM (dNm)		11.01	13.31	16.73

Table 3.5 Dynamic mechanical and vulcanization properties of rubber compounds at 130^0C compounding temperature.

The responses of the composites to dynamic deformations were compared among compounds using silica-reinforced compounds as a reference. The reinforcement of the green compounds prepared with APS was high compared with silica prepared TESPD. Both the vulcanized and unvulcanized

compounds of APS showed higher reinforcement, indicating good dispersion and higher crosslink density. The G' values of APS prepared compounds at 100% deformations were reasonably high also. Considering the fast vulcanization kinetics of the APS compounds, t_{90} is achieved at 3.32 minutes with reversion of the curing curve starting afterwards. Regardless of this occurrence, the properties of APS functionalized compounds have been remarkable. The CNC-TESPD compounds although similar with silica-TESPD is shown to have improved properties except for a higher hysteresis, which could be attributed to the higher storage modulus, probably because of strong filler-filler interactions and higher filler volume (equal weight of silica and Cellulose were employed). The reinforcement of CNC-TESPD compound were higher than the reference silica, this also correlated to the higher Payne effect and tangent delta, which are indications of filler network breakdown and lower filler-polymer interactions. It was evident that compounding at 130^0C partly reduces the problems of reproducibility of compounds as compounding and dumping temperatures remains relatively the same.

3.3.1.3 Percentages of silanes

Previously, compounds have been prepared by adding silanes amounting to 8% of filler content. That means, for a 30 phr of filler, a 2.4 phr of silanes were added. Considering the performance of some of the silanes, it was necessary to vary the amount of silanes from 12, 5 and 2% to understand if reduction or increase would bring remarkable properties.

Samples were prepared by adopting the mixing protocol of table 3.4 and compared with silica as a reference. The vulcanization properties of the various compounds are presented in table 3.6. The results for APS vulcanized compounds showed a trend that is usual of APS compatibilized composites. The increase of APS silane amount from 2% to 12% reduced immensely the scorch time and the optimum vulcanization time (T90) and increased the curing rate index (CRI) drastically. This shows that APS silanes acts as a secondary accelerator, with critical reduction of processability window. Although at 12%, the difference between the minimum and maximum torque reduced remarkably. This could be attributed to the beginning of curing already during mixing, as witnessed by the increase in ML, together with attainment of t_{100} earlier with an early reversion.

Parameter	S-TESPD	CNC-TESPD	CNC-APS	S-TESPD	CNC-TESPD	CNC-APS	S-TESPD	CNC-TESPD	CNC-APS
	2%			5%			12%		
TS2 (min)	9.00	7.22	4.63	9.72	7.58	2.62	9.26	7.42	1.29
T90 (min)	14.55	11.30	7.80	14.93	11.98	4.62	14.53	12.29	2.74
CRI (min-1)	18.02	24.51	31.55	19.19	22.73	50.00	18.98	20.53	68.97
ML (dNm)	2.10	1.75	2.32	2.03	1.73	3.18	1.59	1.92	4.13
MH (dNm)	12.96	18.56	22.64	13.17	18.88	22.45	14.14	17.99	18.17
ΔM (dNm)	10.86	16.81	20.32	11.14	17.15	19.27	12.55	16.07	14.04

Table 3.6 Vulcanization properties of silica and CNC compounds at different silane loading.

The TESPD compatibilized compounds of CNC and referenced silica shared similar trends with longer scorch time and optimum vulcanization time. Silica is generally known to absorb curatives and slowly releasing them, which makes the curing process slow. But in this scenario, the crystalline CNC which has not been known to have this behaviour, also behaves similarly. This could partly be attributed to the silane structures within the matrix. Perhaps there could be difficulty in hydrolysing the ethoxy groups with the unhydrolyzed species of TESPD impeding on the vulcanization kinetics. Ordinarily, only an effective hydrolysis could determine the effectiveness of the TESPD silanes, which may be difficult to ascertain. In fact, an in-situ silane functionalization cannot control the extent of silane hydrolysis. For CNC-TESPD compounds, beyond 5% silanes the vulcanization properties slightly reduced especially the ΔM and the curing rate index. This could be an indication that more TESPD silanes may not confer outstanding properties beyond 5%. Generally, it is evident that silanes perform better with CNC as filler compared to silica in natural rubber composite.

The observed mechanical response to deformations shows a trend and is presented in figure 3.1. The reinforcement of the filler particles showed a trend from lower silane amount to higher silane loadings. For all the CNC compounds, the storage modulus was higher than the reference silica compounds both at 1% and 100% deformations. Higher reinforcements as shown on the storage modulus G' were observed with APS silanized compounds, as expected from the higher crosslinking density.

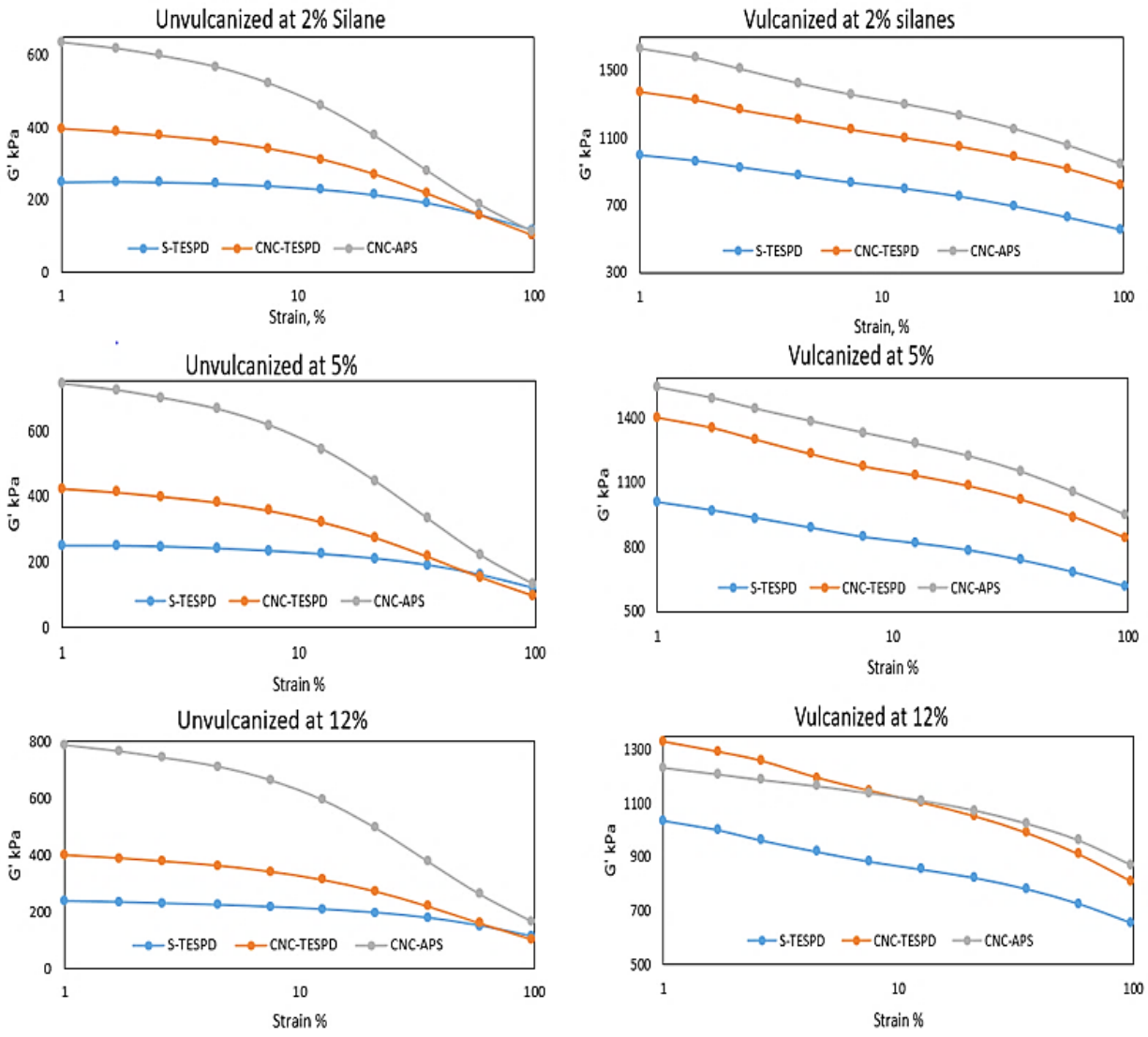

Figure 3.1 Storage modulus of silica and CNC compounds at different silane loading.

Although the modulus reduced with increasing silane content, the Payne effect (shown in table 3.7) also reduced showing an increase in filler-polymer interaction. This increase in filler-polymer interactions is also related to the filler dispersions as the storage modulus of unvulcanized APS silanized compounds were observed to have increased remarkably at low strain. The trends obtained for APS shows that the properties of the compounds are directly correlated to the amount of APS silane used. This gives the clue that APS is more reactive than TESPD with easier silane structures that relates to the amount of APS present. These trends of APS silanized compounds were also visible on the tangent delta. It was greatly reduced as the silane content was increased,. This is an indication of the increase in the elastic portions of the compounds, as expected in relation to higher crosslinking. However, this may not be obtainable for TESPD silanized compounds. There are

similar trends as the storage modulus of TESPD modified CNC are always higher than silica-TESPD compounds.

Payne effect	S-TESPD	CNC-TESPD	CNC-APS	S-TESPD	CNC-TESPD	CNC-APS	S-TESPD	CNC-TESPD	CNC-APS
		2%			5%			12%	
Unvulcanized	130.84	295.73	522.06	127.48	326.31	609.56	123.51	297.34	624.64
Vulcanized	442.75	552.15	690.57	389.93	562.6	595.18	379.46	518.83	362.07

Table 3.7 Payne effect of silica and CNC compounds at different silane loading

Tan delta	S-TESPD	CNC-TESPD	CNC-APS	S-TESPD	CNC-TESPD	CNC-APS	S-TESPD	CNC-TESPD	CNC-APS
		2%			5%			12%	
1%	0.047	0.05	0.052	0.037	0.048	0.042	0.039	0.046	0.037
100%	0.063	0.065	0.082	0.060	0.072	0.075	0.061	0.070	0.072

Table 3.8 Tangent delta of silica and CNC compounds at different silane loading.

Above 5% silane loading, the behaviour of TESPD modified compounds changes and there is no general trend. The two ethoxy groups on the TESPD molecules would require sufficient hydrolysis and the properties it impacts on the compounds would largely be dictated by it and not necessarily the amount of TESPD silane that was added.

3.3.1.4 Tensile properties

The tensile behaviour of APS and TESPD modified compounds were studied for compounds made at 130^0C, four minutes silanization and 8% silane loading. The results of these tensile mechanical properties are shown in table 3.9 with behaviours typical of the silane types. APS modified compound showed a different behaviour as the strain induced stress increased significantly. However, the strain increase did not proceed up to 300% MPa. The elongation at break also was low compared to the reference silica compound and subsequent CNC-TESPD compound. This is an indication of a very stiff material resulting from restrictions of its polymer chains. From physical observations, the material was overtly stiff compared to other compounds. The reductions in chain mobility resulting from filler-polymer interactions and contributions from vulcanization crosslinking may have made the APS silanized compounds relatively brittle.

Property	S-TESPD	CNC-TESPD	CNC-APS
Stress 10% [MPa]	0.38	0.68	0.71
Stress 50% [MPa]	1.08	2.57	3.30
Stress 100% [MPa]	1.91	5.54	7.76
Stress 300% [Mpa]	10.02	15.87	-
Elongation at break [%]	386.82	352.08	156.93
Tensile strenght [MPa]	16.22	17.90	12.32

Table 3.9 Tensile properties of silica and CNC compounds.

Brostow *et al.* [15] had developed a correlation to estimate the brittleness of polymer filled materials from the storage modulus and elongation at break as shown in equation 3.1.

$$B = 1/\varepsilon_0 G' \tag{3.1}$$

Where B is brittleness, ε_0 is elongation at break and G' is the storage modulus. Considering the storage moduli at 100% deformation for vulcanized compounds, estimated values of brittleness for APS compounds were significantly higher than silica and CNC-TESPD compounds. Although chemical composition and chain structure could give indication on the possible behaviour, the significance of elongation to brittleness has been explained [16]. The strain response of CNC-TESPD compounds compared with silica compounds also showed improved mechanical properties. CNC particles are crystalline and more reinforcing with higher restrictions on chain mobility. These tensile properties are indications for designs to maintain a trade-off on the amount of CNC and silanes to be loaded into the matrix to maintain good interactions while not tending towards brittleness. For the CNC-APS compounds not being able to be stressed up to 300%, it is suggestive that lower amount of silane may serve as an alternative means to reduce the brittleness.

3.3.2 Cyclic silanes

Cyclic silanes are new set of silanes that are explored to understand the compatibilization mechanism in filler-polymer composites. The usual alkoxy silanes undergo hydrolytic reaction to form bonding structures. Eventually, hydrolysis of the silanes is a critical step but for in situ composite preparation, it is difficult to control. Therefore, there are possibilities of insufficient

hydrolysis or self-polymerization of the compatibilizing silanes with bulk structures leading to low surface coupling. Considering the low energy bond of Si-N (355 kJ/mol) and Si-S (293 kJ/mol) compared with conventional silane bonds Si-O (452 kJ/mol) [17], there is a considerable driving force for the formation of a Si-O bond which promotes the reactivity of these cyclic silanes. The reaction also proceeds from ring opening because of loss of ring strain energy without requiring water as catalyst [18]. With these possible benefits, the cyclic silanes could be effective alternatives to conventional silanes.

Cyclic silanes have been studied with silica [19, 20] to functionalize the surface and it was used to understand how its high reactive nature would be beneficial in the preparation of CNC composites.

Compounds were prepared as described in section 3.2.2 while the mixing procedure is described in table 3.4. The various compounds were mixed in a brabender internal mixer with variation in the silane content amounting up to 12, 5 and 2 % silane content. Formulation recipe is presented below in table 3.10.

Ingredients	SSIB	CSIB
Polymer/filler system		
Natural rubber	100	
Silica	30	
100PHR NR + 30PHR CNC		130
Compatibilizer		
SIB	3.6, 1.5, 0.6	3.6, 1.5, 0.6
Vulcanization system		
Soluble sulfur	2	2
Zinc oxide	5	5
Stearic acid	2	2
CBS	2	2
Antioxidants/antiozonants		
TMQ	1	1
6PPD	1.5	1.5

Table 3.10 Formulation recipe for silica-cyclic silane compounds (SSIB) and CNC-cyclic silane compounds (CSIB).

3.3.2.1 N-n-butyl-aza-2,2-dimethoxysilacyclopentane (SIB)

- **Vulcanization**

The SIB silane has a Si-N bond in the ring and was used to prepare CNC and silica compounds at various silane loadings. The vulcanization kinetics, dynamic mechanical and tensile measurements were studied. In table 3.11 is shown the vulcanization behaviour of the various compounds.

The trends of the vulcanization for CNC are very similar with silica compounds. It was observed that the vulcanization starts early and achieves early curing with increasing silane content. However, the torque ΔM corresponding to the crosslinking density increased with reducing silane content. The same was observed for silica compounds. This could imply a silane-silane interaction when added in large amount that would impede a better networking. Although the matrix could be flooded with silanes which leads to early optimum vulcanization and higher curing index probably because of short distances within the silane molecules, the networking of the silanes could pose another problem. It was observabed that increasing the amount of silane for all the compounds reduces the scorch time at the start of the vulcanization and increases the cure rate index. However, a higher crosslinking density is not necessarily achieved. The curing kinetics therefore revealed that it is advantageous to use lower amount of silanes to achieve higher crosslinking density. Although there may be a little delay at achieving optimum curing T90, a higher crosslinking is achieved.

Parameters	CSIB12	CSIB5	CSIB2	SSIB12	SSIB5	SSIB2
TS2 (min)	1.26	2.26	3.66	1.52	3.48	4.95
T90 (min)	3.16	4.28	6.3	3.06	6.11	8.33
CRI (min-1)	52.63	49.51	37.88	64.94	38.02	29.59
ML (dNm)	2.39	1.89	1.86	1.29	1.43	1.85
MH (dNm)	15.43	18.42	18.69	12.46	13.94	14.23
ΔM (dNm)	13.04	16.53	16.83	11.17	12.51	12.38

Table 3.11 vulcanization kinetics of SIB compatibilized compounds. CSIB: CNC compounds; SSIB: silica compound; 12, 5, 2 correspond to the percentage of silanes.

With the trend observed with the SIB silanes, optimum curing is achieved very early, and a longer curing could compromise the integrity of the crosslinking network. Silica in general is known to frequently absorbing curatives thereby leading to a delay curing. However, with this silane, the optimum curing time T_{90} was also achieved very early. Reversion also started afterwards for all

compounds which would have affected the properties of the composite. For improve and fast curing of silica filler particles, this silane has shown to be a promising agent.

- **Dynamic mechanical analysis**

The dynamic mechanical properties were studied to understand the reinforcing mechanism provided by the SIB silane in both silica and CNC compounds. In figure 3.2 is shown the storage modulus of the different compounds from 1% to 100% strain.

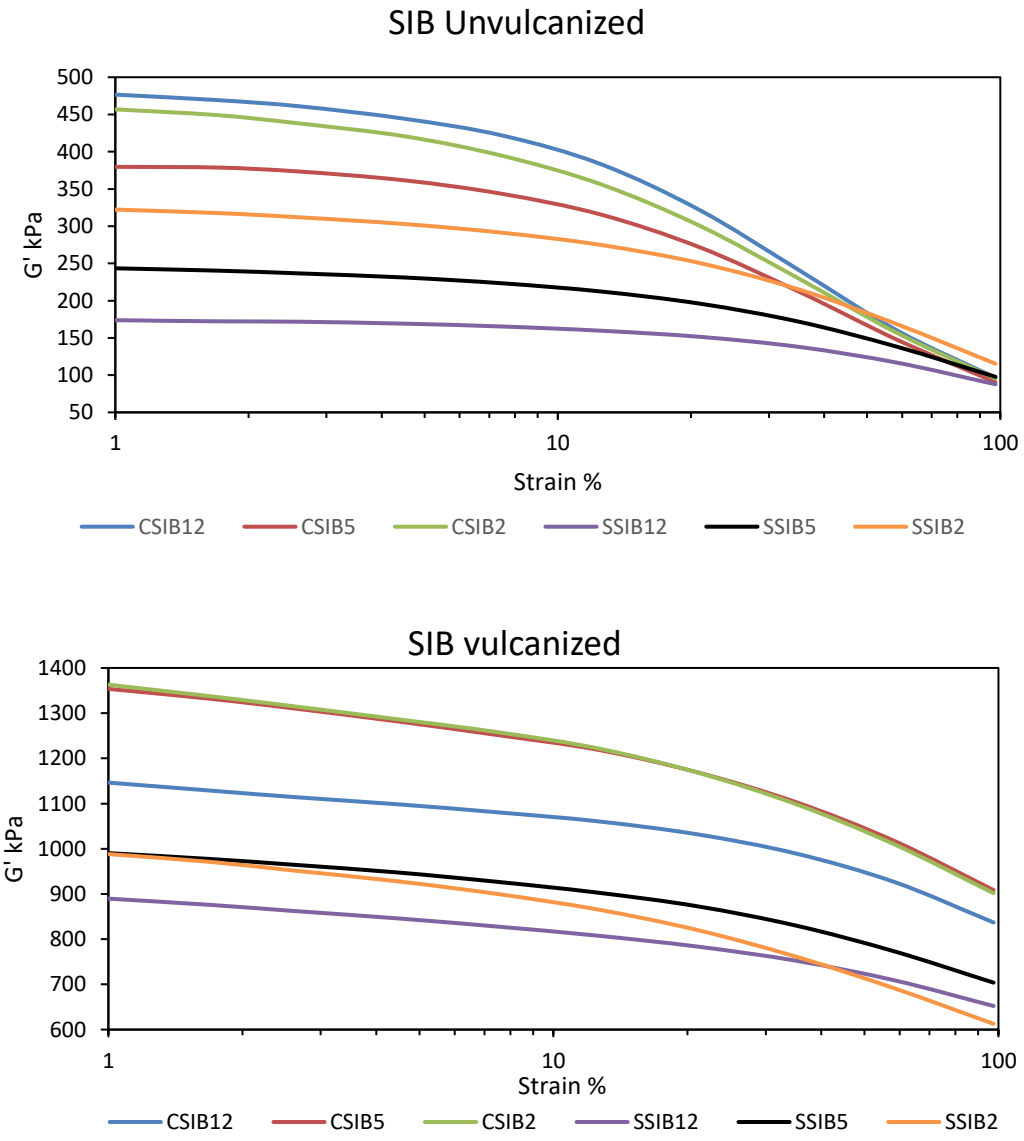

Figure 3.2 Storage moduli as a function of strain for unvulcanized and vulcanized SIB silanize compounds. CSIB and SSIB corresponds to CNC and silica compounds while 12, 5, 2 corresponds to silane percentages.

The viscoelastic properties of the various compounds show that the properties of CNC compounds were improved better than silica compounds. This also alludes to the easy dispersion of rod-like particles compared to spherical silica particles. At low strain, the storage modulus of CNC compound in the green state prepared with 12% silanes was remarkably high and closely followed by CNC compound prepared with 2% silane. This implies that irrespective of the amount of silanes added, a good processing of the compounds can effectively promote dispersion and reinforcement. In fact, it is visible that lower amount of silanes could play the same role as large amount of silanes. The silica compounds attest to this. At low silane loading the dispersion and reinforcement improved as shown in the green compounds. When the compounds were vulcanized, the trend also continued. The storage modulus G' of compound with the least amount of silanes was remarkably high at low strain and it follows that order up to the highest amount of silane. There is the possibility that a higher amount of SIB silane may end up providing structures that could lead to steric hindrance to the coupling reaction because of possible dense networking created in the matrix. Although the cyclic silanes are very promising, a full reaction mechanism has not been developed. However, it is evident that this silane can effectively promote dispersion in CNC compound especially at lower silane loading.

Payne effect	CSIB12	CSIB5	CSIB2	SSIB12	SSIB5	SSIB2
Unvulcanized	380.12	289.22	361.29	86.07	145.67	206.92
Vulcanized	309.36	445.01	461.23	237.50	286.48	375.53

Table 3.12 Payne effects of cellulose compounds prepared with SIB silane (CSIB) and silica compounds prepared with SIB silane (SSIB) at different silane loading.

At high strain, it is not uncommon to have a corresponding higher Payne effect and this was observed as shown in table 3.12. With lower silane loading, the Payne effect increased accordingly especially for the vulcanized compounds. This is evident when compared with the reference silica compounds. As part of interpretations leading to this, it is plausible to consider the effect of the silanes as playing more of a dispersive role than coupling role. That is why at lower silane loading, the effectiveness of the silanes is lower leading to a higher Payne effect because of possible poor dispersions. Although they are reactive, the interaction between the polymer and filler may not be effective compared to the prevailing filler networking. It is important to note that comparing CNC compounds with reference silica does not necessarily make the results of the CNC compounds very

outstanding especially as they are of different morphology, and reinforcement mechanism is also different. But in this case, a rather more holistic expectations of far-reaching interesting properties are expected. Besides this, the behaviour of the tangent delta over a range of strain amplitude alludes to the results of the Payne effect. At low silane loading the tangent delta values increased for the CNC compounds and the silica compounds as shown in figure 3.3.

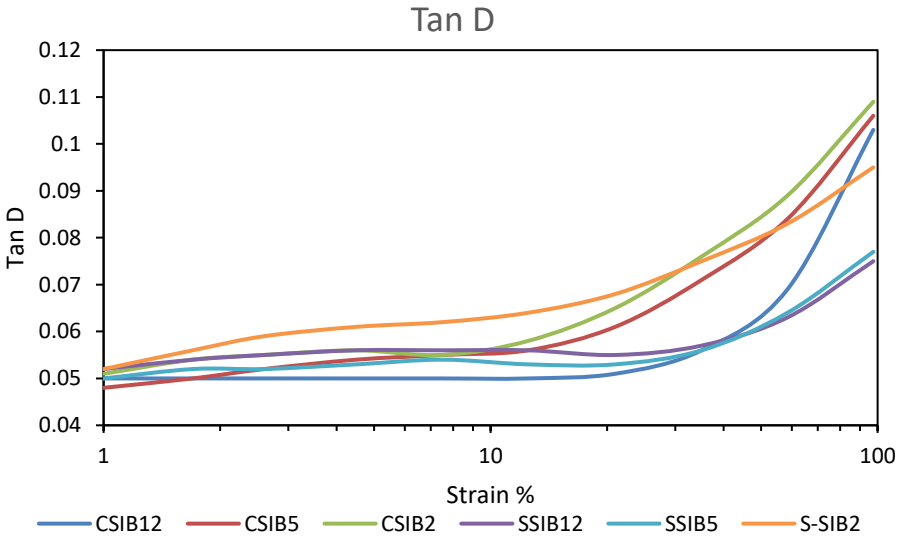

Figure 3.3 Tangent delta of vulcanized cnc compounds prepared with SIB silane (CSIB) and silica compounds prepared with SIB silane (SSIB) at different silane loading.

It is revealing that at high strain the progressive filler network breakdown resulting in the possible debonding of polymer chains increased the viscous portions of the compounds leading to a higher tangent delta. Irrespective of the variation in silane content, the difference in tangent delta values were not remarkably different for CNC compounds. In this scenario, different silane loading merely play negligible role in the tangent delta values.

- **Tensile properties**

The tensile properties of the various CNC compounds were conducted and compared with reference silica compound and results presented in table 3.13. The stress strain behaviour of the material under static applied strain is a combination of the filler type and the role played by the silanes. As could be seen at high silane loading the tensile properties gradually deteriorated and eventually improved at lower silane loading. For CNC compounds, addition of the silanes up to 12% resulted in a near brittle material that could not be strain up to 300%. Physical observation confirmed the stiffness of these materials when these silanes were added in large amount. In table 3.10, especially

for CNC compounds, it could be seen that reducing the amount of silanes reduced the minimum torque M_L. This is an indication that adding large amount of silanes could initiate pre mature vulcanization during compounding. Also, it could be that the silanes are very reactive and primarily increases crosslinking that results into a strong coupling between filler and polymer matrix [21]. Other factors such as possible self-condensation of the reactive silane which could form glassy structures will interfere with filler-polymer interactions and form rigid interface on the polymer chains. This would restrict mobility of the polymer chains and lead to deterioration in tensile properties. A good trade-off is maintaining silane loading below 5% percent.

Property	CSIB12	CSIB5	CSIB2	SSIB12	SSIB5	SSIB2
Stress 10% [MPa]	0.54	0.53	0.56	0.33	0.37	0.36
Stress 50% [MPa]	2.06	2.32	2.05	1.00	0.97	0.88
Stress 100% [MPa]	4.63	4.84	4.28	1.93	1.61	1.35
Stress 300% [Mpa]	-	13.89	12.56	9.60	6.65	5.19
Elongation at break [%]	386.82	369.21	387.89	364.03	513.67	578.54
Tensile strenght [MPa]	6.32	17.76	17.47	13.90	19.67	21.36

Table 3.13 Tensile properties of CNC compounds made with SIB silanes (CSIB) and silica compounds (SSIB) alongside different amount of silanes 12, 5, 2%.

In terms of the tensile strength, the silica compounds showed better properties compared to CNC compounds. Also, more elongation is observed for silica compounds at lower silane loading. However, the tensile properties at 300% strain makes CNC compounds more outstanding. In fact, for tire compounds, a 300% strain is one of important parameter that gives an insight about real application possibilities and the CNC compounds possessed better properties in this aspect. In general, the tensile properties suggest that SIB silane loading beyond 5% for CNC compounds may compromise the tensile properties of the compounds.

3.3.2.2 2,2-dimethoxy-1-thia-2-silacyclopentane (SID)

In the previous section, the role played by the SIB silanes was explored. Here, the SID silane was also studied to understand the properties possessed by compounds made with it. The formulation recipe is presented in table 3.14 while mixing procedure has been outlined in table 3.4.

Ingredients	SSID	CSID
Polymer/filler system		
Natural rubber	100	
Silica	30	
100PHR NR + 30PHR CNC		130
Compatibilizer		
SIB	3.6, 1.5, 0.6	3.6, 1.5, 0.6
Vulcanization system		
Soluble sulfur	2	2
Zinc oxide	5	5
Stearic acid	2	2
CBS	2	2
Antioxidants/antiozonants		
TMQ	1	1
6PPD	1.5	1.5

Table 3.14 Formulation recipe of silica-cyclic silane compounds (SSID) and CNC-cyclic silane compounds at different silane loading

- **Vulcanization properties**

CNC compounds compatibilized with different amount of SID silane were cured at 150^{0}C and at 30 minutes and compared with silica compounds as reference and results are reflected in table 3.15. There is a relative trend in the vulcanization characteristics with silane loading of 5 and 2% always having very close vulcanization properties. For the CNC compounds, the scorch time increased with reduced silane content. This was also observed for silica compounds. The optimum curing time which was considered as when 90% of the entire vulcanization was achieved also increased when the silane content was reduced. This is an indication that low silane content was able to provide networks that facilitates the sulphur crosslinking, probably due to the presence of S-H functionality after reaction with filler surface.

Parameters	CSID12	CSID5	CSID2	SSID12	SSID5	SSID2
TS2 (min)	1.21	1.67	3.47	1.41	5.85	6.54
T90 (min)	2.75	3.45	6.23	5.18	9.67	10.49
CRI (min-1)	64.94	56.18	36.23	26.53	26.18	25.32
ML (dNm)	4.44	2.19	1.71	2.01	2.05	2.06
MH (dNm)	16.49	17.99	18.51	12.04	13.36	13.18
ΔM (dNm)	12.05	15.8	16.8	10.03	11.31	11.12

Table 3.15 Vulcanization properties of CNC compounds (CSID) compared with referenced silica compounds (SSID) at different silane loadings 12, 5, 2%.

The vulcanization kinetics of the CNC compounds were relatively fast compared to the silica compounds and the curative absorptive nature of silica could still be attributed to this. While the silica would have absorbed some curatives even at different silane loading, the cure rate index, minimum torque, and maximum torque were relatively the same for silica compounds. To an extent, higher crosslinking that corresponds to higher torque was achieved at lower silane loading for silica compounds. It is rational to assume that large amount of the reactive silanes can self-condense and form dense structures that can restrict the already absorbed curatives from being released by silica particles during the curing process. Therefore, lower silane loading could be a better bargain. On the CNC compounds, reducing the silane content also increased the crosslinking density. In actual sense, the stiffness of the material was overtly higher when low amount of silanes were added, and it is therefore beneficial to process the various compounds with lower silane loading. In comparison, the CNC compounds achieved higher crosslinking density compared to the silica compounds. The reversion after the maximum torque was achieved very early. At about 10 minutes of the vulcanization process, all the CNC compounds were cured and the possibility of compromising the crosslinking network will dictate that the curing process be not extended far beyond the 10 minutes.

- **Dynamic mechanical analysis**

After the curing process, CNC and silica compounds were subjected to different strain amplitude and the viscoelastic behaviour of the various compounds are presented in figure 3.4. The storage

modulus G' of CNC compounds at low strain were reasonably high at high silane loading for unvulcanized compounds. It followed that order even for silica compounds. At 12 percent silane loading, the dispersion of the filler was remarkable. Although at high strain, the filler network is broken down and storage modulus is remarkably decreased. For unvulcanized compound, it is usual, and the storage modulus is only indicative of the dispersion and filler-filler interaction. Filler-polymer interaction at the unvulcanized state is dictated by physical interaction.

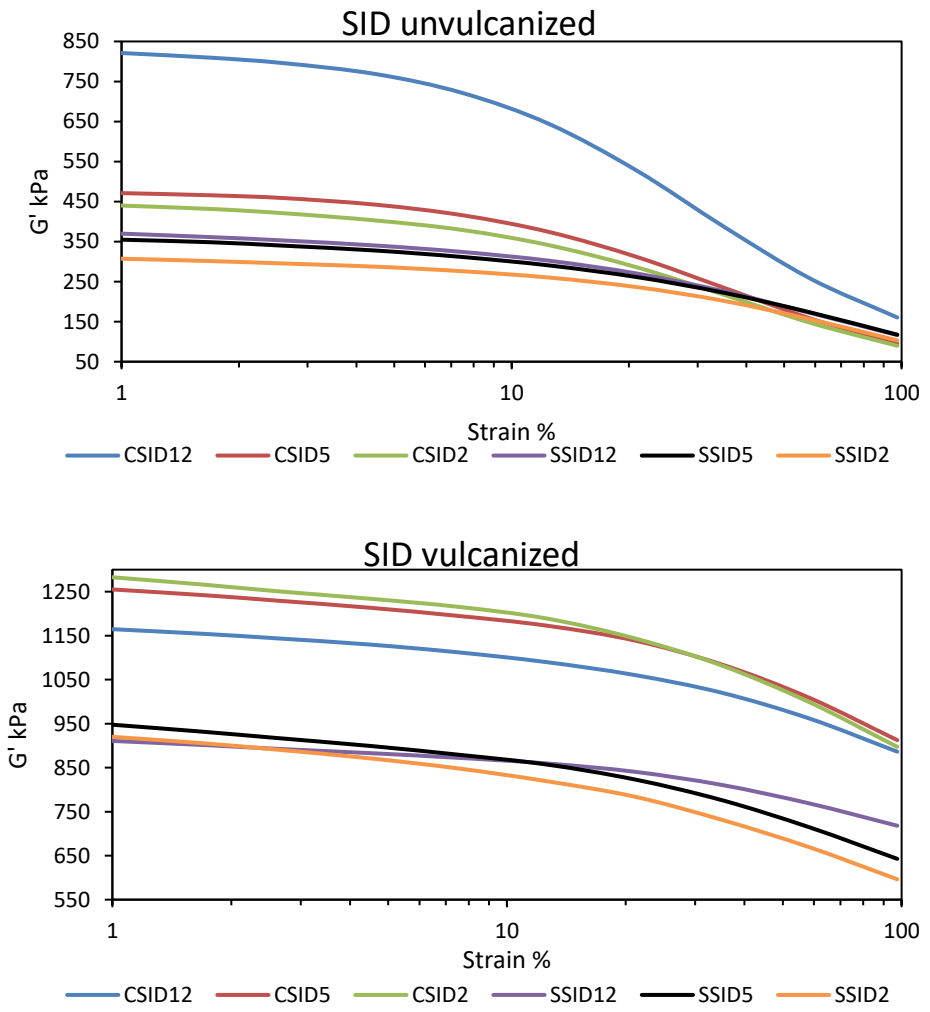

Figure 3.4 Storage moduli versus strain of CNC compounds (CSID) and silica compounds (SSID) at different silane loadings 12, 5, 2%.

However, when the various compounds were vulcanized, a different trend dominated. In this time, higher storage modulus was recorded at low strain for the CNC compounds with the lowest silane content. As explained earlier, the possibility of large amount of silanes self-condensing to form structures that interfere with the crosslinking process is observed with the SID silanes accordingly.

This in essence can disrupt the filler-filler networking which in the vulcanizates reduced the storage modulus when compared to lower silane loading.

Although, the Payne effect eventually increased when the silanes were reduced in the vulcanized compounds, it is not uncommon especially when compounds have higher storage modulus.

Payne effect	CSID12	CSID5	CSID2	SSID12	SSID5	SSID2
Unvulcanized	661.56	376.13	350.27	253.57	237.27	204.12
Vulcanized	278.41	342.45	385.46	192.78	304.82	323.67

Table 3.16 Payne effect of vulcanized and unvulcanized CNC compounds (CSID) and silica compounds (SSID) at 12, 5, and 2% silane loading.

This is due to strain amplification and the effective networking of the filler in polymer matrix which at higher deformations, leads to filler network breakdown. Alternatively, we can also attribute this Payne effect to a lower filler-polymer interaction, but the concept of occluded rubber is a model that reasonably offers a good insight. Here, we can visualize a filler networking at lower silane loadings forming effective filler-filler networks that can exclude some rubber molecules (occluded rubber) and in doing so, the filler volume fraction increases. At high strain, the strain amplification is so remarkable because of the short inter aggregate distance and reduced matrix content. The possible exclusion of a part of the polymer matrix in the composite (supposedly from occluded rubber) would eventually lead to reduced filler-polymer interaction. This concept could be more pronounced for cellulose nanocrystals. The rod-like morphology can form a loosely packed network with possible internal cavities large enough to accommodate large polymer compounds in the occluded region. As shown in figure 3.5, the tangent delta curves attest to this. At lower silane loading, the tangent delta values were reasonably higher for CNC and silica compounds. The higher storage modulus was interesting at low strain for CNC compounds which was indicative of good filler-filler networking. However, the structural formation leading to occluded rubbers could have created huge viscous portions of the polymer that are excluded from forming a continuous matrix phase. In essence, it may not effectively participate as the continuous phase while also not rigid enough to behave like a reinforcing filler. Higher tangent delta values are indicative of the poor interactions with the clue that the viscous portions are higher for the lower silane loading.

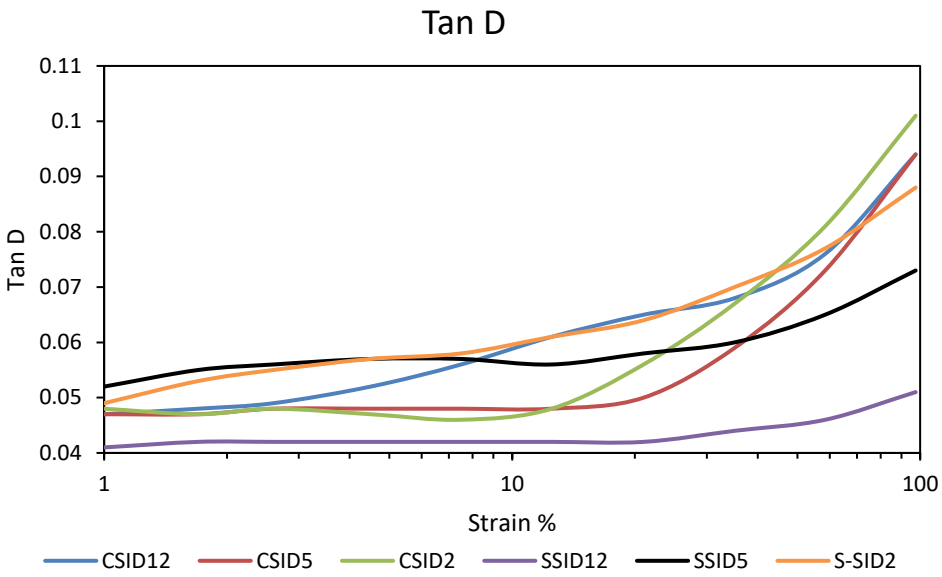

Figure 3.5 Tangent delta curves of vulcanized CNC compounds (CSID) and silica compounds (SSID) at 12, 5, 2% silane loading.

Silica compounds by far were considered to have relatively lower tan D values at higher strains. In essence better interactions took place for silica compounds. The explanation about the structural formation excluding a large portion of the matrix from filler-polymer interactions could be confirmed with the silica particle morphology forming a rather different structure that may not remarkably promote occluded rubber. Silica is spherical and quite different from the rod-like structure of CNC particles. The experience with the cyclic silanes shows that higher silane loading does not necessarily results to remarkable improvement in properties. Even for the tan D of CNC compounds, the 12 and 5% silane loading behave typically the same and increment in the silane content beyond 5% does not result to much desired properties.

- **Tensile properties**

The variations in the silane content showed that the cyclic silanes were promising and at higher silane loading, remarkable dynamic properties were not recorded. It was also important to understand the resulting properties under static strain loadings. The tensile properties of both silica and CNC compounds are shown in table 3.17.

Property	CSID12	CSID5	CSID2	SSID12	SSID5	SSID2
Stress 10% [MPa]	0.40	0.61	0.55	0.45	0.36	0.37
Stress 50% [MPa]	1.20	2.53	2.04	1.68	0.95	0.92
Stress 100% [MPa]	2.64	5.84	4.40	3.77	1.54	1.50
Stress 300% [Mpa]	-	-	13.09	-	6.76	7.10
Elongation at break [%]	225.19	235.47	348.47	114.98	533.4	519.44
Tensile strenght [MPa]	8.43	13.98	15.14	4.29	21.73	20.41

Table 3.17 Tensile properties of CNC compounds (CSID) and silica compounds (SSID) made with SID silanes at 12, 5, 2% silane loading.

The tensile properties for CNC compounds were observed to have improved at lower silane loadings. At 5 and 12%, the material became stiff and was unable to be strained up to 300%. Comparable to that of silica, the tensile properties were better than CNC compounds. However, at 12% silane loading, the tensile properties of silica compounds deteriorated. Most times, the tensile properties of a poorly processed compound could deteriorate. This drawback was given attention and compounds properly processed. But for the consistency in deteriorated tensile properties of compounds at higher silane loading alludes to the fact that poor properties was not due to a poorly processed compound but from the large amount of cyclic silanes which may not provide good benefits to the various compounds.

3.3.3 Cyclic silane in CNC/silica hybrid

Silica fillers have been known to confer good properties to tire compounds. The lower hysteresis as well as lower rolling resistance is considered an appropriate edge over carbon black. Some of these properties could be associated with the filler morphology, particle sizes and surface chemistry of which silica is unique. Ordinarily, particle sizes at much lower nano meter range are good medium to judge the reinforcement of a compound. But silica, despite meeting this criterion do not confer reasonable reinforcement when compared to cellulose nanocrystals. For CNC, the rod-like morphology with high aspect ratio is one of the major contributions to reinforcement in CNC compounds. In all, both fillers share the same surface chemistry with abundant hydroxyl groups on the surface. The combination of these fillers in a rather hybrid system could bring the different properties of the filler to the new composite.

To actualize this, CNC compounds were coagulated with natural rubber as described earlier in this work. The dried coagulated CNC/natural rubber compounds were mixed in a brabender mixer with the right amount of silica filler and SID silanes at 8% of filler content as shown in table 3.16. The amount of fillers used were varied by starting with a 30 phr silica compound (S30C0) and progressively reducing to 25 phr of silica with a 5 phr of cellulose (S25C5), a 20 phr of silica and a 10 phr of cellulose (S20C10). The compounds were varied until a CNC compound prepared without silica (S0C30). Subsequently, the compounds were characterized to understand their properties.

The mixing procedure was adopted in table 3.4 and applied to all the hybrid compounds.

- **Vulcanization properties**

The various hybrid compounds were cured at 150^0C and at 30 minutes and the resulting vulcanization parameters are presented in table 3.19. In the start of the vulcanization, the scorch time for all the hybrid compounds were relatively the same. At this point, the contributions of the inherent filler morphologies were negligible. Recall that in table 3.15, the scorch time when the SID silanes were used for silica and CNC compounds, similar values were recorded especially when the amount of silane were beyond 5%.

ingredients	S30C0	S25C5	S20C10	S15C15	S10C20	S5C25	S0C30
polymer/filler system							
NR	100.0						
100PHR NR + 30PHR CNC		105.0	110.0	115.0	120	125	130.0
Silica (U. 7000)	30.0	25.0	20.0	15.0	10	5	
compatibilizer							
SID	2.4	2.4	2.4	2.4	2.4	2.4	2.4
vulcanization system							
Zinc oxide	5.0	5.0	5.0	5.0	5.0	5.0	5.0
Stearic acid	2.0	2.0	2.0	2.0	2.0	2.0	2.0
Sulfur	2.0	2.0	2.0	2.0	2.0	2.0	2.0
CBS	2.0	2.0	2.0	2.0	2.0	2.0	2.0
antioxidant/antiozonants							
TMQ	1.0	1.0	1.0	1.0	1.0	1.0	1.0
6PPDS	2.0	1.5	1.5	1.5	1.5	1.5	1.5

Table 3.18 Mixing formulation for CNC/silica hybrid compounds. S corresponds to silica, C corresponds to cellulose, with their various amounts in PHR.

Parameters	S30C0	S25C5	S20C10	S15C15	S10C20	S5C25	S0C30
TS2 (min)	1.29	1.23	1.1	1.08	1.11	1.12	1.09
T90 (min)	3.34	3.3	3.08	3.02	2.89	3.03	2.87
CRI (min-1)	48.78	48.31	50.51	51.55	56.18	52.36	56.18
ML (dNm)	1.9	2.46	1.68	1.92	2.27	3.67	3.08
MH (dNm)	11.12	10.68	11.74	13.7	15.91	15.22	18.04
ΔM (dNm)	9.22	8.22	10.06	11.78	13.64	11.55	14.96

Table 3.19 Vulcanization properties of hybrid compounds.

Comparing the amount of silane used in the hybrid (8%), properties tends to be similar. The optimum curing time T90 among all compounds showed no remarkable difference. Ordinarily, it would be expected that when the amount of silica and CNC were varied in the compound, the curing process would show a trend. However, there is no remarkable trend. Most importantly is the observation that the optimum curing time was reached early even when silica was the only filler used in the compound. The role played by the silane to promote an early vulcanization is evident and could not be attributed to any other factor. Cyclic silanes are very reactive and the structures they form within the matrix are associated with a higher curing index as shown in table 3.19. Although a much higher curing index was observed when there was an increase in the added CNC, there was also a corresponding increase in torque when the CNC filler was increased. At a CNC content of 15 phr, up to a 30 phr, the vulcanization kinetics seemed closely related. At this point, it is possible to allude that higher crosslinking was achieved when the CNC content was increased.

- **Dynamic mechanical properties**

The strain dependent viscoelastic properties of the various hybrid compounds are shown below in figure 3.7. In the unvulcanized compounds, the compounds with an increasing CNC amount tend to show a higher storage modulus at lower strain. Ordinarily, CNC rod-like particles are easily dispersible more than the spherical shaped particles of silica. Usually at high strain, the filler network is broken down and dispersion is useful at the green state. The reinforcement in form of storage modulus is another vital factore and the compounds with lower storage modulus were those of filler content having a 20/10 and 15/15 phr of silica and CNC fillers. At this hybrid composition, a specific morphology distribution may find it difficult to dominate and dispersion could encounter some drawbacks. Although the SID silanes are reactive and are effective is enhancing filler dispersion, it

was not witness with these hybrid compounds. When the various compounds were vulcanized, the resultant behaviour changed. At this point, a trend seemed to appear. The storage modulus seemed to be higher with the CNC content and lower with silica content. It comes to reveal that the filler networking was not homogeneous and perhaps it may not be proper to term the system a hybrid as both filler morphologies prevail according to their content. It is important to note that the storage modulus of the compound made with only silica (during the hybrid preparation) do not compare to the properties of the silica compound prepared previously at various amount of silane loading. This may be attributed to the degradation of the silane because of likely poor storage conditions. With the compounds having higher CNC content, at 8% silane loading, the possible degradation of the silanes because of storage conditions could make the effective silane content to be lower. This would make the behaviour of the compound to be similar with compounds prepared at lower silane loading.

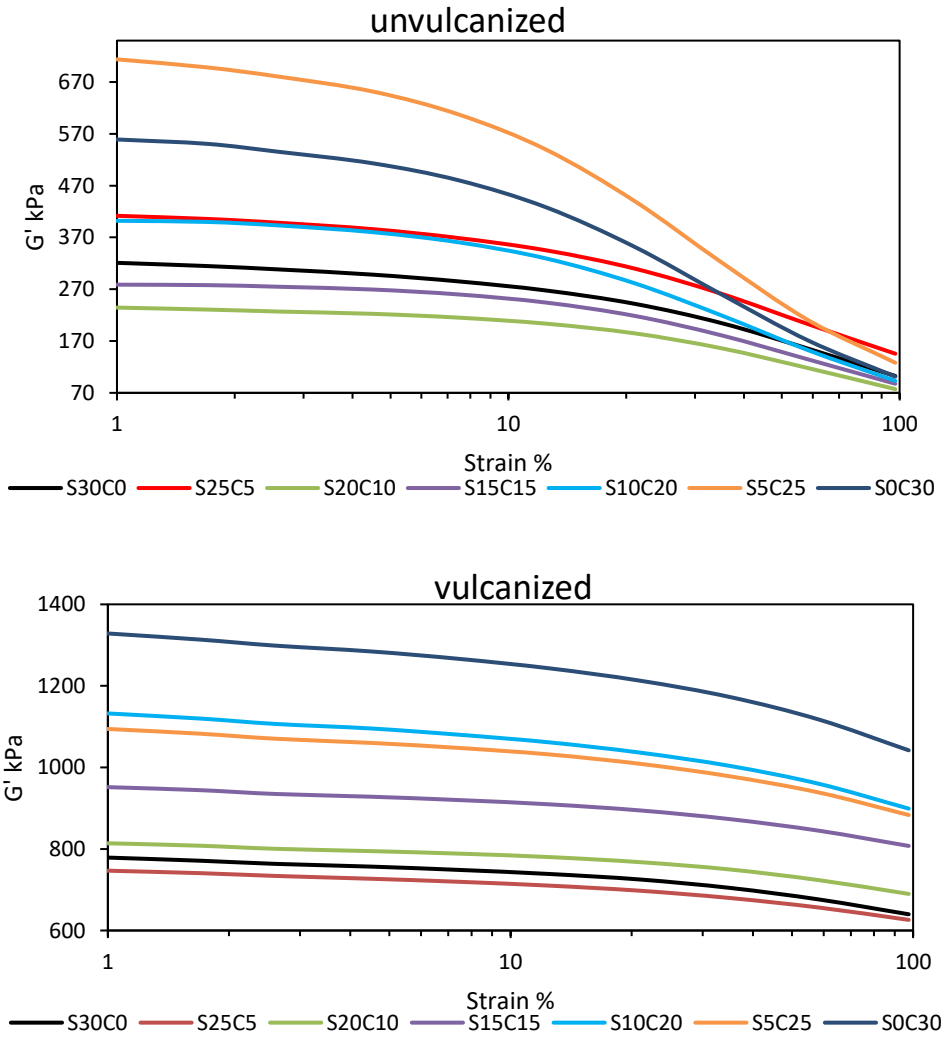

Figure 3.7 Storage modulus versus strain for unvulcanized and vulcanized hybrid compounds.

At lower SID silane content, the storage modulus of CNC compounds at low strain was improved which is witness in the hybrid. The nature of the various compounds prepared somewhat shows a regime of properties dominated by silica and CNC content. The CNC were coagulated with natural rubber, washed, and dried before compounding with silica. When the CNC network structure has been formed in the rubber matrix, it may be difficult to incorporate other filler structures. At such, the response of the compounds under shear deformations showed properties typical of the filler with a higher content.

Payne effect	S30C0	S25C5	S20C10	S15C15	S10C20	S5C25	S0C30
Unvulcanized	218.44	266.18	157.4	191.28	308.87	585.71	457.79
Vulcanized	139.06	120.64	124.24	144.24	233.47	211.09	286.62

Table 3.20 Payne effect of CNC/silica hybrid compounds.

The Payne effect of the various compounds also displayed irregular trend. However, for compounds with higher silica content, the Payne effect was relatively lower. This is not unusual as the storage modulus was lower compared to the compound prepared with only CNC (S0C30) having the highest Payne effect. In essence, at CNC content beyond 15 phr, the Payne effect becomes remarkable because of the reinforcement. This is an indication that beyond 15phr of CNC a percolation network is formed. Therefore, it is easy to visualize that despite the presence of two fillers with different morphologies, the properties of the composite are dictated by the type of filler that is having a higher content. To understand the filler-polymer interaction of the vulcanizates, the tangent delta curves are shown below in figure 3.8.

The various compounds showed distinct behaviour. The compounds having 20, 25 and 30 phr of CNC showed a higher tangent delta values at high and low strain and this is an indication that the material have a larger viscous portion. This is typical of CNC fillers and as it dominates the matrix, the formation of occluded rubber could possibly contribute to exclusion of large part of the rubber chains which should have participated in the interaction. For highly dispersible silica used in the compounds, filler-filler interactions may be lower than CNC filler, likewise the reinforcement. At 30, 25, 20 and 15 phr of silica, the effect is obvious as it showed that the compounds had more filler-polymer interactions as depicted by the low tangent delta values.

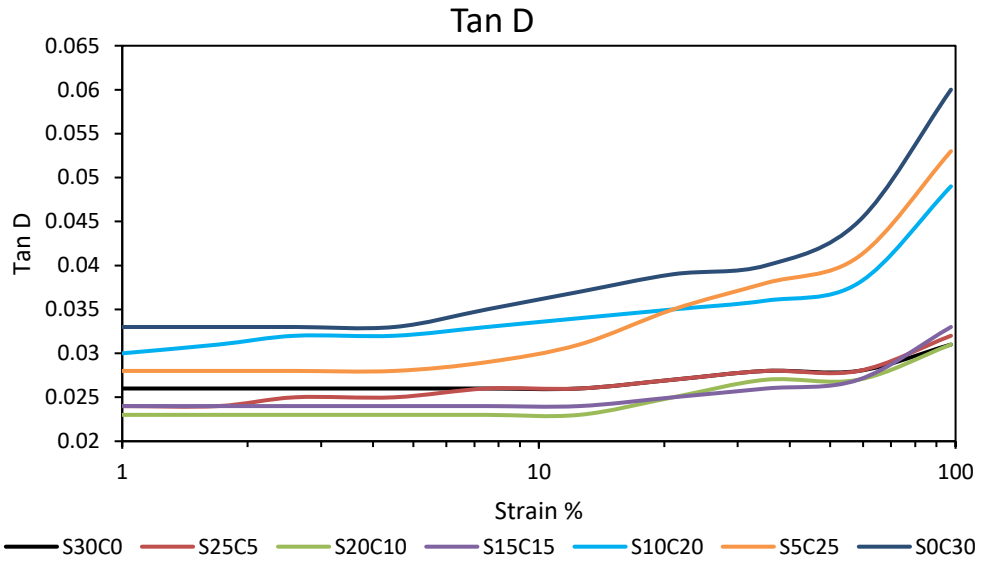

Figure 3.8 Tan D curves of vulcanized hybrid CNC/silica compounds.

Besides the trends observed in the properties, beyond 15 phr of filler content when CNC is expected to form a percolation network, the tangent delta values seemed to be higher.

- **Tensile properties**

The tensile properties of the hybrid compounds are shown in table 3.21. From the table below, the properties of the compounds showed properties that are similar with the amount of filler volume. When observed at 10% strain, the stress values showed that compounds with higher silica content were very similar in properties while those with higher CNC filler were with similar properties. In fact, at equal filler loading, the properties of the hybrid served as mid-point to transit to properties typical of the filler with higher content.

Property	S30C0	S25C5	S20C10	S15C15	S10C20	S5C25	S0C30
Stress 10% [MPa]	0.42	0.48	0.44	0.53	0.63	0.66	0.70
Stress 50% [MPa]	0.44	1.77	1.66	2.13	2.74	2.81	3.23
Stress 100% [MPa]	3.11	3.99	3.81	4.88	6.30	6.85	7.51
Stress 300% [Mpa]	-	-	-	-	-	-	-
Elongation at break [%]	125.04	107.56	123.99	211.9	198.73	114.48	198.84
Tensile strenght [MPa]	4.32	4.25	5.11	11.96	12.34	7.73	13.84

Table 3.21 Tensile properties of CNC/silica hybrid compounds

This trend continued up to 100% strain. But at 300% strain the material were stiff and could not be strain up to this point. Recall that for cyclic silanes, amount exceeding 5% especially for CNC compounds often results to deterioration of the properties and the resulting tensile properties are not so much desirable beyond this point even in the presence of silica fillers . At 300% strain, tensile properties are very useful for tire applications and in this scenario, it is difficult for this compound to serve for such purpose. The tendency to brittleness is also observe as the elongation at break is lower. However, even at such properties, compounds containing a 15 phr of CNC and higher possessed relatively better tensile properties as could be seen in the tensile strength. In all, it is evident that the SID cyclic silanes are very reactive and addition of these silanes beyond 5% may compromise the tensile properties.

3.4 Conclusions

The preparation of various CNC compounds with different silanes have been studied and compared with silica compounds as reference. As explored in this chapter, it is evident that there are several contributions to the properties of the composite. At the processing stage, allowing sufficient time for silanization, processing temperature and addition of zinc oxide are very crucial. For example, zinc oxide can form complexes with the vulcanization additives which can lead to masking the surface of the filler and thereby preventing good silane coupling. Adding zinc oxide after silanization was observed to be advantageous. More so, during compound preparation, processing at lower temperatures often create a temperature profile that is different among compounds. At higher temperatures, there is no remarkable difference in temperatures profile, and this can promote properties that are reproducible. Therefore, for CNC compounds, allowing a 4 minutes silanization, 130^0C processing temperature and addition of zinc oxide at the second stage of mixing could enhance better properties and make the compounds reproducible. Evaluation of different types of silanes also showed different contributions. For aliphatic silanes involving the use of APS and TESPD, their reaction proceeds first by hydrolysis which was different with explored cyclic silanes. The properties of APS silanized compounds were very interesting although the compounds often tend to brittleness at higher silane loading, most likely because with early vulcanization also comes early reversions which compromised the sulphur networks. For TESPD compounds, the properties are also good. CNC compounds showed that it is advantageous to cure the various compounds made with aliphatic silane less than 11 minutes at 150 °C. Similar behaviour was observed with cyclic silanes. There was an early vulcanization. The dynamic mechanical properties and tensile properties

were interesting. But at higher silane loading beyond 5%, the tensile properties deteriorate making the material brittle. The materials could not be strain up to 300% and this shows that the reactive nature of the silanes can achieve interesting properties only at very low silane loading. When the cyclic silanes were applied to hybrid CNC/silica compounds, the properties obtained were dictated by the filler that was having a higher content. It was observed that the processing method of first coagulating the CNC and rubber before incorporating the dry silica does not promote a very homogeneous hybrid system. While it is necessary to adopt a different processing method for the hybrid, cyclic silanes may not be ideal silanes for this study.

References

1. Eichhorn, S.J., Dufresne, A., Aranguren, M., Marcovich, N.E., Capadona, J.R., Rowan, S.J., Weder, C., Thielemans, W., Roman, M., Renneckar, S., Gindl, W., Veigel, S., Keckes, J., Yano, H., Abe, K., Nogi, M., Nakagaito, A.N., Mangalam, A., Simonsen, J., Benight, A.S., Bismarck, A., Berglund, L.A., Peijs, T. (2010) Review: Current international research into cellulose nanofibres and nanocomposites. Journal of Materials Science, 45, 1-33.

2. Baghaei, B., Skrifvars, M. (2020) All-Cellulose Composites: A Review of Recent Studies on Structure, Properties and Applications. Molecules, 25, 2836.

3. George, J., Sabapathi, S.N. (2015) Cellulose nanocrystals: synthesis, functional properties, and applications. Nanotechnology, Science and Applications, 8, 45-54.

4. Manoharan, P., Naskar, K. (2016) Exploring a highly dispersible silica-elastomer composite for tire applications. J. Appl. Polym. Sci., *133*, 43531.

5. Brinkle, J.W., Debnath, S.C., Reuvekamp, L., Noordermeer, J. (2003) Mechanistic aspects of the role of coupling agents in silica-rubber composites. Composites Science and Technology, 63, 1165-1174.

6. Ko, J.Y., Prakashan, K., Kim, J.K. (2012) New silane coupling agents for silica tire tread compounds. Journal of Elastomers & Plastics, 44, 549-562.

7. Ali, S.D. (2018) Biofillers from renewable lignocellulosic feedstock for elastomers. PhD thesis-University of Milano-Bicocca.

8. Rostamzadeh, P., Mirabedini, S.M., Esfandeh, M. (2014) APS-silane modification of silica nanoparticles: effect of treatment's variables on the grafting content and colloidal stability of the nanoparticles. J. Coat. Technol. Res., 11, 651-660.

9. Lee, J., Kim, J.H., Choi, K., Kim, H.G., Park, J.A., Cho, S.H., Hong, S.W., Lee, J.H., Lee, J.H., Lee, S., Lee, S.Y., Choi, J.W. (2018) Investigation of the mechanism of chromium removal in (3-aminopropyl)trimethoxysilane functionalized mesoporous silica. Scientific report, 8, 12078.

10. Lim, H.T., Ahn, K.H., Lee, S.J., Hong, J.S. (2012) Design of new HDPE/silica nanocomposite and its enhanced melt strength. Rheologica Acta, 51, 143-150.

11. Maciejewska, M., Sowinska, A. (2019) Thermal characterization of the effect of fillers and ionic liquids on the vulcanization and properties of acrylonitrile-butadiene elastomer. J. Thermal Analysis and Calorimetry, 138, 4359-4373.

12. Hayichelaeh, C., Reuvekamp, L.A.E.M., Dierkes, W.K., Blume, A., Noordermeer, J.W.M., Sahakaro, K. (2017) Reinforcement of natural rubber by silica/silane in dependence of different amine types. Rubber Chemistry and Technology, 90, 651-666.

13. Brinke, J.W., Swaaji, P.J., Reuvekamp, L.A.E.M., Noordermeer, J.W.M. (2002) The influence of silane sulphur rank on processing of silica-reinforced tyre tread compound. Elastomers and plastics, 244-254.

14. Thomas, M.G., Abraham, E., Jyotishkumar, P., Maria, H.J., Pothen, L.A., Thomas, S. (2015) Nanocelluloses from jute fibers and their nanocomposites with natural rubber: preparation and characterization. Int. J. of biological macromolecules, 81, 768-777.

15. Brostow, W., Lbland, H.E.H. (2010) Brittleness of materials: implications for composites and a relation to impact strength. J. material sci., 45, 242-250.

16. Menges, G., Boden, H-E. (1986) In: Brostow, W., Corneliussen, R.D. (eds) Failure of plastics. Hanser Publishers, Munich.

17. King, R.B., Crabtree, R.H., Lukehart, C.M., Atwood, D.A. (Eds), (2006) Bond Energies, in Encyclopedia of Inorganic Chemistry, John Wiley and Sons, Ltd, Chichester, UK.

18. Arkles, B., Pan, Y., Larson, G.L., Berry, D.H. (2004) Cyclic azasilanes: volatile coupling agents for nanotechnology, In, Mittal, K.L. (Ed.) Silanes and other coupling agents. Vol 3, 179-191.

19. Kim, D., Zuidema, J.M., Kang, J., Pan, Y., Wu, L., Warther, D., Arkles, B., Sailor, M.J. (2016) Facile surface modification of hydroxylated silicon nanostructures using heterocyclic silanes. J. Am. Chem. Soc., 138, 15106-15109.

20. Ju, L., Strandwitz, N.C. (2016) Cyclic azasilanes as a volatile and reactive precursor for atomic layer deposition of silicon dioxide. J. Mater. Chem. C, 4, 4034-4039.

21. Xie, Y., Hills, C.A.S., Xiao, Z., Militz, H., Mai, C. (2010) Silane coupling agents used for natural fiber/polymer composites: A review. Composites: part A, 41, 806-819.

Chapter 4

CNC as a biofiller: role of sulphate esters on composite properties

4.1 Introduction

Cellulose nanocrystals have interesting properties which makes them useful as good reinforcing fillers. The production route of these nanocrystals also contributes to some of its unique properties. As explained earlier, several mineral acids are used to selectively hydrolyse the amorphous regions to obtain nanocrystals [1-4] and among them, sulphuric acid is the most employed method. When sulphuric acid is used, the resulting nanocrystals are imparted with sulphate half esters leading to a stable colloidal suspension. This change in surface properties has influenced potential use of CNC's in different applications. For instance, in composite preparations, the sulphates half ester which maintains stable colloidal suspension helps in the preparation of the composite by coprecipitation or solution blending. There are other processes such as electrospinning which the presence of the sulphate half esters can create difficulties because of the repulsions between CNC particles.

Understanding the role of these sulphate half esters on the CNC is drawing attention. Several research have affirmed the impact of sulphates half esters on the thermal stability of the CNC's [5,6,] and also the role it plays as a flame retardant in pyrolysis and combustion because of its ability to promote dehydration reactions [7]. In general, it is believed that the presence of sulphates half esters reduces the thermal stability of CNC. But on the contrary, there are results that also show a moderate increase in thermal degradation temperatures at higher level of sulphate groups [8,9] and this issue is almost inconclusive. It is difficult to make a direct comparison on the effects of sulphates half esters on CNC because the structural characteristics, thermogravimetric protocols, hydrolysis conditions and counter ions also influence the thermal properties of CNC [5]. It is therefore not strange to expect different composite properties when CNC has various amounts of sulphate half ester groups on the surface.

The esterification of the surface hydroxyl groups of CNC during sulphuric acid hydrolysis makes the sulphate half esters to also occupy substantial active sites meant for further functionalization. Compatibilization of CNC with hydrophobic polymers in composites takes place on the hydroxyl groups and the issue of sulphate half esters occupying the hydroxyl groups could be of concern. The hydroxyl groups on the surface are relatively few compared to the bulk and several reactions are targeted at the surface to reduce impact on the crystallinity. Reducing the amount of sulphate esters could make more hydroxyl groups available for coupling reaction. Although, there are propositions that the surface hydroxyl groups are sufficiently abundant irrespective of the presence of the sulphate half esters, it was needful to study the role they play during composite preparation.

In this chapter, desulphation was conducted with the intent of having different amount of sulphate esters on the surface and to prepare composites thereon. Subsequent characterizations of these compounds were compared with silica made compounds and are expected to give a better understanding on the properties it confers on the composite. In this regard, the pristine CNC is not of so much important. This is because each synthesized CNC have their various amount of sulphate esters grafted on the surface and the properties, they confer on composites are expected to corelate to the amount of sulphates present.

4.2 Experimental method

4.2.1 Materials

CNC suspension was procured from Celluforce and freeze dried. Bis(triethoxysilylpropyl)disulfide (TESPD), 3-aminopropyltriethoxysilane (APS) silanes, natural rubber latex, antioxidants and vulcanizers were provided by Pirelli tires, while sodium hydroxide and acetic acid was bought from Sigma Aldrich. All materials were used as received

4.2.2 Method

4.2.2.1 Desulphation

The desulphation procedure was adopted from the literature [10] with modifications. Briefly, about 20 g freeze dried CNC was transferred into a round bottom flask. A determined concentration of sodium hydroxide (NaOH) solution was prepared taking into consideration the CNC. The solution

was added to the CNC and made to reach the necessary concentration. From 0.3 to 1.2 molar concentrations, the entire volume of the mixtures was kept at 300 ml. Thereafter, it was stirred to near homogeneity and placed in an oil bath and stirred continuously at 65^0C for 3 hours. The reaction was ended by pouring cold water and dialyzed for days until the pH of the suspension was relatively neutral. Earlier, hydrochloric acid was used to quench the reaction, but it was observed that there was lower yield and likely contaminations of the CNC surface with the salts formed from the possible acid-base reaction. Therefore, dialysis was opted to remove the sodium hydroxide from the suspension.

The suspension was removed from the dialysis tubes and transferred to a beaker to be concentrated. All samples were concentrated at 100^0C for 2 days until the samples attained a 9.8 - 15wt % for easy coprecipitation.

4.2.2.2 Composite preparation

A 30 phr concentrated desulphated CNC suspension was weighted and mixed with natural rubber latex. The mixture was homogenized for about 20 minutes and coagulated with concentrated acetic acid. The coagulated sample was pressed and washed to remove undesired components and chopped into smaller pieces. The sample was soaked to remove acetic acid and dried in an oven at 40^0C till constant weight. Thereafter, silanes, vulcanizers and additives were added and compounded in a brabender internal mixer with the procedure in table 4.1 while the formulations recipe is shown in table 4.2.

Mixing stage	Time (min)	Temperature (0C)	Activity
Step 1	0	130	Load rubber and filler
	2		Add silanes
	6		Add stearic acid
	7		Unload
Step 2	0	60	Load masterbatch from Step1
	1		Add sulfur, CBS, TMQ, 6PPD, zinc oxide
	3		Unload

Table 4.1 Mixing procedure for desulphated compounds.

Ingredients (PHR)	S-TESPD	CNC-TESPD	CNC-APS
		Polymer/filler system	
Natural rubber	100		
Silica	30		
100PHR NR + 30PHR CNC		130	130
		Compatibilizer	
TESPD	2.4	2.4	
APS			2.4
		Vulcanization system	
Soluble sulfur	2	2	2
Zinc oxide	5	5	5
Stearic acid	2	2	2
CBS	2	2	2
		Antidegradants	
TMQ	1	1	1
6PPD	1.5	1.5	1.5

Table 4.2 Formulation recipes for silica compounds made with TESPD silanes (S-TESPD), desulphated CNC compounds prepared with TESPD silanes (CNC-TESPD) and desulphated CNC compounds made with APS silanes (CNC-APS).

4.2.2.3 Characterizations

- **DLS/ZP**

The particle size and the zeta potential were estimated by dynamic light scattering and zeta potential measurements. Both measurements were conducted on a Malvern Zetasizer, Malvern UK at a scattering angle of 90^0.

- **Elemental analyses**

Elemental analysis was conducted to understand the elemental composition of CNC before and after desulphation. The elemental analyser used is a CHNS/O Series II analyser from PerkinElmer using cysteine as calibration standard with the composition: C - 29.99%, H - 5.03%, N - 11.67%, and S - 26.69%. The main intent is to know the percentage of sulphur that has been removed in the desulphation process which correlates to the amount of sulphates groups that were removed.

- **X-Ray Diffraction (XRD)**

The crystallinity of CNC is an important property as it has contributions to the reinforcement in the composite. The crystallinity of the CNC particle was studied with an X'Pert PRO diffractometer from Malvern Panalytical, UK. The X-ray source was from Cu Kα with data acquisition starting from 2θ = 5 to 50.

- **TGA analyses**

Thermogravimetric analysis was employed to study the thermal stability of CNC before and after desulphation. The analysis was conducted with a Mettler Toledo TGA 1 instrument. Samples were added to crucibles and were heated from 30 - 600^0C in the presence of nitrogen. The nitrogen flow rate was maintained at 50ml/min while the heating was at 20^0C.

- **SEM analyses**

Scanning electron microscopy was used to ascertain the preservation of the particle morphology before and after desulphation. The instrument used was a Zeiss UltraPlus Field Emission Scanning Electron Microscope (FESEM) operating at 7.0 kV. Samples were prepared by dispersing 10 ml of the various suspensions in a 30 ml of distilled water. The mixture was then sonicated for few minutes. 1 ml of the sonicated suspension was thereafter dispersed in ethanol and sonicated again for about 10 minutes. About 1 microliter of the sample was deposited on a stub for analysis. To overcome the drawback of the non-conductive nature of CNC, a 5-7 nm gold or carbon was deposited on the surface to aid image acquisition.

- **Composite characterizations**

The dynamic mechanical and tensile properties of the composite prepared from desulphated cellulose nanocrystals were performed as described in chapter 3, section 3.2.3.

4.3 Results and discussions

4.3.1 Particle size

The estimations of particle sizes of CNC after desulphation were intended to serve for relative comparison [12]. The average particle sizes estimated from DLS are in most cases approximately

half of the size obtained from electron microscopy [13]. However, it is a fast means to understand the particle size distribution.

As shown in figure 4.1, samples from the CNC suspension before desulphation were estimated to be averagely 104.8 nm. The sizes gradually increased up to 259.7 nm at a 1.2 molar concentration of sodium hydroxide. This trend of increase in particle sizes was an indication that the removal of sulphate groups and impact of the soda concentration was promoting agglomerations of the particles leading to larger particle sizes. Often, desulphated samples may not meet measurement quality criteria when impact on the surface charges results in larger agglomerates leading to particle sedimentation. Also, the sulphate esters affect the rheological properties of the particles at certain concentrations [11] and it was necessary to dilute samples in large folds and to decant gel-like flocculating particles that could influence results.

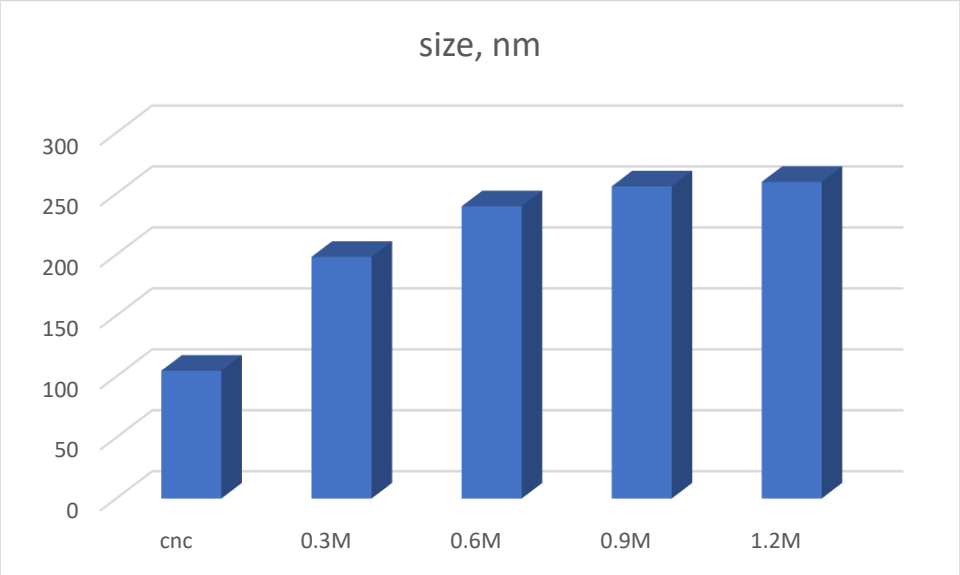

Figure 4.1 Particle sizes of desulphated CNC samples.

In general, the trend of the particle sizes corresponds to the CNC treatments conditions as it increases along with increase in soda concentration.

The size of the particles as measured by DLS could be double if measured by electron microscopy. However, the sizes of the desulphated CNC samples are within nanometre range and still posses' properties similar to the starting material.

4.3.2 Zeta potential

Sulphate half esters contributes to the colloidal stability of CNC suspension due to electrostatic repulsion and the zeta potential reflects this by measuring the potential difference between the electric double layer of the particle and the layer of dispersant (water). Samples were prepared for analysis by diluting in large fold to have a clear suspension without particle flocculation or sedimentation particles. As obtainable in other works where few drops of electrolytes are added to the suspension before a zeta potential analysis, electrolytes were avoided. Samples were analysed after dialysis at neutral pH and the results are presented in Table 4.3.

Sample	Zeta potential (mV)
CNC	**-50.9**
0.3M	**-35.5**
0.6M	**-27.7**
0.9M	**-34.7**
1.2M	**-32.1**

Table 4.3 Zeta potential of CNC before and after desulphation.

The highest zeta potential was obtained for CNC sample before desulphation at -50.9 mV. Similarly, high zeta potential of CNC suspension has been published from sulphuric acid catalysed hydrolysis of filter paper with −52 to −58 mV [12] and -78.3 mV obtained from sulphuric acid hydrolysis of microfibrilated cellulose [13]. The sample with the lowest zeta potential is from 0.6 M sodium hydroxide desulphated CNC which correlate to the lowest amount of sulphur content from elemental analysis as shown in Table 4.4 This implies that more sulphate half esters were removed from the surface of the particles leading to a reduction in zeta potential. From visual observations, the 0.6 M sample had several sediments indicating large reduction in the sulphate half esters and it was almost unfit for zeta potential measurement. To make it fit for analysis, samples were dried, and equal mass was measured from all samples and re-suspended in water after series of sonication.

For suspensions stabilized by electrostatic repulsions, a zeta potential of ±30 mV is required minimum [14] to maintain colloidal stability. Albeit large zeta potentials do not always guarantee stability as van der Waal attractive forces may cause agglomeration [15, 16]. Samples showed a relatively high zeta potential, and the differences can be attributed to the amount of sulphate half

esters present on the surface of the CNC particles. Zeta potential is mostly influenced by concentration, ionic strength, and pH and samples were prepared with keen attention to maintaining the same conditions. Generally, depending on the process condition, CNC preparation could be targeted at achieving high yield or increasing the amount of sulphate half esters.

Composites were made with the desulphated CNC after dialysis to a neutral pH immediately. This took into consideration the unstable colloidal suspension of some of the desulphated samples which could not be kept for a longer period because of aggregating sediment particles.

4.3.3 Elemental analysis

The sulphate content estimated by elemental analysis as percentage sulphur is presented in table 4.4. The percentage sulphur content of CNC before desulphation was 2.05% and reduced to a minimum of 1.66% for 0.6 M solution. There was no further reduction irrespective of increase in soda concentration. During the desulphation process, it was observed that as the molarity increased, the samples became highly viscous and inter molecular diffusion would have reduced leading to a reduction in the efficiency of the desulphation process. As shown, there are slight variations in the sulphur content when the concentration was increased from 0.9 to 1.2 M. This would imply that a further increase in the concentration of sodium hydroxide may not necessarily lead to further sulphur removal. Further desulphation could be achieved if the weight percent of CNC is reduced in the mixture to allow proper interdiffusion of reacting species. However, this may affect good comparisons for the different samples. The amount of CNC in the suspension subjected to desulphation, temperature and time are all major contributing factors to the extent of sulphur removal.

Cellulose nanocrystals are mostly prepared by sulphuric acid hydrolysis which confers sulphate half esters on the surface. Depending on the preparation conditions, different amount of sulphate group is grafted onto the surface of CNC. This sulphate groups could be expressed in percentage sulphur (% S) or mmol sulphate per kg of CNC (mmol kg^{-1}) which are mostly not reported [17] when CNC are produced with sulphuric acid. Elemental analysis and conductometric titration are among the widely used method employed to determine the amount of grafted sulphates group.

Sample	Sulfur (%)
cnc	2.05
0.3M	1.86
0.6M	1.66
0.9M	1.76
1.2M	1.71

Table 4.4 Sulphur content of CNC before and after desulphation.

The elemental analysis can determine the total sulphur contents which are always higher than values reported from conductometric titration [18]. Sulphur is essential to living cells and for some plant species, sulphur found in tissues could range from 0.1% to 6% [19]. This amount may not be accessible by titrimetric method [20]. Also, when cellulose nanocrystals are produced, after the centrifugation step, there are often residual amount of sulphuric acid. This amount could be removed by neutralization and dialysis. For neutralization, sodium hydroxide is used leading to the formation of sodium sulphates. If adequate centrifugation is not carried out, the sulphate ester contents which are estimated by deducing the elemental content of sulphur may reach higher levels. This contribution apart from inherent sulphur content of materials from living cells are major contributors to large amount of sulphur content during elemental analysis of sulphate half esters of CNC. As shown in table 4.4, the sulphur content of the starting CNC seemed relatively high and the explanation above could be the reason.

The sulphate groups have also been a subject of controversies bringing inconclusiveness to the idea that it affects the thermal stability. However, large amount of the sulphate groups during CNC synthesis process for sulphuric acid content exceeding 62wt % impacts negatively on the yield leading to a <20% yield [21]. The sulphate content during CNC preparation and after is therefore a subject that would require more attention to explore even their role in composite.

4.3.4 XRD

An X-ray diffraction was conducted to understand the changes in the crystallinity of the CNC before and after desulphation. The crystalline peaks of CNC treated with different concentrations of NaOH are shown in figure 4.2. The crystalline peaks of pristine CNC showed higher intensity followed by

0.3 molar NaOH solution. The lowest intensity was recorded with 0.6 molar NaOH solution. This sample also had the lowest sulphur content which implies that the more efficient in the desulphation process, the more the crystallinity of the sample was impacted. For decades, mercerization by treating cellulose with sodium hydroxide has been used in the textile industry to swell cellulose and it has been adopted to activate cellulose for further reaction [22-24]. This treatment process also often results to large impact on the crystallinity of cellulose. During CNC preparations by sulphuric acid hydrolysis, the functionalization by the sulphate half esters takes place on the hydroxyl groups. The removal of the sulphate half esters by desulphation interrupts the hydrogen bonding network within the cellulose structure. Depending on the degree of desulphation, it will correspond to the crystallinity of the sample.

The crystalline peaks of the various samples were found along the 2theta planes of 12.3^0, 14.9^0, 22.3^0 and 34.5^0 corresponding to the planes of (1 ī 0), (1 1 0) (2 0 0) and (0 0 4). These are typical of cellulose I and cellulose II [25, 26]. Cellulose II is more stable than native cellulose I and it is typical of commercial CNC having portions of both I and II. As seen in the various peaks, the impact of the desulphation process did not lead to a total conversion of the material to cellulose II.

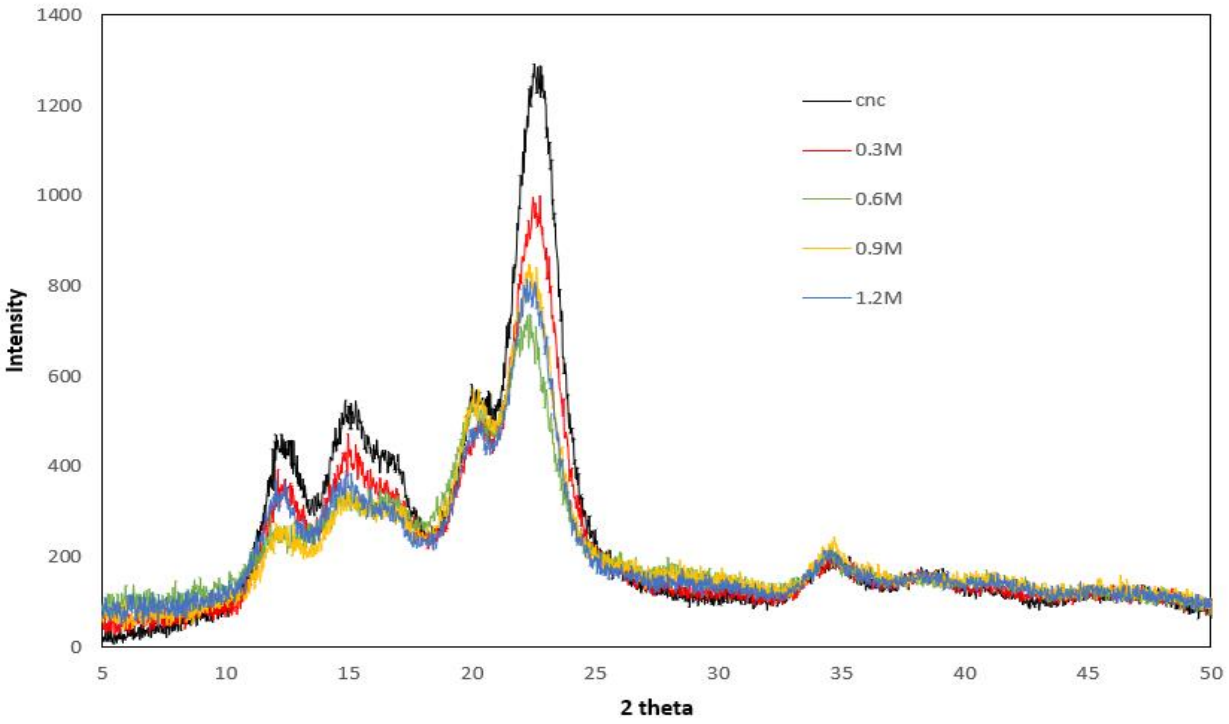

Figure 4.2 crystalline peaks of pristine and desulphated CNC.

The crystallinity index of the various samples was estimated by the deconvolutional method using Gaussian distribution to deduce the ratio of the crystalline regions to the amorphous regions [27-29]. The crystallinity index of the pristine CNC (86.35%) reduced to the minimum at 72.17% for 0.6 M concentration while samples at 0.9 M and 1.2 M had a close crystallinity. The results are in accordance with the sulphur content and it is easy to conclude that more sulphur removal affected the crystallinity of the CNC.

	CNC	0.3M	0.6M	0.9M	1.2M
Crystallinity index %	86.35	83.38	72.17	78.55	77.83

Table 4.5 Crystallinity indexes of pristine and desulphated CNC.

4.3.5 TGA

The thermogravimetric analyses of cellulose nanocrystal before and after desulphation are presented in figure 4.3. The onset loss in weight is attributed to possible adsorbed water and organics. The main degradation of the various materials was close to each other at around 250^0C.

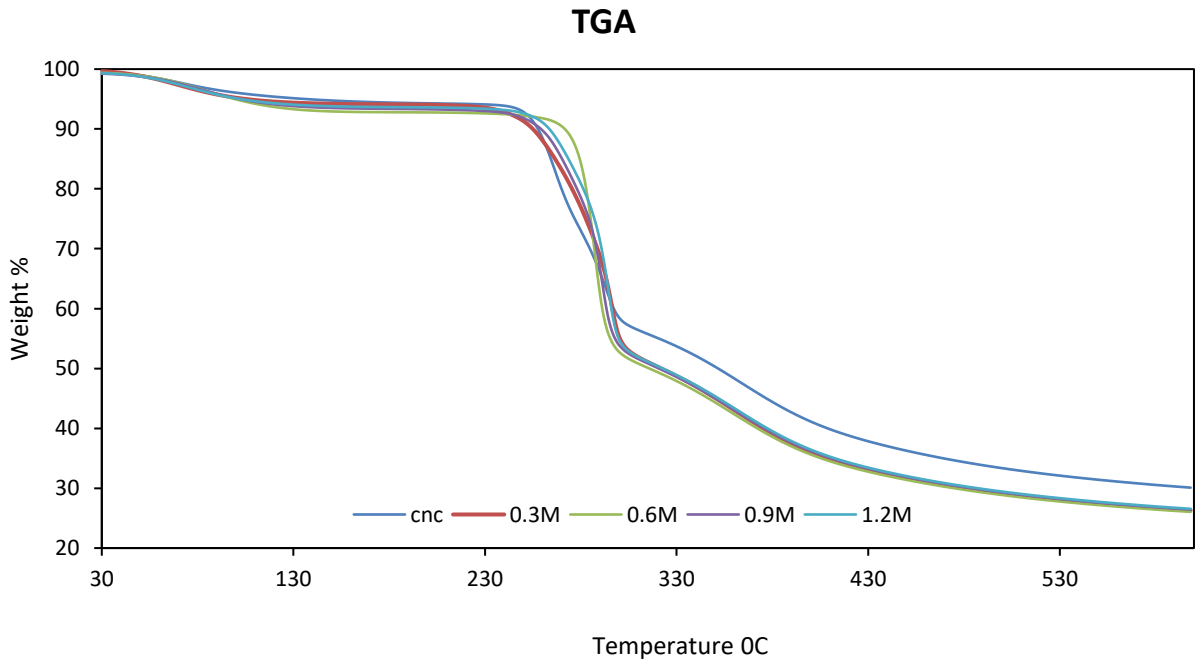

Figure 4.3 Thermogravimetric curves of CNC before and after desulphation.

However, the sample desulphated at 0.6 M, having the lowest percentage of sulphur after desulphation was shown to have a slightly higher degradation temperature around 270^0C. In essence, reducing the sulphate content on the CNC can slightly improve the thermal stability of the CNC. This supports the assertion that sulphates groups catalyse early degradation [30, 31]. However, the differences in the degradation process are not remarkable as they are within the same band. Probably, there could be remarkably differences in the thermal behaviour if the difference in the sulphate content vary widely among the different samples. The pristine CNC showed a reduced weight loss even at 600^0C which could be attributed to the higher crystalline content. Besides the reduction in the sulphate groups, the crystallinity of the samples made contributions that showed all desulphated samples having higher loss in weight compared to the pristine CNC. The possible explanation is the contributions of the crystallinity in slowing the impact of degradation especially for pristine CNC.

4.3.6 SEM analysis

Scanning electron microscopy imaging was used to observe the preservation of the particle morphology before and after desulphation and results shown in figure 4.4.

The morphology of cellulose nanocrystals is rod-like in shape and the fibres are mostly networked to each other in a three-dimensional networking. The morphology of the pristine CNC and the morphology of the material after desulphation was observed to be the same. However, there are slight variations showing some degree of aggregations. While the sulphate groups are removed, the particles tend to aggregate.

The images shown below are of different magnifications. This and the preparation methods are major contributions to obtaining precise images. Samples were prepared within the same concentration range, however, the highly desulphated sample at 0.6 molar concentration shows more of CNC aggregations with particles fusing to each other. This sample is of more interest because the large amount of sulphate groups that were removed were expected to impact heavily on the morphology. The particles tend toward elongated spheres. Despite the large extent of the desulphation at this molar concentration, it is obvious that the morphology is still similar to the pristine CNC. The other desulphated samples still show strands of the CNC particles not as highly fused as the highly desulphated material.

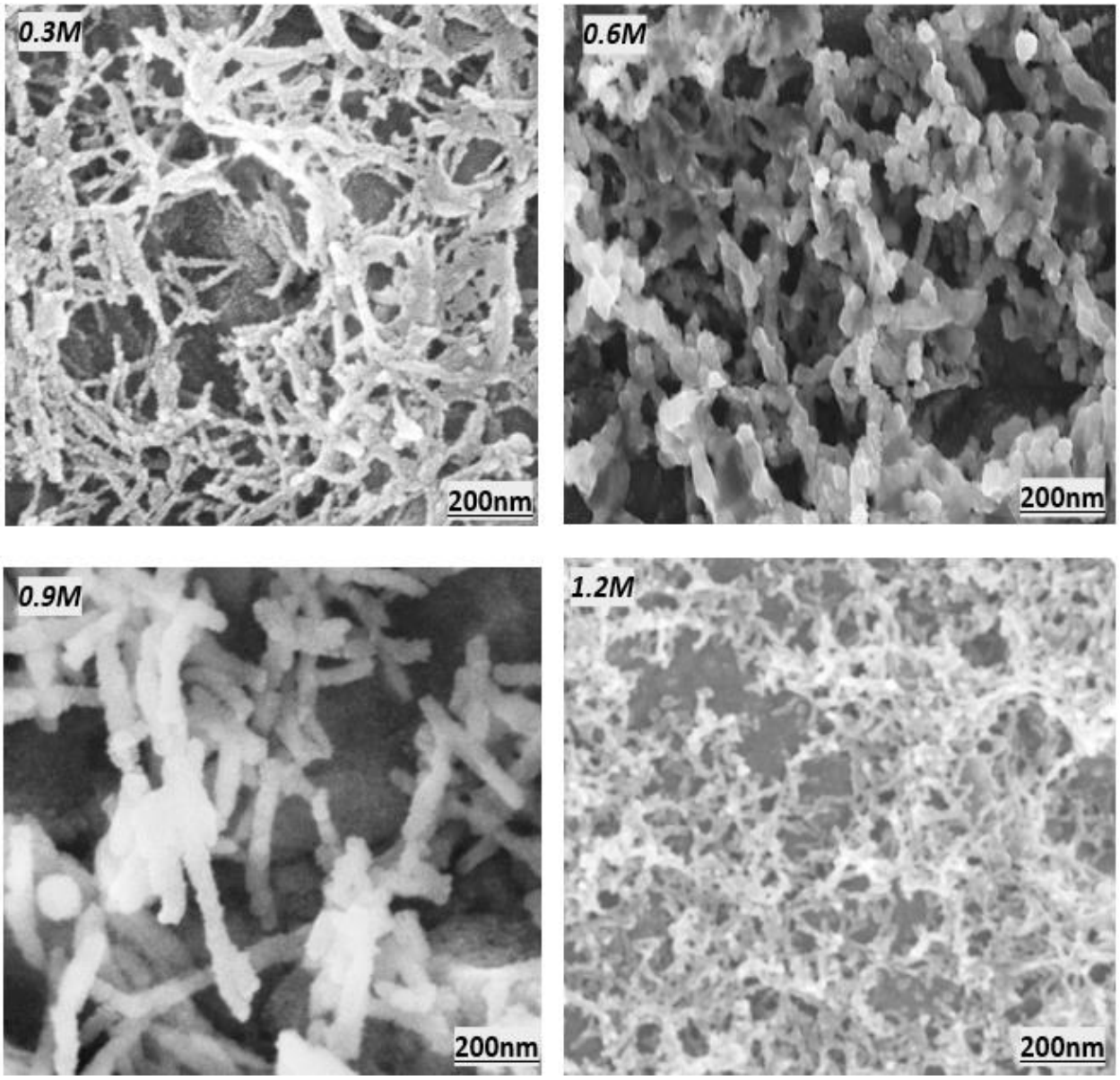

Figure 4.4 SEM images of desulphated CNC.

With the images above, it could be inferred that the desulphated samples still maintain morphology typical of cellulose nanocrystal.

4.3.7 Vulcanization properties

The desulphated rubber compounds were prepared using APS and TESPD silanes and materials cured at 150^{0}C. The curing kinetics is shown below in table 4.6 and 4.7 with S-TESPD indicating silica compatibilized compounds, 0.3, 0.6, 0.9, 1.2 APS and TESPD showing the various molar concentrations. All desulphated cnc compounds were compared with silica-TESPD prepared compounds as reference.

In both tables, the vulcanization trends were heavily influenced by the compatibilizing silanes. APS silanes showed an early optimum curing time and higher cure rate index (CRI) compared with TESPD compatibilized compounds. This is very similar to pristine CNC compounds that were earlier prepared with APS silanes. In this regard, the different amount of sulphate groups on the CNC were not observed to have made a remarkable influence on the vulcanization process when compounded with APS silanes. The vulcanization properties of the highly desulphated samples were seen to be similar with the 0.3M desulphated compounds. Albeit all desulphated compounds maintained a relatively higher crosslinking density when compared with the reference silica as shown in the difference between the lowest and highest torque.

Parameters	S-TESPD	0.3APS	0.6APS	0.9APS	1.2APS
TS2 (min)	9.72	2.91	2.78	2.45	2.53
T90 (min)	15.73	5.36	5.28	4.57	4.73
CRI (min-1)	19.96	40.82	40.00	47.17	45.46
ML (dNm)	1.61	1.92	2.14	1.78	1.84
MH (dNm)	12.30	15.53	15.36	13.28	15.50
ΔM (dNm)	10.69	13.55	13.22	11.50	13.66

Table 4.6 Vulcanization kinetics of desulphated CNC prepared with APS silanes.

Parameters	S-TESPD	0.3TESPD	0.6TESPD	0.9TESPD	1.2TESPD
TS2 (min)	9.72	5.32	5.14	5.79	5.41
T90 (min)	15.73	9.49	9.32	10.08	9.52
CRI (min-1)	19.96	23.98	23.92	23.31	24.33
ML (dNm)	1.61	1.61	1.87	1.32	1.65
MH (dNm)	12.30	15.13	15.67	12.71	14.25
ΔM (dNm)	10.69	13.52	13.80	11.39	12.60

Table 4.7 Vulcanization kinetics of desulphated CNC prepared with TESPD silanes.

In all the CNC-TESPD silanized compound, the 0.6 M desulphated compound showed a relatively higher crosslinking density as shown in the ΔM torque. The optimum curing time was also slightly lower than all the compounds. It is possible the aggregating particles can contribute to the stiffness

of the composite thereby resulting to an increase in higher torque required to monitor the vulcanization. While assessing the impact of desulphation on the various samples, the contributions of the crystallinity index are worthy of consideration. In essence, samples that were not heavily desulphated had a higher crystallinity which alongside the crosslinking, increases the vulcanization torque. Comparing with silica prepared compounds, the vulcanization kinetics of the CNC compounds were better. In general, the results have shown that desulphation or treatment of CNC with soda concentration below 1.2 M would not interfere remarkably on the vulcanization kinetics. The idea of acidic groups interfering with vulcanization mechanism [32, 33] was not observed as results are within the same trend. It is possible to attribute this to the fact that the margins in the amount of sulphate removed were not remarkable to affect the vulcanization process.

4.3.8 Dynamic mechanical analysis

The reinforcement mechanism of the desulphated cellulose nanocrystals was studied and compared with silica filled compounds. The results of APS compatibilized compounds and TESPD compatibilized compounds are shown in figure 4.5 and 4.6.

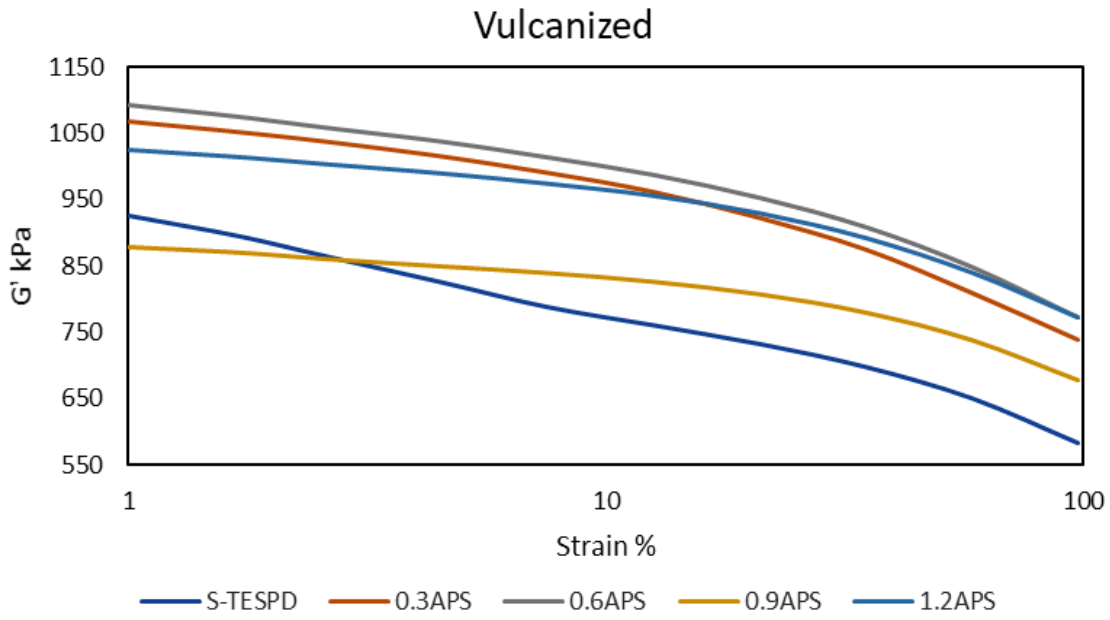

Figure 4.5 Storage moduli of desulphated CNC compatibilized with APS silanes in NR compounds.

Among the desulphated compounds, the storage modulus of the highest desulphated CNC sample (0.6 M) prepared with APS silanes was higher compared to all the compounds, even the reference silica. At low strains, the storage moduli were up to 1093.93 kPa, with the lowest storage modulus

at low strain from 0.9 M samples. This may be attributed in part to the possibility of more hydroxyl groups being made available from the desulphation process thereby creating more sites for the coupling reactions. At 100% strain, the values of the highest desulphated samples were still high compared to other compounds. However, it was expected that the sample with the lowest desulphation (0.3 M) should have the lowest modulus going by the postulations that when desulphation is initiated, more active sites are provided for coupling which would contribute to the reinforcements. But it is on the contrary. A possible explanation in this scenario is to understand the contributions of the crystallinity of the least desulphated samples which was reasonable higher and possibly contributing to compensate the reinforcement. The desulphations effect are obvious in the various compounds. However, other contributing factors such as the crystallinity of the particles, silane structures etc could have contributed in a way that its difficult to connect the improvement of properties to the freed hydroxyl groups alone.

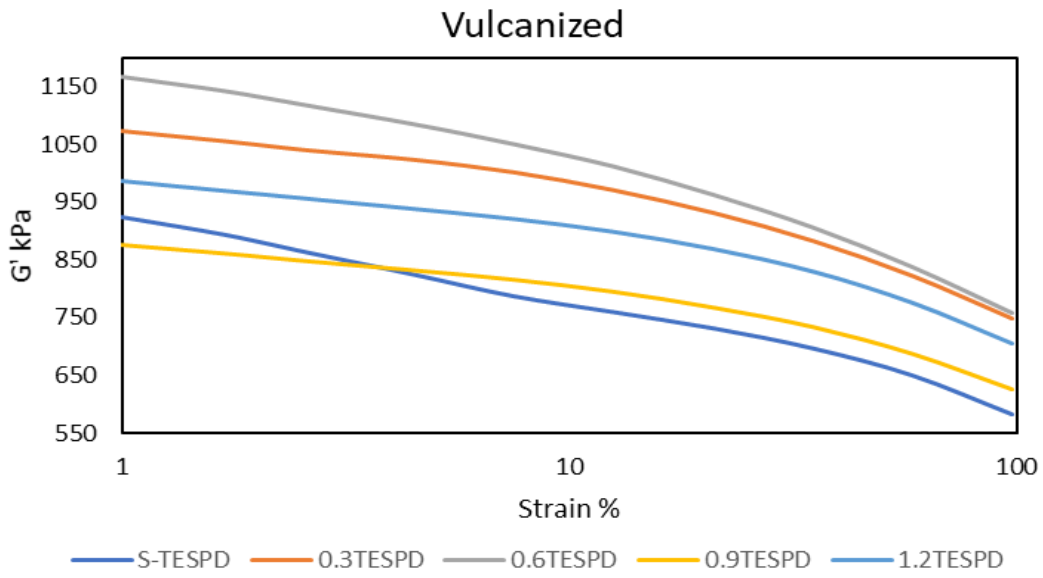

Figure 4.6 Storage moduli of desulphated CNC compatibilized with TESPD silanes in NR compounds.

The storage modulus of the desulphated compounds compatibilized with TESPD silanes showed similar trend. The compound with highest storage modulus was from 0.6M samples which were highly desulphated. Even at 100% strain the values were higher compared to the rest of the compounds. This also alludes to the possibility of more hydroxyl groups being made available for the coupling reaction. The deformations imposed on the 0.6M sample of interest was remarkable at about 12.5% strain when filler network breakdown was more obvious. The Payne effects of the samples are also displayed below.

Payne effect	S-TESPD	0.3APS	0.6APS	0.9APS	1.2APS	0.3TESPD	0.6TESPD	0.9TESPD	1.2TESPD
Unvulcanized	108.03	282.44	561.02	240.84	296.3	261.57	353.54	157.73	243.94
Vulcanized	343.18	330.95	322.39	200.32	254.29	323.85	407.99	249.52	281.8

Table 4.8 Payne effects of desulphated compounds.

From table 4.8 showing the Payne effect for both silanes compatibilized compounds, the highly desulphated compounds had a higher Payne effect both for the vulcanized and unvulcanized compounds which may be attributed to aggregations and poor dispersions. In the vulcanized state, the Payne effect for APS highly desulphated compound reduced and was relatively compared to others. However, it increased for TESPD compounds. It is important to highlight that vulcanizations for APS reach optimum at early time while that of TESPD silanized compound also achieved an optimum curing at about 40% of the entire curing time. Reversions set in afterward with the subsequent loss of part of the crosslinking bridges. The high values of the Payne effect and possibly the storage modulus could improve if the curing process is ended early to avoid reversion that would lead to loss of vulcanization networks.

Tan Delta	S-TEPSD	0.3APS	0.6APS	0.9APS	1.2APS	0.3TESPD	0.6TESPD	0.9TESPD	1.2TESPD
1%	0.047	0.029	0.03	0.02	0.021	0.027	0.036	0.026	0.026
100%	0.053	0.061	0.059	0.048	0.055	0.06	0.065	0.058	0.055

Table 4.9 Tangent delta of APS and TESPD silanized desulphated compounds.

The tangent delta of the various desulphated compounds are shown in Table 4.9 for vulcanized compounds. The response of the compounds is indicative of the synergistic effect of the elastic portions of the compounds. When compared to the silica prepared compound, several samples exhibited a slightly higher tangent delta at high strain. As said earlier, the difference in the margin of the sulphate content as reflected in the amount of sulphur is relatively close and it is difficult to observe sharp differences in the properties. However, the contributions of the highest desulphated compound are reflected in the properties of the various composites. For the APS silanized compound, the tangent delta of the highly desulphated compound is relatively the same with 0.3M desulphated compound which were higher than all APS silanized compounds. With the TESPD silanes, the highly desulphated compound (0.6M) showed a higher tangent delta. This could be

attributed to aggregations and poor dispersions leading to poorer filler-polymer interactions. The removed sulphates groups have shown to be vital to aid dispersion when present in reasonable amount.

4.3.9 Tensile properties

The tensile measurements of the desulphated compounds made with APS and TESPD silanes and compared with silica compounds are presented in table 4.10 and 4.11. The tensile properties of CNC compounds were higher than the reference silica except 1.2 M desulphated CNC compound prepared with APS silane at 300% strain. The material was unable to be stressed up to 300%. The possible explanation may be due to brittleness of the materials which were reasonably stiff to the point of not been able to stress up to 300%. More so, high reactivity of APS silanes and the high impact of the soda treatment could have made contributions to this.

Property	S-TESPD	0.3APS	0.6APS	0.9APS	1.2APS
Stress 10% [MPa]	0.38	0.48	0.51	0.40	0.48
Stress 50% [MPa]	1.08	1.63	1.71	1.39	1.84
Stress 100% [MPa]	1.91	3.60	3.71	3.11	4.34
Stress 300% [Mpa]	10.02	14.93	15.66	14.17	-
Elongation at break [%]	386.82	353.93	398.07	310.22	268.87
Tensile strenght [MPa]	16.22	19.53	22.46	15.24	13.85

Table 4.10 Tensile properties of desulphated compounds prepared with APS silanes.

Property	S-TESPD	0.3TESPD	0.6TESPD	0.9TESPD	1.2TESPD
Stress 10% [MPa]	0.38	0.48	0.54	0.43	0.47
Stress 50% [MPa]	1.08	1.58	1.73	1.42	1.64
Stress 100% [MPa]	1.91	3.29	3.44	2.96	3.59
Stress 300% [Mpa]	10.02	13.07	12.98	11.78	13.87
Elongation at break [%]	386.82	395.25	412.85	445.33	348.90
Tensile strenght [MPa]	16.22	18.07	20.10	21.08	17.16

Table 4.11 Tensile properties of desulphated compounds prepared with TESPD silanes.

There is the possible reaction taking place in APS silanized compounds where there is an electrostatic interaction of sulphates groups with amine moieties. This type of interaction can cause restrictions of polymer chains, thereby making them to tend towards the glassy behaviour. It is important to highlight that not all the immobility of polymeric chains is caused by covalent bonds. Therefore, when the restriction of chains is majorly not a result of covalent interactions, the material resistance to deformations may be poor. Although, chain immobility due to other factors can influence some properties of the composite to a large extent. An increase in tensile strength also show increase in the elastic portions of the material. This is brought about by the increase of filler-polymer interactions. For APS silanized compounds, the tensile strength of 0.6 M desulphated compound showed the highest values. It is possible more coupling sites were made available for interaction with the polymer matrix even though the material was known to have aggregations. The values from 10 to 300% elongation were also noticed to be higher than the referenced silica. It showed a combination of properties from being strong, stiff, and tough. While the desulphated compounds showed properties relatively better than the referenced silica, the 1.2 M desulphated compound for both APS and TESPD silanized compounds showed lower properties. This may be possible as the impact of the highly concentrated soda used in the treatment process would have influenced the material. It was expected that for samples with higher tensile strength, demonstrating large elastic portions, there supposed to be a relative reduction in elongation at break showing the possibility of reduction in polymer chain mobility. However, as observed in this case the response of the materials to tensile stress showed combined improved properties with chain flexibility. The filler networking structures, and crystallisation properties would have also made contributions to this.

4.4 Conclusions

Cellulose nanocrystals are widely produced with sulphuric acid which grafts on the surface a sulphate half ester group. Understanding the effect, they have on CNC composite have been studied. The CNC material was subjected to desulphation using sodium hydroxide. The sulphate ester content deduced from the amount of sulphur was 2.05% for pristine CNC and reduced to 1.66% for the highest desulphated sample at different sodium hydroxide concentrations. Composites were prepared with the desulphated CNC and compatibilized with APS and TESPD silanes. The properties of the composites were relatively indicative of the degree of desulphation. The highly desulphated samples had a high reduction in crystallinity index. It was observed that the

removal of the sulphate groups slightly improved the thermal properties of the filler material and provided more reactive sites for the coupling reaction which led to improvement in the compounds properties. This is an indication that cellulose nanocrystals produced with lower amount of sulphates groups on the surface could lead to better cellulose nanocrystal composites. There was also a corresponding improvement in the tensile properties of the desulphated compounds especially the compound with the lowest values of sulphate content. In this regard, it would be advantageous to produce CNC with lower amount of sulphate half esters.

References

1. Cheng, M., Qin, Z., Chen, Y., Hu, S., Ren, Z., Zhu, M. (2017) Efficient extraction of cellulose nanocrystals through hydrochloric acid hydrolysis catalyzed by inorganic chlorides under hydrothermal conditions. ACS Sustainability Chem. Eng., 5, 4656-4664

2. Dhar, P., Bhasney, S.M., Kumar, A., Katiyar, V. (2016) Acid functionalized cellulose nanocrystals and its effect on mechanical, thermal, crystallization and surfaces properties of poly (lactic acid) bionanocomposites films: A comprehensive study. Polymer, 101, 75-92.

3. Camarero Espinosa, S., Kuhnt, T., Foster, E.J., Weder, C. (2013) Isolation of thermally stable cellulose nanocrystals by phosphoric acid hydrolysis. Biomacromolecules, 14, 1223-1230.

4. Reid, M.S., Villalobos, M., Cranston, E.D. (2017) Benchmarking Cellulose Nanocrystals: From the Laboratory to Industrial Production. Langmuir, 33, 1583-1598.

5. Vanderfleet, O.M., Reid, M.S., Bras, J., Heux, L., Godoy-Vargas, J., Panga, M.K.R., Cranston, E.D. (2018) Insight into thermal stability of cellulose nanocrystals from new hydrolysis methods with acid blends. Cellulose, 26, 507-528.

6. Roman, M. and Winter, W.T. (2004) Effect of sulphate groups from sulphuric acid hydrolysis on the thermal degradation behavior of bacterial cellulose. Biomacromolecules, 5, 1671-1677.

7. Tang, W. K.; Neill, W. K (1964) Effect of flame retardants on pyrolysis and combustion of α-cellulose. J. Polym. Sci., Part C, 6, 65.

8. Voronova, M.I., Surov, O.V., Zakharov, A.G. (2013) Nanocrystalline cellulose with various contents of sulphate groups. Carbohydr. Polym., 2013, 98, 465-469

9. Zhao, Y., Zhang, Y., Lindstrom, M.E., Li, J. (2015) Tunicate cellulose nanocrystals: preparation, neat films and nanocomposite films with glucomannans. Carbohydr Polym 117:286-296.

10. Hasani, M., Cranston, E.D., Westman, G., Gray, D.G. (2008): Cationic surface functionalization of cellulose nanocrystals, Soft Matter, 4, 2238-2244.

11. Abitbol, T., Kam, D., Levi-Kalisman, Y., Gray, D.G., Shoseyov, O. (2018) Surface Charge Influence on the Phase Separation and Viscosity of Cellulose Nanocrystals. Langmuir, 34, 3925-3933.

12. Boluk, Y., Danumah, C. (2014). Analysis of cellulose nanocrystals rod lengths by dynamic light scattering and electron microscopy. J. Nanopart Res., 16, 2174.

13. Borjesson, M., Sahlin, K., Bernin, D., Westman, G. (2018) Increased thermal stability of nanocellulose composites by functionalization of the sulphate groups on cellulose nanocrystals with azetidinium ions. J. Appl. Polym. Sci., 45963.

14. Jacobs, C.; Müller, R.H. (2002) Production and characterization of a budesonide nanosuspension for pulmonary administration. Pharm. Res., 19, 189-194.

15. Beyene, D., Chae, M., Dai, J., Danumah, C., Tosto, F., Demesa, A.B., Bressler, D.C. (2018) Characterization of cellulase-treated fibers and resulting cellulose nanocrystals generated through acid hydrolysis. Materials, 11, 1272.

16. Bhattacharjee, S. (2016) DLS and zeta potential—What they are and what they are not? J. Control. Release, 235, 337-351.

17. Jordan, J.H., Easson, M.W., Condon, B.D. (2019) Alkali hydrolysis of sulphated cellulose nanocrystals: optimization of reaction conditions and tailored surface charge. Nanomaterials, 9,1232.

18. Dong, X. M., Revol, J.-F., & Gray, D. G. (1998). Effect of microcrystallite preparation conditions on the formation of colloid crystals of cellulose. Cellulose, 5, 19-32.

19. Gu, J., Catchmark, J.M., Kaiser, E.D., Archibald, D.D. (2013) Quantification of cellulose nanowhiskers sulphate esterification levels. Carbohydrate polymers, 92, 1809-1816.

20. Araki, J., Wada, M., Kuga, S., & Okano, T. (1998) Flow properties of microcrystalline cellulose suspension prepared by acid treatment of native cellulose. Colloids and Surfaces A: Physicochemical and Engineering Aspects, 142, 75-82.

21. Cheng, L., Wang, Q., Hirth, K., Baez,C., Agarwal, U.P., Zhu, J.Y. (2015) Tailoring the yield and characteristics of wood cellulose nanocrystals (CNC) using concentrated acid hydrolysis. Cellulose, 22, 1753-1762.

22. Mansikkamäki, P., Lahtinen, M., Rissanen, K. (2007) The conversion from cellulose I to cellulose II in NaOH mercerization performed in alcohol-water systems: An X-ray powder diffraction study. Carbohydrate Polymers, 68, 35-43

23. B. J. C. Duchemin, B.J.C. (2015) Mercerisation of cellulose in aqueous NaOH at low concentrations. Green Chem., 17, 3941-3947.

24. Dinand, E., Vignon, M., Chanzy, H., and Heux, L. (2002) Mercerization of primary wall cellulose and its implication for the conversion of cellulose I → cellulose II. Cellulose 9: 7-18.

25. Gong, J., Li, J., Xu, J., Xiang, Z., Mo, L. (2017) Research on cellulose nanocrystals produced from cellulose sources with various polymorphs. RSC Adv., 7, 33486-33493.

26. Cheng, G., Varanasi, P., Li, C., Liu, H., Melnichenko, Y.B., Simmons, B.A, Kent, M.S, Singh, S. (2011) "Transition of Cellulose Crystalline Structure and Surface Morphology of Biomass as a Function of Ionic Liquid Pretreatment and Its Relation to Enzymatic Hydrolysis. Biomacromolecules, 12, 933-941.

27. Rongpipi, S., Ye, D., Gomez, E.D, Gomez, E.W. (2019) Progress and opportunities in the characterization of cellulose - An important regulator of cell wall growth and mechanics. Front. Plant Sci., 9, 1894.

28. Rambo, M.K.D., Ferreira, M.M.C. (2015) Determination of cellulose crystallinity of banana residues using near infrared spectroscopy and multivariate analysis. J. Braz. Chem. Soc., 26, 1491-1499,

29. Park, S., Baker, J.O., Himmel, M.E., Parilla, P.A., Johnson, D.K. (2010) Cellulose crystallinity index: measurement techniques and their impact on interpreting cellulase performance. Biotechnology for Biofuels, 3,10.

30. Roman M., Winter W.T. (2004) Effect of sulphate groups from sulphuric acid hydrolysis on the thermal degradation behavior of bacterial cellulose. Biomacromolecules. 5, 1671-1677.

31. Lin, K.-H., Enomae, T., Chang, F.-C. (2019) Cellulose nanocrystal isolation from hardwood pulp using various hydrolysis conditions. Molecules, 24, 3724.

32. Cotton, R. (1972) effects of carbon black surface properties and structure rheometer cure behavior. Rubber chemistry and technology 45, 129.

33. Cotten, G., Boonstra, B.B, Rivin, D., Williams, F.R. (1979) Effect if chemical modification of carbon black on its behaviour in rubber. Kautschuk gummi und kunststoffe 9, 477.

Chapter 5

Alpha-1,3-glucan as a biofiller

5.1 Introduction

Alpha-1,3-glucan is a water insoluble polysaccharide found mostly in different fungi species. It is medicinally valuable and several research have been published about this [1-5]. Another occurrence of this insoluble polymer is in dental plaques where the presence of 1,6 linkages can make them soluble in water [6,7]. A viable means of making them soluble is by modifications where ester derived alpha-1,3-glucans have been published [8-10]. At the present there is need to reduce the heavy reliance on fossil derived polymeric material and alpha-1,3-glucan could serve as one of a potential replacement in some industrial applications if properly researched.

The biosynthetic procedure of the alpha-1,3-glucan molecule is different according to different fungi species because there is the presence of other competing polysaccharides such as the beta linkages. The synthesis leading to the formation of dental plaques has been studied and replicated [8]. Here, glucosyltransferase (Gtfs) enzymes catalyse the reaction from sucrose which can lead to the formation of alpha-1,3-glucan chains with high degree of control of the synthetic process. The resulting glucan material maintains interesting properties which could be explored for possible use as reinforcing filler in the tire industry.

Because of the presence of hydroxyl groups on the surface of the glucan, aggregations and agglomerations are unavoidable. Therefore, glucan materials are mainly obtained with particle sizes in the range of 1-5 micrometre. At bigger particle sizes, fillers are unsuitable for use as reinforcing agent in rubber matrix because of huge reduction in the effective particle surface area and problems dispersing the filler in the polymer matrix. Plausible options available to avoid this challenge are to break down the particle sizes or graft some functionality that can reduce the surface energy and increase its hydrophobicity.

In chapter 4, the role of sulphates half ester on CNC surface was explored. CNCs are widely produced with sulphuric acid which confers on the surface half sulphate ester functionalities leading to stable

colloidal suspension. From this stable suspension, it is easier to prepare a composite without the filler sedimenting out of the matrix. Also, when desulphation were carried out, the role of sulphate half esters were obvious and it makes sense to see if sulphates groups could also be grafted on the glucan surface to maintain a stable suspension.

The approach used in Chapter 4 was therefore replicated here by using sulphuric acid to reduce the chain length and to understand the possibility of grafting sulphate half esters on the surface of alpha-1,3-glucan. This is intended to create an alpha-1,3-glucan suspension that could be used to co-precipitate with natural rubber for composite preparation. This approach was considered necessary as the glucan is insoluble in water with huge particle aggregations. Subsequently, the treated 1,3-glucans were used to reinforce natural rubber compounds using silanes as compatibilizing agents. The procedures adopted and characterization results have been explained below.

5.2 Experimental method

5.2.1 Materials

Alpha-1,3-glucan was obtained as described elsewhere [11]. Natural rubber latex, bis(triethoxysilylpropyl)disulphide (TESPD), 3-aminopropyltriethoxysilane (APS) silanes, antioxidants and vulcanizers were provided by Pirelli tyres. Sulphuric and acetic acid were bought from Sigma Aldrich. All materials and reagents were used as received.

5.2.2 Procedure

5.2.2.1 Alpha-1,3-glucan treatment

A 30, 40 and 50% wt./wt. solution of sulphuric acid was prepared and 10 ml each was transferred into a beaker. About 1 g of alpha-1,3-glucan was also added into the beaker and homogenized by stirring. Later, the mixtures were placed on a magnetic stirrer and stirred at 55^0C for several minutes. Reaction time was evaluated from 30 minutes to 120 minutes. At the end of the reaction, about three-fold cold water was used to quench the reaction. Thereafter, it was centrifuged. For the subsequent cycle of centrifugation, samples were refreshed with deionized water, sonicated before repeated centrifugation. After repeated centrifugations, a relatively stable suspension appeared

and was decanted while the residue is discarded. The obtained suspension was transferred into dialysis tubes and dialyzed for 3 days until neutral pH. Subsequently, the suspensions were characterized by DLS, zeta potential and SEM analysis.

Alternatively, for large compounds that would meet the requirement for brabender compounding of compounds up to 10-20 g, the sulphuric acid treatment process is conducted with few centrifugation cycles and endless dialysis with the intent to recover all glucan materials.

Ingredients (PHR)	S-TESPD	G-TESPD	G-APS
		Polymer/filler system	
Natural rubber	100		
Silica	30		
100PHR NR + 30PHR CNC		130	130
		Compatibilizer	
TESPD	2.4	2.4	
APS			2.4
		Vulcanization system	
Soluble sulfur	2	2	2
Zinc oxide	5	5	5
Stearic acid	2	2	2
CBS	2	2	2
		Antidegradants	
TMQ	1	1	1
6PPD	1.5	1.5	1.5

Table 5.1 Compounding formulation for silica compounds made with TESPD silanes (S-TESPD), alpha-1,3-glucan compound made with TESPD silanes (G-TESPD) and alpha-1,3-glucan compounds made with APS silanes (G-APS)

5.2.2.2 Composite preparation

The alpha-1,3-glucan suspension was concentrated at 100^0C until percentage content of glucan reached about 10%. A determined amount corresponding to 30 phr of glucan was weighed and mixed with natural rubber latex. The mixtures were homogenized by magnetic stirring for 20 minutes. Thereafter, glacial acetic acid was added dropwise, and the mixtures were coagulated. The coagulated samples were pressed, chopped in smaller pieces, and soaked overnight. After which, they were dried in an oven until constant weight. The dried materials were compounded in a brabender internal mixer with the recipe shown in table 5.1.

The compounding procedure has been outlined in table 4.1.

5.3 Results and discussions

5.3.1 Particle sizes

The particle sizes of the glucan material were estimated with dynamic light scattering (DLS) and is presented in figure 5.1. The hydrolytic reactions were evaluated from 30 minutes to 120 minutes using sulphuric acid at 30, 40, and 50% wt./wt. The procedure followed the principle of obtaining cellulose nanocrystals using sulphuric acid.

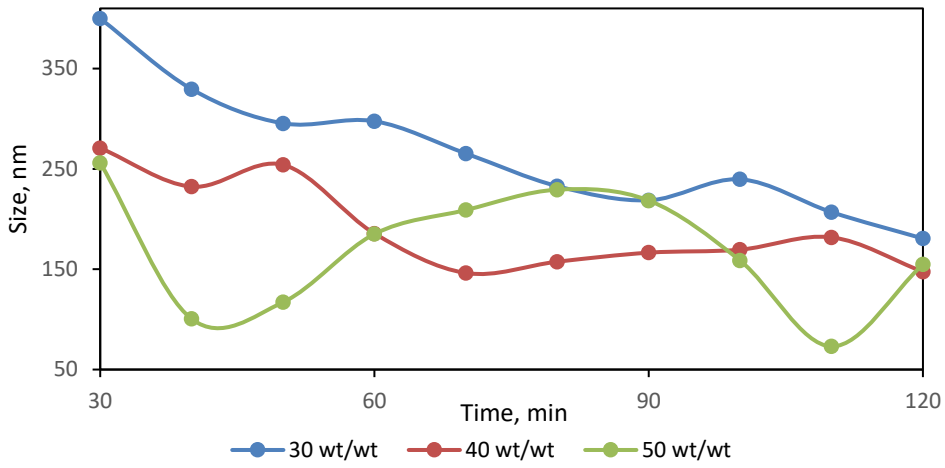

Figure 5.1 Particle sizes of alpha-1,3-glucan hydrolysed with sulphuric acid.

It was intended that the amorphous regions would be hydrolysed to recover glucan nanocrystals in suspension. The suspension obtained and subjected to DLS analysis showed a reduction in glucan particle sizes as the hydrolytic time increased. The glucan particle size was reduced to about 400 nm at 30 minutes and continued to a minimum of 180 nm for 30% wt./wt. acid. The reductions in particle sizes were also enhanced by the particle agitations during hydrolysis. It was observed that a vigorous agitation with mixing incorporating all regions of the beaker was one of the key-factor to effective size reduction. Also, during the several cycles of centrifugation to produce glucan suspension, the samples were sonicated for at least five minutes and this contributed immensely to the particle size reduction.

To produce a nano suspension, the glucan residue needs to be continuously refreshed with water and sonicated until components from the residue are unable to be resuspended. In this case, there is the possibility of increasing the yield. The highest yield that was obtained was when the sample

was hydrolysed with 40% wt./wt. and it was achieved at about 70min of hydrolytic time. The other acid concentration did not produce a yield comparable to that of 40% wt./wt.

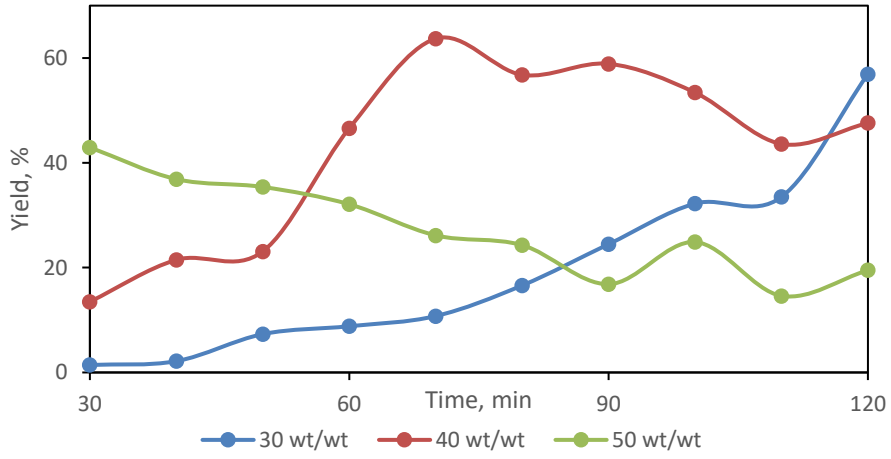

Figure 5.2 Percentage yield of alpha-1,3-glucan hydrolysed with sulphuric acid.

While the intention was to create a stable glucan suspension by also grafting sulphate half esters on the surface as obtainable with cellulose nanocrystals, a large portion of the material could be lost due to the hydrolysis. This is because, all the materials could not be transformed into a suspension as the yield showed that about 40% of the material could be lost. Alternatively, it was observed that the process could be considered as sulphuric acid treatment to reduce particle size instead of producing alpha-1,3-glucan nanocrystals. Therefore, all the materials were recovered after the acid treatment without any losses. As it would be shown subsequently, the treatment was sufficient to reduce the particle sizes by reducing particle size and recovering all the matter. With this treatment, an unstable suspension is created with eventual precipitation after concentrating the suspension. The size of particles in the treated suspension (when studied with DLS) were true estimates as the morphology of the glucan was later resolved to be spherical in shape.

5.3.2 SEM

The particle morphology was studied with scanning electron microscopy and presented in figure 5.3. The morphology gives a clue on the aggregate structures that can be formed within the polymer matrix. The suspension obtained after alpha-1,3-glucan treatment was sonicated. A few amounts of the sample were dispersed in distilled water and sonicated again. Thereafter, a few drops of the suspension were dispersed in ethanol, sonicated, and deposited on a stub for analysis. About 5 to 7 nm of carbon nanoparticles were sputtered on the surface to aid in image acquisition.

The morphology of the glucan showed a spherical-like particles aggregating into irregular shapes. It is indicative of a broad range of particle size distribution with more primary particles fusing into aggregates. Glucan in several species was revealed to be fibrillar with a thickness of 10-14 nm [11-13]. The same synthetic procedure using glucosyltransferase enzymes showed glucan with fibrillar morphology [14]. There are possibilities that the glucan acid treatment resulted in chain dissolution leading to small fragment of glucose units. In general, the morphology depicts spherical particles with low structural disordered aggregates.

The images were acquired at 200 nm scale with different magnifications. At the lower part of the image with higher resolutions, the particle sizes showed a broad range of sizes corresponding to the DLS measurements which estimated the average particle sizes. On the large particle size estimated with SEM, fused particles measured about 249 nm longitudinally were observed. It was also observed that on the surface of the large particles, smaller sized particle not expected to measure up to 30 nm were fused on the surface, indicated by the arrows. With this type of morphology, there is the indication of very high aggregations and the aggregate structures are combination of wide range of primary particle sizes than may find difficulty establishing a well-ordered aggregating structure. In general, alpha-1,3-glucan morphology was irregular spherical structure tending to fuse to each other. This type of morphology is different from the rod-like cellulose nanocrystals. However, it is relatively similar to silica nanoparticles and the reinforcement behaviour is expected to be similar to that of silica filled compounds.

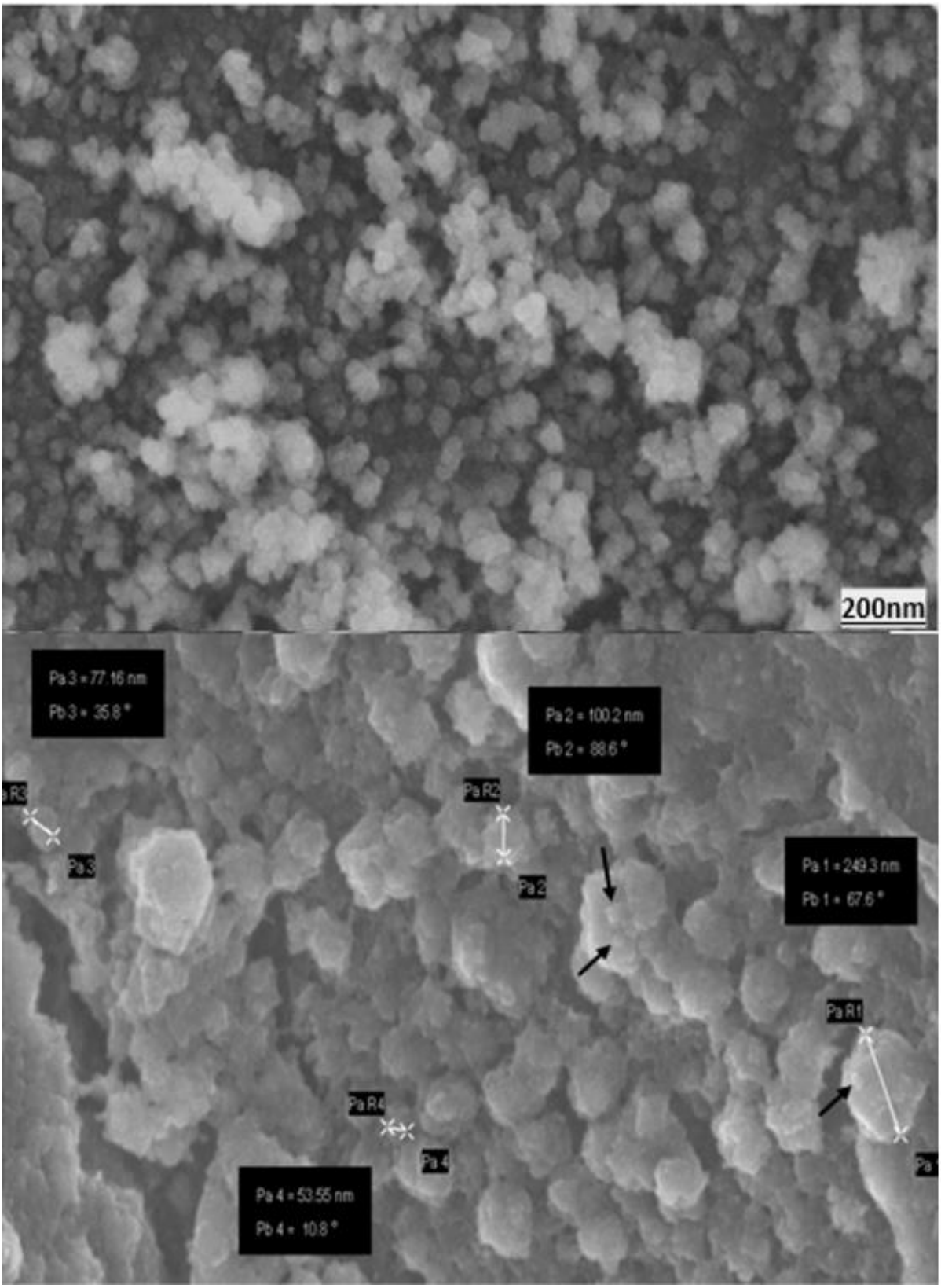

Figure 5.3 SEM image of alpha-1,3-glucan morphology.

5.3.3 XRD

An X-ray diffraction was used to study the crystallinity of the glucan polysaccharide before and after treatment. In figure 5.4 is shown the crystalline peaks of the alpha-1,3-glucan and the treated glucan (N-Glucan). The peaks showed a higher intensity of the untreated glucan. The higher intensities in part may be attributed to contributions from water crystallites as the sample was relatively hydrated. Although it was dried before data acquisition, the peaks are closely related to hydrated glucan XRD data reported elsewhere [3, 14]

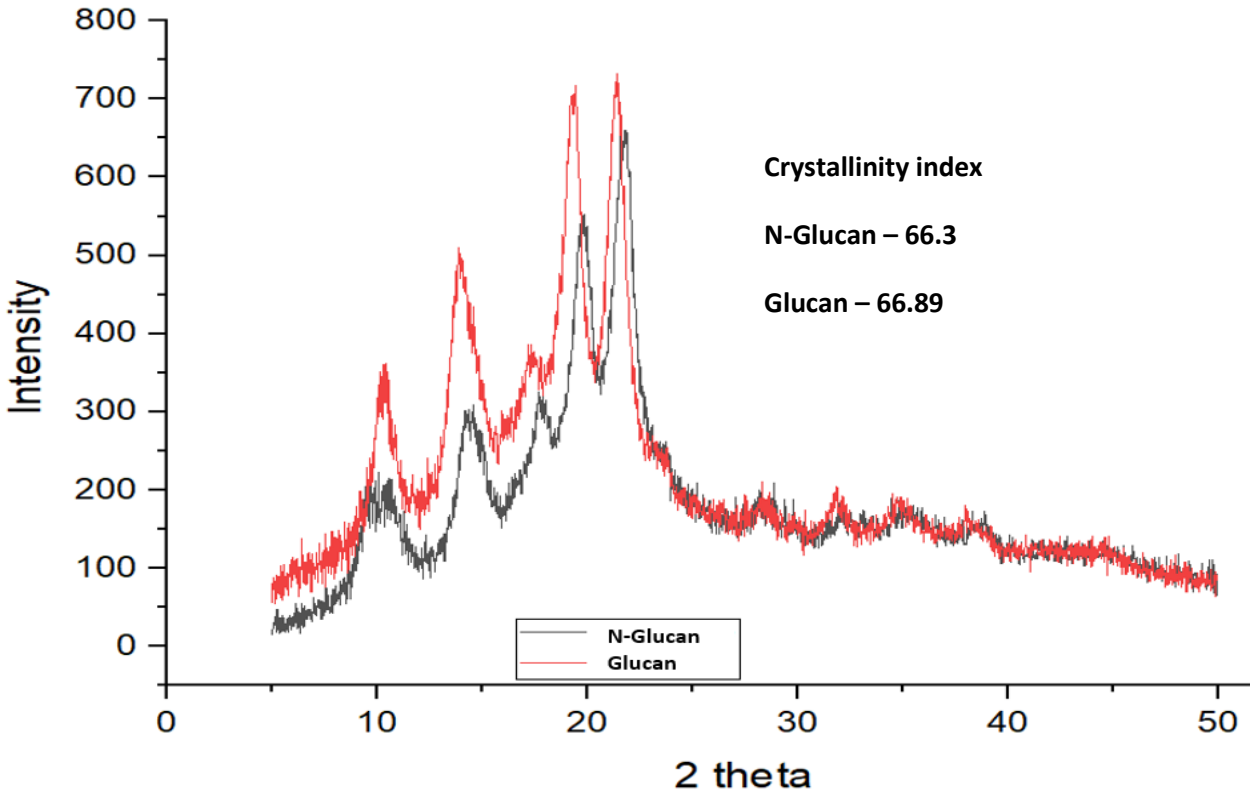

Figure 5.4 Crystalline peaks of untreated (Glucan) and treated (N-Glucan) alpha 1,3 glucan.

About four glucan polymorphs have been established. Polymorph II exists as hydrated glucan while polymorph IV exists as anhydrous glucan [15]. The treated glucan has crystalline peaks that is very similar to the hydrated glucan and in the same crystalline planes, but at different intensities. After the treatment, there was a slight reduction in the crystallinity as shown on the crystallinity index. This may infer that the treatment had not particularly hydrolysed the amorphous regions to produce nanoparticles. Rather, it could be assumed that there was partly a chain dissolution or opening of the glucan structure where part of the water formed crystallites was removed. Despite the

treatment, the results still show that a considerable part of the glucan compound remains crystalline and the hydrogen bond networking has not been destroyed.

5.3.4 TGA

Thermogravimetric analysis was conducted on the glucan filler to understand the thermal properties. This is very important as certain processing temperatures may require thermal stability of fillers for composite preparation. Below is shown the evolutional response of glucan in a wide range of heating temperatures.

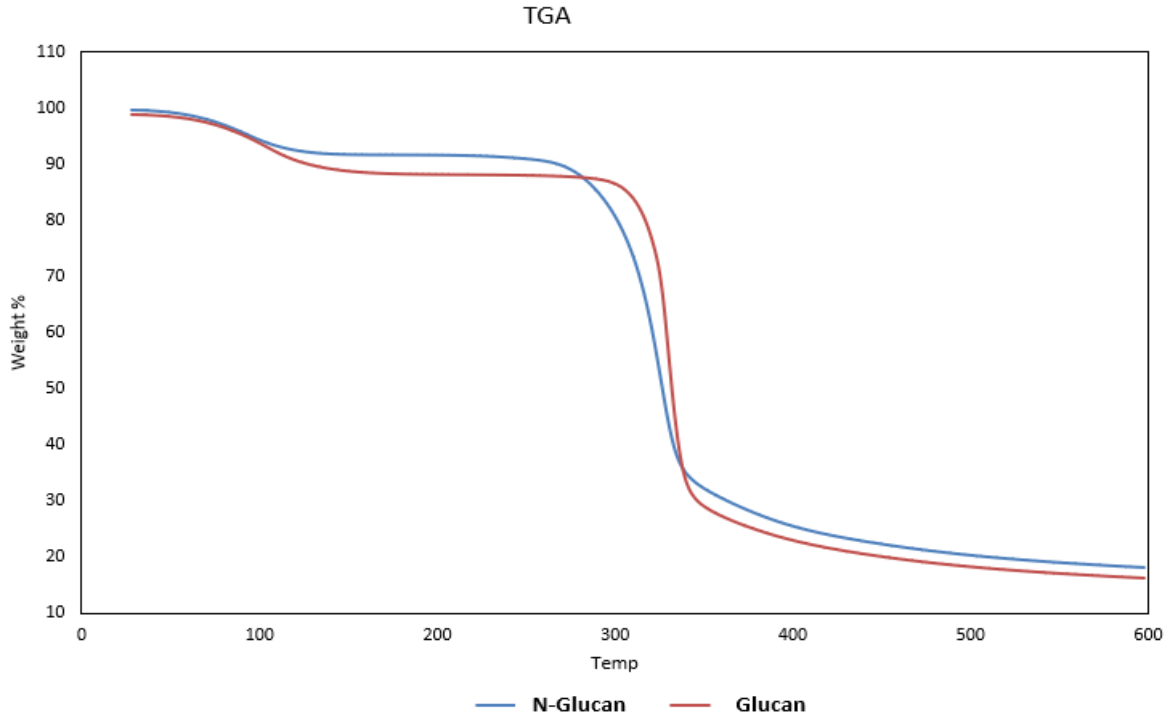

Figure 5.5 Thermogravimetric curve of treated (N-Glucan) and untreated (Glucan) alpha 1,3-glucan

From figure 5.5, there was a percent loss in weight of both glucan materials from 30 to 100^{0}C. This could be attributed to absorbed water. From 100^{0}C, the loss in weight remained constant over a wide range of temperatures with the untreated glucan having a higher loss in weight. At 270^{0}C, thermal degradations start for the treated glucan. However, the start of thermal degradation for untreated glucan delayed until at 303^{0}C. Similar thermal behaviour of glucan has been published [16, 17] with many improvements recorded only when they were functionalized to ester derivatives and subsequent substitution of the hydroxyl groups. The early degradation observe with the treated glucan could partly be explain that the chain scissoring has exposed the material to higher thermal impact. However, at this temperature, it is tenable for processing with some polymeric compounds.

5.3.5 Vulcanization properties

The vulcanization properties of alpha-1,3-glucan compounds were conducted to understand the extent of crosslinking that was achieved with glucan compounds. Compounds were prepared with TESPD and APS silanes and compared with silica compounds. The curing conditions were at 150^0C and at 30 minutes and results shown in table 5.2.

Parameters	S-TESPD	G-TESPD	G-APS
TS2 (min)	9.72	4.73	2.33
T90 (min)	15.73	8.13	4.42
CRI (min-1)	19.96	29.41	47.85
ML (dNm)	1.61	1.38	1.7
MH (dNm)	12.3	13.4	13.22
ΔM (dNm)	10.69	12.02	11.52

Table 5.2 Vulcanization properties of alpha-1,3-glucan compounds.

The vulcanization kinetics of glucan in comparison to the reference silica compounds showed an improved trend. Silica particles are spherical with the tendencies of adsorbing curatives. From the SEM image analysis, glucan was considered spherical just as silica. However, the crystallinity index which may not be applicable to silica because of the amorphous nature would have influenced the curing kinetics by restricting the absorption of curatives. For both silanes, the scorch time of glucan compounds was lower, and the optimum curing time T90 was higher compared to silica compounds. The curing behaviour of glucan is considered similar to that of cellulose nanocrystals by being faster. Although the types of silanes used, including an effective hydrolytic and condensation reactions, influences the vulcanization kinetics, it seems, the curing behaviour of glucan and cellulose are similar. Considering the high torque generated during the curing, glucan compounds had a higher crosslinking density as shown on the difference in torque ΔM. The curing rate index of the glucan compounds were higher compared to that of silica compounds and this also could be attributed to the crystallinity of glucan not promoting curative absorption. With the early vulcanization, also comes early reversion and it is expected that if the glucan compounds are cured before 14 minutes, there would be improved properties. Curing up to 30 minutes as it was done leads to the loss of sulphur bridges which can compromise the quality of the composite.

5.3.6 Dynamic mechanical analysis

The dynamic mechanical analysis of alpha-1,3-glucan compounds were studied to understand the strain dependence of the viscoelastic properties of glucan compounds. Glucan compounds were prepared and compared with silica made compounds as reference and results both for green and vulcanized compounds showed in figure 5.6 and 5.7.

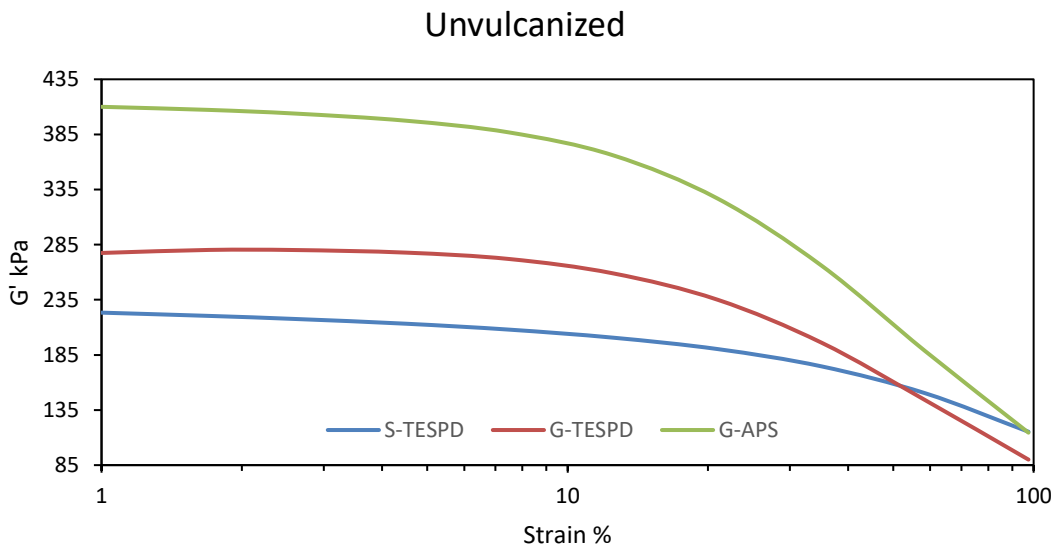

Figure 5.6 Storage moduli of unvulcanized alpha-1,3-glucan compounds made with APS silanes (G-APS), TESPD silanes (G-TESPD) and compared with silica compounds made with TESPD silanes (S-TESPD)

Green glucan compounds made with APS silanes had a higher storage modulus at lower oscillatory strains. It was followed by glucan compounds made with TESPD silanes. This is an indication of higher filler dispersion as well as good filler-filler interactions which APS silanes are most remarkable at providing. At progressive strain sweep, the filler networking was broken down. For APS glucan compound, the un-recoverability of filler network was mostly observed at about 20% strain. At this point, there were huge breakdown of filler networking. The green state of the various compounds is a clear indication of glucan interesting properties being more reinforcing than silica compounds. In this case, for the silanes that were used, efficient dispersion was achieved with a better filler-filler networking. Although at higher storage modulus, there is a relatively correlation to a higher Payne effect when the material is subjected to higher oscillating deformations. As shown in table 5.3, in the unvulcanized compounds, there is more hysteresis for APS prepared compounds which is because of the filler-networking breakdown.

Payne effect	S-TESPD	G-TESPD	G-APS
Unvulcanized	108.03	187.44	295.56
Vulcanized	343.18	193.73	147.84

Table 5.3 Payne effects of vulcanize and unvulcanized glucan compounds compared with silica compounds.

The green compounds were cured at 150^0C and at 30 minutes and the contributions of sulphur bridges to the various compounds were studied. Comparable to the green compounds, the storage modulus increased remarkably with silica compound showing the highest storage modulus at low deformations, although the differences were not overtly remarkable. When considering the reinforcement pattern, it is easy to observe that the reinforcement mechanism was almost the same as reflected in figure 5.7. From the SEM images, the alpha-1,3-glucan fillers showed spherical-like particles closely related to the morphology of amorphous silica. These spherical-like particles are not highly reinforcing compared to rod-like fillers with higher aspect ratio such as cellulose derivatives. It is therefore easier to infer that the reinforcement mechanism of both silica and glucan compounds are relatively the same.

On the account of glucan compounds having lower storage modulus at lower strain in the vulcanized state, it is possible to infer that the fused nature of the primary particles with a broad range of particle size distribution were highly irregular with possibilities of not being able to form high aggregate structures that can network and confer good reinforcement on the compounds. This is not minding the fact that the green compound has already shown good dispersion.

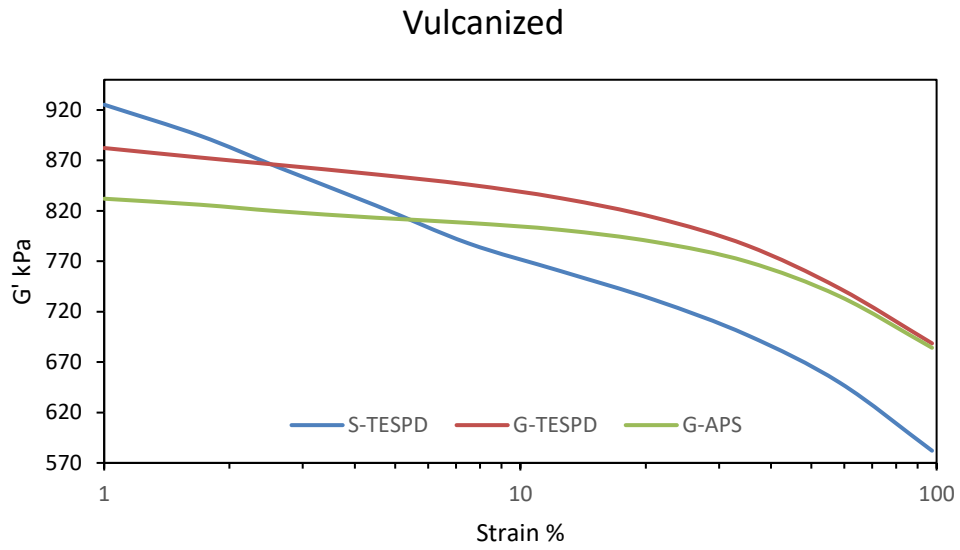

Figure 5.7 Storage moduli of vulcanized glucan compounds made with APS silanes (G-APS), TESPD silanes (G-TESPD) and compared with silica compound (TESPD).

In the uncured state, the properties of APS silanized compounds showed better reinforcement which is the opposite compared to the vulcanized. This occurrence could be attributed to the realization of early reversion because of over curing. In essence, at about 8 minutes, a t_{100} was achieved for APS silanized glucan. With the tightest torque achieved at this time, the remaining vulcanization process (additional 22minutes) were seen as a period where the necessary features that promotes reinforcements were compromised and it is not unusual to see the storage modulus of APS compounds at the vulcanized state being reduced. In general, it is possible to conclude that the reinforcement of glucan compounds is very similar to silica, and the storage modulus G' could have been higher than that of silica if not for the vulcanization conditions that were imposed on the glucan compounds.

The tangent delta as estimated below is the ratio of the elastic portion to the viscous portions of a viscoelastic material. It shows the damping properties of rubber compounds and results of the tangent delta behaviour are shown in figure 5.8.

Recall that it was highlighted earlier about the good dispersion and possible polymer-filler interaction promoted by APS silanes. This polymer-filler interactions and high degree of crosslinking is a key-factor to increasing the elastic portions of the composite and thereby reducing the tangent delta. At low strain, the tangent delta properties of glucan compounds were lower than silica referenced compound. This shows that glucan compounds had a higher filler-polymer interaction

thereby increasing the elastic portions of the material. However, at high strain, the tangent delta values increased which could be attributed to the strain amplification effect destroying the filler networks and releasing polymer chains not having contact with filler networks.

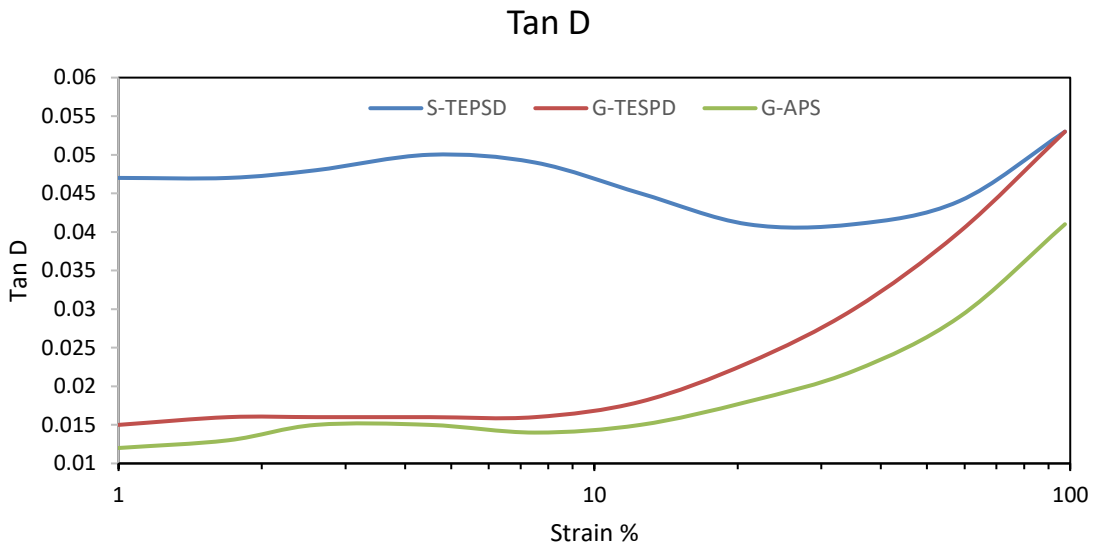

Figure 5.8 Tangent delta of vulvanized alpha-1,3-glucan and silica compounds

The aggregate formations of glucan fillers are indicative of low structures and reinforcement. In the polymer mix, there could be good polymer-filler interactions on the surface. But a large portion of the glucan fillers are fused in a manner that may not be accessible to adjacent polymeric chains for interactions, thereby increasing the viscous response of the polymer chains during dynamic deformations. This assertion may be considered realistic when considering the Tan D curves of glucan compounds and silica compound. For silica compound, the response evolved by an increment in the values, and then forming a plateau before going upward again at high strains. The filler structures could be related to this nature of response, whereas that of glucan showed a steady increase to high strains. The values of tangent delta were low compared to the reference material, and it would be expected that much lower Tan D values could be obtained if glucan compounds are prepared in a way that polymer chains are processed to extend interactions to the severally fused inaccessible filler particles. Or maintaining treatment conditions that can promote particle sizes of similar distribution and able to form higher aggregate structures.

5.3.7 Tensile properties

Alpha-1,3-glucan compounds prepared with APS silanes and TESPD silanes alongside reference silica compounds were subjected to tensile measurements to understand the response of the material in tensile shear mode. Results are shown in table 5.4.

Property	S-TESPD	G-TESPD	G-APS
Stress 10% [MPa]	0.38	0.36	0.40
Stress 50% [MPa]	1.08	1.08	1.45
Stress 100% [MPa]	1.91	1.89	3.13
Stress 300% [Mpa]	10.02	6.48	-
Elongation at break [%]	386.82	389.30	178.84
Tensile strenght [MPa]	16.22	10.20	5.95

Table 5.4 Tensile properties of glucan compounds made with APS silanes (G-APS), TESPD silanes (G-TESPD) and silica compounds made with TESPD silanes (TESPD).

The tensile properties of silica compounds serving as reference was relatively similar to glucan compounds made with TESPD. Beginning at 10% strain, the stress values of G-APS were higher than both silica and glucan TESPD compounds. The trend of G-APS increased remarkably and was also higher than TESPD prepared compounds up to 100% strain. At 300% strain, the G-APS silanized compound was seen to providing no values. It shows that the material could not be strain up to 300%. Subsequently, the elongation at break of this compound was remarkably lower compared with the reference silica. This incidence could be attributed to high crosslinking and reversion and the tendency of the material becoming brittle. Ordinarily, when polymeric materials are brittle, they can fail at few strains. The contributions of voids could also remarkably contribute to such failure. It is difficult to observe the impact of these voids in a composite during cyclic deformations because they can realign themselves and may be unnoticed. They are most noticeable when materials are subjected to tensile deformations. In the previous chapters on cellulose nanocrystals, this feature was observed that it was difficult to strain some APS-cellulose material up to 300%. It seems the role played by the amine groups in the amino silane structure does not only promote dispersion, but it also creates rigid siloxane structures [18] within the polymeric composite and thereby restricting the tendency to flexibility of polymeric chains. In this scenario, it may be preferable to reduce the amount of the amino silanes that are used.

Strains at 300% are crucial for the tire industries and the reference silica compound was shown to have better properties. Generally, good filler-polymer interaction is important to achieving high

tensile properties. However, irrespective of any possible interactions, the intrinsic properties and the structural formations of filler compound within the polymeric matrix are other major contributions. In the case of alpha-1,3-glucan, it could be seen that the filler has low structures, and the reinforcement is low. Tensile properties of alpha-1,3-glucan films at 70^0C were published [19] and results were much lower than the results obtained in this work. This is partly also, the contributions of the composite processing method which if studied and improved, could improve the tensile properties to be higher than the reference silica.

5.4 Conclusions

The use of alpha-1,3-glucan as a potential reinforcing filler has been explored in this chapter. There are different synthetic route to synthesizing alpha-1,3-glucan, but the process gaining industrial relevance is the enzymatic polymerization of sucrose using glucosyltransferase enzymes. Most often, the resulting glucan polymer agglomerates to large particle sizes extending to the micrometre range which is not suitable to be used as reinforcing filler. This work therefore employed similar technique used in cellulose nanocrystal hydrolysis to hydrolyse the glucan compounds with intent to obtain glucan nanocrystals. This procedure gave a glucan suspension with a relatively colloidal stability and yield reaching 60% depending on the acid concentration. However, for the preparation of compounds large enough for composite preparation and characterization, the treatment was done, and all samples were recovered through dialysis. In this case the process of glucan was considered as targeted at scissoring the length of the polymeric chains and not producing glucan nanocrystals which was confirmed with relatively the same crystallinity before and after treatment. The SEM images of the treated glucan showed spherical-like fused structures which were deemed low reinforcing. Thereafter, they were prepared with TESPD and APS silanes in natural rubber compounds. When compared with silica prepared compounds, the reinforcement of glucan was seen to be lower for both silanes that were used. The tensile properties were slightly inferior also to silica. However, the vulcanization kinetics were relatively better than silica. From observations, the glucan filler would need higher filler loading compared with the 30 phr used in the studies. Although it is promising filler, more studies targeting at exploring the use of different silanes or modification methods, and processing techniques would be needful to establish the entrant of glucan as potential reinforcing filler.

References

1. Buddana, S.K., Varanasi, Y.V.N., Shetty, P.R. (2015) Fibrinolytic, anti-inflammatory and anti-microbial properties of -(1-3)-glucans produced from Streptococcus mutans (MTCC 497) Carbohydrate polym., 115, 152-159.
2. Pingyi, Z., & Peter, C. K. C. (2002). Evaluation of sulphated Lentinus edodes - (1-3)-D-glucan as a potential antitumor agent. Biosciences, Biotechnology and Biochemistry, 66, 1052-1056.
3. Złotko, K., Wiater, A., Wasko, A., Pleszczynska, M., Paduch, R., Jaroszuk-Scisel, J., Bieganowski, A. (2019) A Report on Fungal (1→3)-α-d-Glucans: Properties, Functions and Application. Molecules, 24, 3972.
4. Leemhuis, H., Pijning, T., Dobruchowska, J.M., Leeuwen, S.S., Kralj, S., Dijkstra, B.W., Dijkhuizen, L. (2013) Glucansucrases: Three-dimensional structures, reactions, mechanism, α-glucan analysis and their implications in biotechnology and food applications. J. Biotechnol., 163, 250-272.
5. Zhang, L., Zhang, M., Chen, J., Zhang, F. (2001) Solution properties of antitumor carboxymethylated derivatives of α-(1→ 3)-d-Glucan from Ganoderma lucidum. J. Polym. Sci., 19, 283-289.
6. Loesche, W. J. (1986) Role of *Streptococcus mutans* in Human Dental Decay. J. Microbiol. Rev., 50, 353-380.
7. Monchois, V., Willemot, R. M., Monsan, P. (1999) Glucansucrases: mechanism of action and structure function relationships. FEMS Microbiol. Rev., 23, 131-151.
8. Puanglek, S., Kinura, S., Enomoto-Rogers, Y., Kabe, T., Yoshida, M., Wada, M., Iwata, T. (2016) *In vitro* synthesis of linear α-1,3-glucan and chemical modification to ester derivatives exhibiting outstanding thermal properties. Scientific report, 6, 30479.
9. Gericke, M., Tied, A., Lenges, C., Heinze, T. (2020) a-1,3-Glucan benzoate - A novel polysaccharide derivative. Advanced industrial and engineering polymer research, 3, 71-76.
10. Kasat, R.B., Paullin, J.L. (2014) Preparation of poly alpha-1,3-glucan esters and films therefrom. WO Patent 2014/105698 A1.
11. Sanchez-Hernandez, M.E., Garcia-Mendoza, C., Novaes-Ledieu, M. (1993) Two-different alkali-soluble alpha-glucans in hyphal wall of the basidiomycete *Armillaria mellea* Microbiología, 9, 34-42.

12. L.M. Carbonell, L.M., Kanetsuna, F., Gil, F. (1970) Chemical morphology of glucan and chitin in the cell wall of the yeast phase of *Paracoccidioides brasiliensis*. J. Bacteriol., 101, 636-664.
13. San Blas, G., Carbonell, L.M. (1974) Chemical and ultrastructural studies of the yeastlke and mycelial forms of *Histoplasma farciminosum*. J. Bacteriol., 119, 602-611.
14. Kobayashi, K., Hasegawa, T., Kusumi, R., Kimura, S., Yoshida, M., Sugiyama, J., Wada, M. (2017) Characterization of crystalline linear (1 → 3)-α-D-glucan synthesized in vitro. Carbohydrate Polymers, 177, 341-346.
15. Ogawa, K., Yui, T., Okamura, K., Misaki, A. (1994) Crystalline Features of Streptococcal (1 → 3)-α-D-Glucans of Human Saliva. Biosci. Biotech. Biochem., 58, 1326-1327.
16. Puanglek, S., Kinura, S., Iwata, T. (2017) Thermal and mechanical properties of tailor-made unbranched α-1,3-glucan esters with various carboxylic acid chain length. Carbohydrate Polymers 169, 245-254.
17. Fukata, Y., Kinura, S., Iwata, T. (2020) Synthesis of α-1,3-Glucan branched ester derivatives with excellent thermal stability and thermoplasticity. Polymer Degradation and Stability 177, 109130.
18. Xie, Y., Hill, C.A.S., Xiao, Z., Militz, H., Mai, C. (2010) Silane coupling agents used for natural fiber/polymer composites: A review. Composites: part A, 41, 806-819.
19. Mok, J.W., Behabtu, N., Lenges, C., Sendijarevic, I., Sendijarevic, A. (2021) Evaluation of the engineered polysaccharide alpha-1,3-glucan in a thermoplastic polyurethane model system. J. Appl. Polym. Sci., 138, 49931

Chapter 6

CNC as a biofiller: Enzymatic modifications

6.1 Introduction

Cellulose nanocrystals are actively explored with wide areas of prospective applications [1-6]. Their use as fillers in polymeric composites is currently promoted due to its fascinating properties and the green nature of CNC. Notwithstanding the enormous benefits, the hydrophilic nature of CNC requires surface modification to be compatible with polymeric matrixes for composite preparation and several methods of surface modifications have been reviewed [4, 7-13].

Among several successful methods of functionalizing fillers for compatibility with polymer matrixes is the use of silanes. These bifunctional silanes are added to the composite during preparation or pre-treated with the filler and are the major compatibilizer in the tire industry. Their inorganic nature and search for sustainable and greener composite has made enzymatic modification one of alternatives. The green character of different cellulose modification processes has been reviewed [14-18] with comparisons on the different processes alongside overall score on a green character scale. This is in line with the principles of green chemistry, considering the green origin of the treatment, avoiding harmful solvents, avoiding toxic materials, minimizing energy use, biodegradability, avoiding material waste, avoiding petrochemicals, recyclability, does not hurt cellulose and scale-up friendly. These are part of reasons enzymatic modification is being explored.

Enzymatic processes which are currently explored takes place at mild reaction conditions, environmentally friendly, and can target reactant molecules preferentially. The bottleneck that comes with the use of enzymes is their non-solubility in organic media and the attendant lack of activity in several polar organic solvents. The solubility of enzymes in aqueous system does not favour synthetic reactions. Chemical modification of enzymes with the use of surfactants and extraction from aqueous buffers to organic solvents [19] are well established procedures to overcome the solubility drawbacks. In most cases, a combination of several organic solvents as reaction media is used to adapt the enzymes. This eventually reduces the green character of the process as more complex waste products may be generated with difficulties in recycling.

Besides the preparation of cellulose nanocrystals enzymatically, there are reports of enzymatic modifications in the literatures. Some reports that evaluated enzymes catalysed modification showed lipases as good candidate for CNC modification [20-24]. But most of these are silent on waste recoveries and efficient purifications. Most of the papers uses esters as donors, at stoichiometric ratios that may defeat a possible scale-up. These drawbacks were studied, and alternative means were explored to overcome the drawbacks.

In this chapter, vinyl acetate and vinyl methacrylate have been considered as ester donors to modify the CNC surface for dispersion and compatibility on one side, and the exploitation of the carbon-carbon double bond in vinyl methacrylate that would not only enhance the dispersion and compatibility of the modified CNC but also promoting a cross-linking between the filler and polymer matrix during vulcanization. The challenges in previous research works would be attempted to address.

6.2 Experimental methods

6.2.1 Materials

CNC suspension was procured from Celluforce and freeze dried for use. Vinyl acetate, vinyl methacrylate, Amano Lipase A from *Aspergillus niger*, dimethyl sulfoxide, sodium phosphate monobasic, and sodium phosphate dibasic were procured from Sigma Aldrich. Natural rubber latex, vulcanization system including soluble sulphur, stearic acid, zinc oxide, and antidegradants were provided by Pirelli Tires and were used as received.

6.2.2 Procedures

6.2.2.1 Lipase catalysed transesterification

The transesterification reaction scheme using vinyl acetate and vinyl methacrylate as ester donor is presented in figure 6.1 and briefly described below.

Vinyl esters that were used subsequently as donors are good leaving groups in nucleophilic substitutions and are suitable for transesterification reactions [19]. In a stable reaction, vinyl

alcohols are the by-products which quickly convert to acetaldehyde thereby favouring the formation of desired cellulose esters.

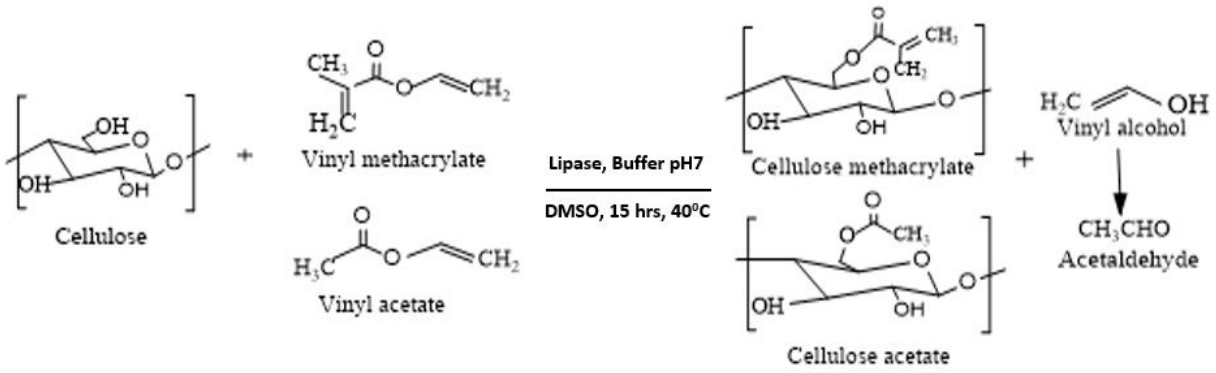

Figure 6.1 Transesterification of CNC with vinyl methacrylate and vinyl acetate

Experimental procedure was adopted from previous work [20] with modifications. Briefly, about 10g of dried cellulose nanocrystals was dispersed in 150-200 ml DMSO by heating at 80^0C for 10 minutes and allowed to cool. Thereafter, 650 mg of lipase from *Aspergillus niger* was added to 100 ml 0.1 M pH 7 phosphate buffer. The dissolved lipase was mixed with the dispersed CNC and allowed to stay for few hours for equilibrations. Afterwards, 50 ml vinyl methacrylate or vinyl acetate was added and reacted at 40^0C for 15-24 hours. Intermittently, the mixture was stirred vigorously to homogenize the biphasic system. At the end of the reaction, about 60 ml ethanol was used to precipitate the mixtures and centrifuged to recover CNC pellets. The sample was dialyzed overnight, and the success of the reaction was confirmed by subsequent characterizations.

6.2.2.2 Composites preparation

Functionalized CNC after dialysis was concentrated to 9wt % by heating at 100^0C for few hours with continuous stirring. At the necessary concentration, about 30 phr of the functionalized CNC filler suspension (measuring up to about 10 g CNC) was weighed and added to latex rubber suspension. The mixture was stirred for 20 minutes till homogeneity. Thereafter, about 20ml acetic acid was used to coagulate the mixture by adding dropwise with continuous stirring. The coagulated sample was washed, pressed to remove trapped acetic acid, and chopped into smaller pieces. The chopped coagulated material was soaked in distilled water overnight and dried in an oven at 40^0C till constant weight. The compound formulation recipe is shown in table 6.1.

Ingredients	S-TESPD	CNC-MET	CNC-ACET
Polymer/filler system			
Natural rubber	100		
Silica	30		
100PHR NR + 30PHR CNC		130	130
Compatibilizer			
TESPD	2.4		
Vulcanization system			
Soluble sulfur	2	2	2
Zinc oxide	5	5	5
Stearic acid	2	2	2
CBS	2	2	2
Antioxidants/antiozonants			
TMQ	1	1	1
6PPD	1.5	1.5	1.5

Table 6.1 Formulations in PHR of silica and CNC compounds. S-TESPD: silica compatibilized with TESPD silanes; CNC-MET: methacrylate CNC co-precipitated with natural rubber; CNC-ACET: acetylated CNC co-precipitated with natural rubber.

The functionalized CNC composite was prepared and compared with silica compounds prepared by dry mixing silica with natural rubber using TESPD as a silane compatibilizing agent. The compounding procedure is shown in Table 6.2.

Mixing stage	Time (min)	Temperature (^{0}C)	Activity
Step 1	0	130	Load rubber and filler
	1		Add silanes (for silica compound)
	5		Add stearic acid
	6		Unload
Step 2	0	60	Load masterbatch from Step1
	1		Add sulphur, zinc oxide, CBS, TMQ, 6PPD
	3		Unload

Table 6.2 Mixing procedure for CNC and silica compounds

The different samples were compounded by first setting the temperature of the brabender internal mixer at 130 ^{0}C. When the mixing temperature was attained, samples were added as outlined in table 6.2. Functionalized CNC composites were prepared without silanes and were mostly homogenized few minutes before the addition of stearic acid.

6.2.2.3 Characterizations

Characterizations were carried out on the filler before and after modification and the properties it conferred on the composite was studied. After the modification reactions, FTIR was used to confirm the success of the reaction. The crystallinity index of CNC before and after modification was measured with XRD while the thermal properties of the CNC were measured with TGA. After composite preparation, the dynamic mechanical properties, tensile measurement, and vulcanization kinetics were studied. Details of the characterization techniques have been explained in chapter 3 (3.2.3) and 4 (4.2.2.3).

6.3 Results and discussion

6.3.1 CNC modification

The success of the transesterification reaction was confirmed by FTIR. The FTIR spectra of pristine and modified CNC is shown in figure 6.2. Appearance of absorbance of the carbonyl stretching vibrations of acetylated CNC was observe in the region of 1737 cm^{-1} while that of methacrylate CNC was observed at 1721 cm^{-1} possibly because of the saturated nature of the methacrylate group tending to a lower wavelength. Ester carbonyl peaks ranges from 1600 to 1750 cm^{-1}. However, for cellulose, there is a broad peak in the region of 1660 cm^{-1} depicting the presence of molecularly bound water which is close to the carbonyl peak of methacrylate CNC. For most samples, the broadness of these peaks did overlap the carbonyl peak and it was difficult to observe the presence of a carbonyl peak.

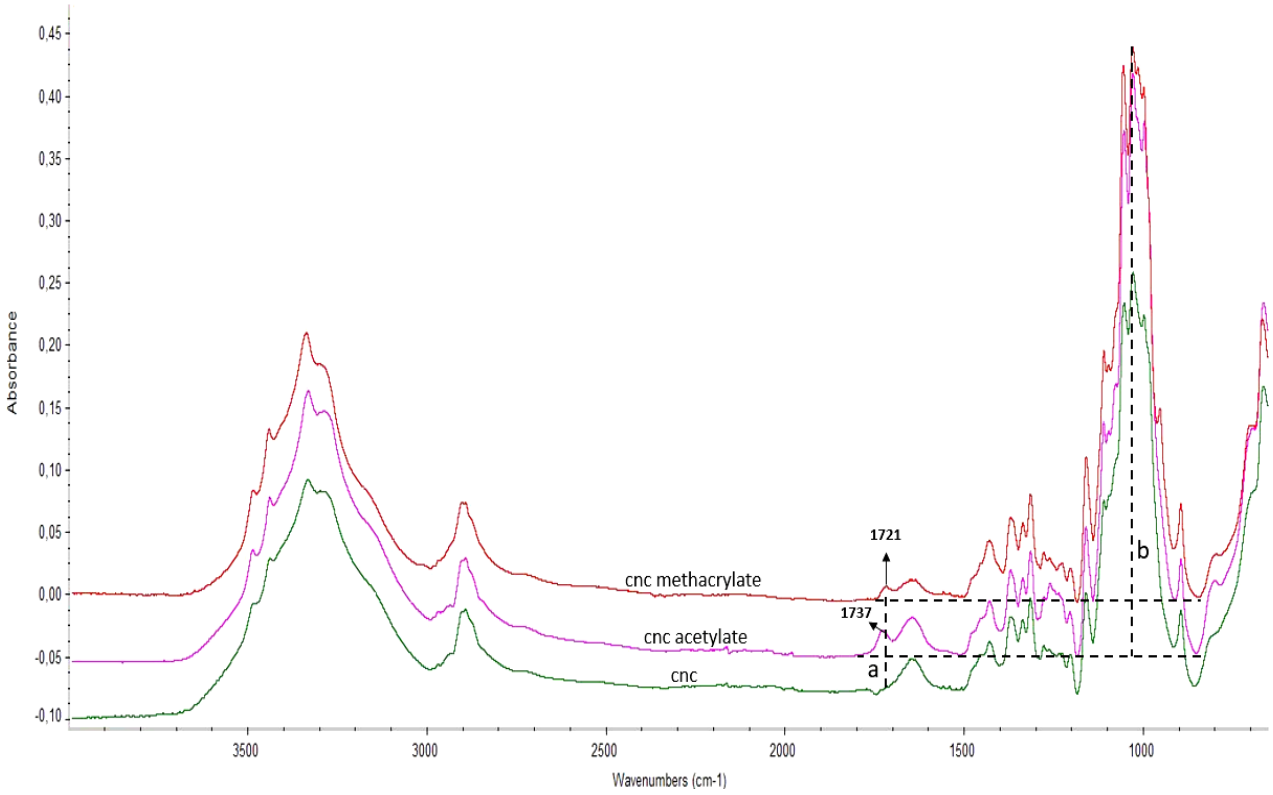

Figure 6.2 FTIR of unmodified and enzymatically modified CNC.

The appearance of the carbonyl peaks was used to estimate the amount of modifying agent that was grafted by using the peak heights ratios (equation 5.1) of the C=O and the C-O stretching vibrations located around 1060 cm^{-1} [25-28].

$$r = a/b \tag{5.1}$$

The C-O assigned to the glucopyranose backbone of cellulose is not affected by the modification and was used as a standard for normalizing the intensity of the carbonyl peaks. A baseline was therefore constructed in the valleys of 1790-1700 cm^{-1} for the carbonyl region and extended to the valleys of 1500 and 860 cm^{-1} to estimate the ratio of $I_{C=O}/I_{C-O}$ which correlates to the percentage of ester that was grafted. For acetylation reaction with grafting taking place on the surface, the intensity of hydroxyl groups in the region of 3400 cm^{-1} is relatively unchanged, as seen also with the methacrylate reaction. It has been established that the esterification reaction follows a first order equation up to 50 hours and this ratio is a valid and reliable means to estimate the amount of grafted modifying agent [29, 30].

From estimation, going by the peak height ratio, the acetylated CNC has a ratio of 0.37 while methacrylate CNC has a ratio of 0.14. However, for esterification reaction, when the ratio (r) deduced from FTIR is less than 0.4, a correlation to the degree of substitution (DS) has been established [29] as shown in equation 5.2. considering that the reaction is taking place on the surface.

$$DS = 0.7r \tag{5.2}$$

The DS estimated from this procedure shows that acetylated CNC had a higher amount grafted on the surface with a DS = 0.26 and the methacrylate CNC having a DS = 0.098.

When DMSO containing solubilized cellulose is mixed with lipase dispersed in buffer, the resulting mixtures are considered exothermic and recorded temperatures had been observed as reaching up to 48 ^{0}C which could affect the enzyme activity. An alternative protocol is to add the enzyme dispersed in the buffer slowly in a bath having a slightly below room temperature with mild shaking to avoid precipitation of CNC. The mixtures are then stayed to equilibrate and to allow the enzymes adjust to the new environment. The addition of the various vinyl esters makes the mixtures heterogeneous and it requires intermittent robust stirring to homogenize the mixtures and create sufficient contact among reactant species.

Figure 6.3 Resultant products after CNC modification

The end of the reaction also comes with the ability of recovering the products of the reaction. After reaction, the products are expected to be CNC, DMSO, unreacted vinyl esters, enzymes, buffer solution and few amounts of acetaldehyde. As shown in figure 6.3, after the precipitation of the mixtures, the entire CNC was recovered and the fluid part of figure 6.3 which possibly contains

DMSO, dissolved enzymes, part of the buffer solution, and unreacted vinyl acetate on the top of the mixtures are meant for recycling. The recovered CNC is expected to contain large amount of the ethanol used for precipitation, part of the buffer solution and probably few amounts of DMSO. By overnight dialysis, they are removed. However, the catalytic activity of the enzymes in the recovered DMSO is expected to reduce although may be sufficient for another cycle of reaction, a buffer solution may not be needed. Hence, it will require dispersing certain amount of CNC for another cycle of reaction without adding additional enzymes and buffer into the system. The possibility of reuse of the reacting solvent was not investigated and could be considered in subsequent research. This reaction procedure shows prospects as reasonable amount of the reacting species could be reused.

6.3.2 SEM

Scanning electron microscopy was used to study the morphology of the modified CNC. The morphology of cellulose nanocrystal is rod or needle-like in nature and the SEM image was needful to understand the impact after modification. SEM images for both cellulose acetate and cellulose methacrylate are shown in figure 6.4a and b. After the modification reaction, the dialyzed suspension of modified CNC was prepared for SEM analysis by dispersing few drops in water and sonicated. Few amounts of the sonicated sample were dispersed again in ethanol and sonicated again before depositing one microliter on a stub. In figure 6.4a is the cellulose acetate which was considered to have a higher grafting. The image showed a preservation of the needle-like structures. Alongside the image acquisition, the particle sizes were also estimated. The length of the longer rod was estimated to be 280.4 nm and a width of 20.98 nm. It is evident that the length of the modified cellulose acetate is still within the nano meter range with little or no aggregations. The image acquisition for cellulose methacrylate was rather different. It showed huge aggregations. Although the needle-like morphology of CNC is visible. This could be attributed to the sample preparation method where it is considered that the sample was not properly diluted and sonicated for a sufficient duration. Ordinarily, estimations from the grafted amount showed that the CNC methacrylate had a lower grafting, and it is expected that there should be lower aggregations on the acquired images. This is on the opposite. Therefore, the preparation method of poor dilution is the only explanation for this occurrence. More so, the image was acquired at lower magnification and the CNC morphology could be considered remarkably preserved.

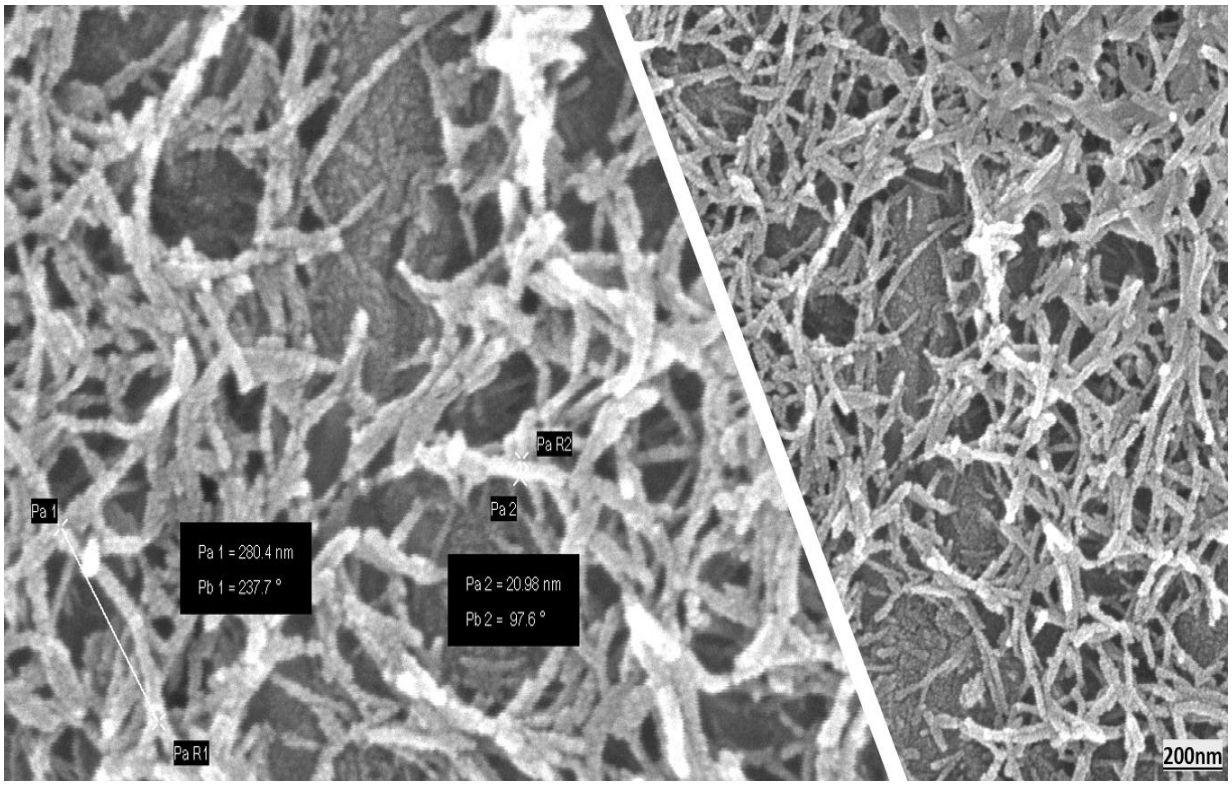

Figure 6.4a SEM image of cellulose at different magnifications.

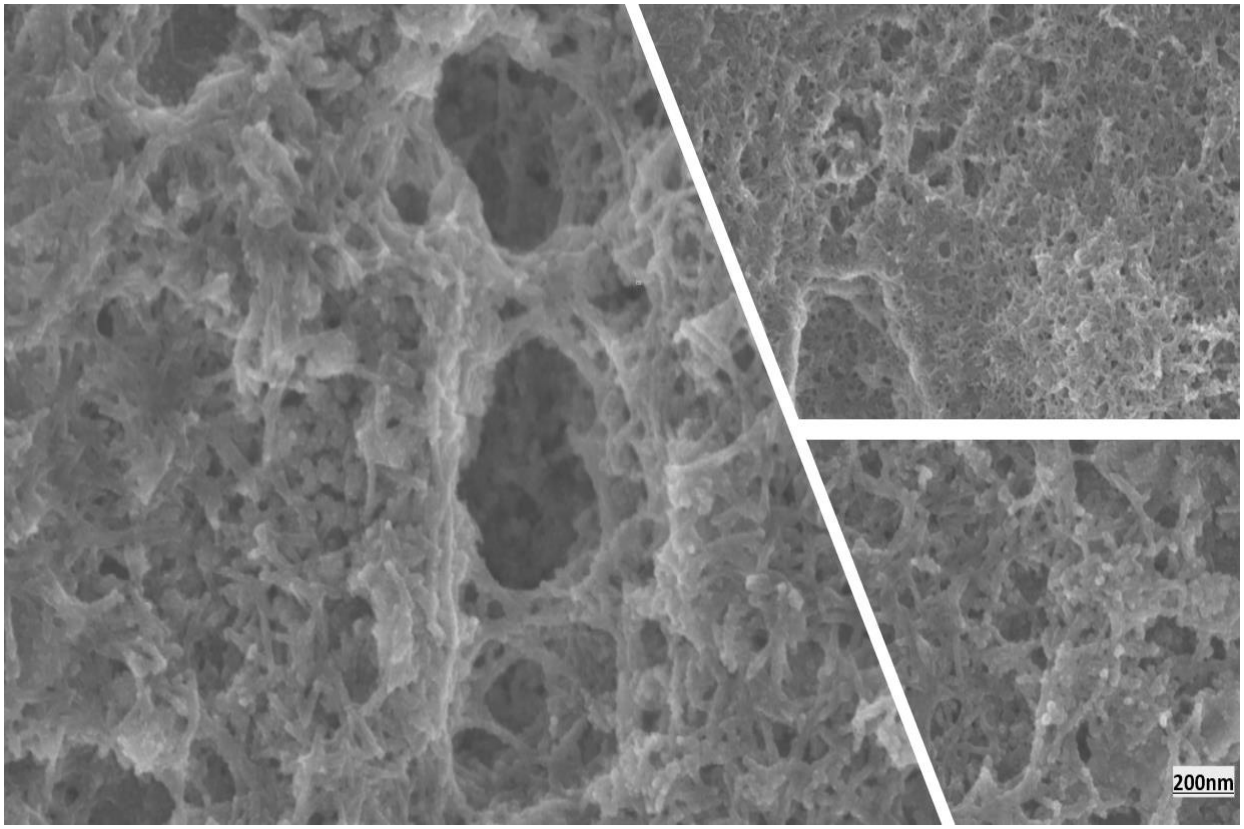

Figure 6.4b SEM image of cellulose methacrylate at different magnifications.

6.3.3 XRD

The crystallinity of the cellulose nanocrystals was confirmed by X-ray diffractions before modifications and after modifications. Generally, after modifications, part of cellulose fibres is opened especially if the reactions proceed to the bulk. In this case, there would be a reduction in the crystallinity index because of the distortion of the hydrogen bonding network and increase in defects within the cellulose fibres. The crystallinity peaks of both cellulose acetate and cellulose methacrylate compared with unmodified CNC are shown in figure 6.5.

From the diagram below, the crystallinity peaks of pristine cellulose, methacrylate, and acetylated CNC at 2Θ is observed around 12.5^0, 15^0, 22.5^0, and 34.8^0 which correspond to the planes of (1 ī 0), (1 1 0) (2 0 0) and (0 0 4). These peaks are typical of cellulose I and II [31, 32] and it is the main form of several commercially available celluloses. Cellulose I is mainly found in native cellulose while cellulose II is obtained by regeneration of cellulose I using sodium hydroxide or other modifications that would result to misalignment of cellulose fibres. The intensities of the crystalline peaks reduced after grafting which showed that the cellulose crystalline structure has been slightly altered. Cellulose has a strong inter hydrogen bonding network that contributes to the ordering of its fibres, hence its high crystallinity. However, DMSO is one of the polar solvents that can solubilize cellulose [33]. The presence of DMSO in the reaction media is expected to have contributed to disrupting part of the hydrogen bonding network which could lead to reduction in the crystallinity, and this could occur even without synthetic reaction. The crystalline peaks up to the 0 0 4 plane are obvious and are considered to contribute mahorly to the crystallinity of cellulose. Therefore, the diffractions from 2-theta range of 5^0 to 50^0 was used and effectively covered the range of these crystalline peaks. There is a faint peak at 38^0 and by extension; Ju *et al.* [34] have identified possible contributions to the crystallinity of cellulose beyond the 2-theta range of 5^0 to 50^0. These subsequent peaks beyond the 0 0 4 planes are extremely low with contributions that could be neglected for comparative purposes.

To estimate the crystallinity of the pristine and modified cellulose, the crystallinity index (CrI) was calculated from the crystalline peaks using Gaussian deconvolution of the crystalline and amorphous regions [35-37] and deducing their ratios subsequently. The crystallinity index of both modified and unmodified cellulose is shown in table 6.3.

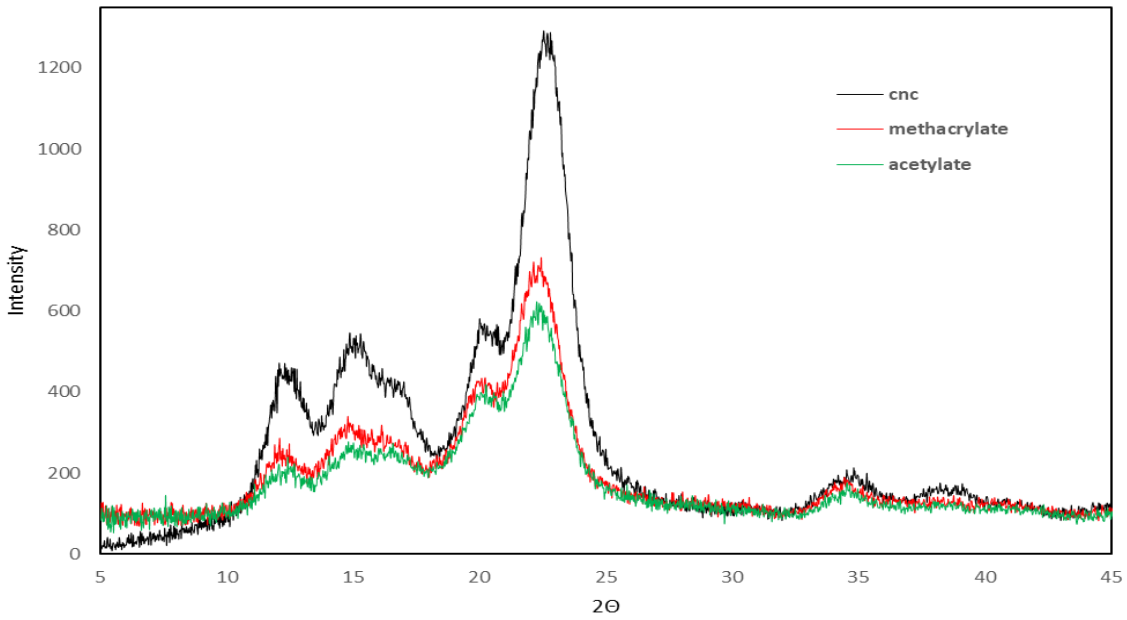

Figure 6.5 XRD diagrams of unmodified CNC and CNC modified with methacrylate and acetate.

	CNC	Acetylate	Methacrylate
Crystallinity index (CrI)	86.35	77.35	79.07

Table 6.3 Crystallinity of pristine and modified CNC

The crystallinity index of pristine cellulose slightly reduced after the grafting reaction. Corresponding to the intensities of the crystalline peaks, the acetylated CNC had the lowest crystallinity index. This is in accordance with the higher grafting achieved during the modification reaction. It is evident that when the grafting is increased, the crystallinity of the material would be compromised.

6.3.4 TGA

A thermogravimetric analysis was conducted for both pristine and modified cellulose to understand the thermal stability of the samples. Usually, when fibres are modified, the macromolecular structures are changed and their response to thermal decomposition can also change. In this regard, it is needful to understand the thermal response of pristine and modified CNC which is shown in figure 6.6.

The behaviour of all the samples was relatively the same from the start of the degradation temperatures. The weight loss followed the same pattern from 30-130^{0}C which could be attributed to adsorbed water. Afterwards, the acetylated CNC continued a gradual loss in weight while pristine CNC and methacrylate CNC maintained a moderately constant weight over a range of temperatures. However, at about 252^{0}C a rather sharp degradation started for the pristine CNC while the methacrylate and acetylated CNC maintained a weight loss without sharp degradation. For the acetylated CNC, a gradual degradation started at 272^{0}C while methacrylate CNC started at 270^{0}C at different weight loses. This showed that the modification of the CNC slightly improved the thermal stability for both acetylates and methacrylate groups.

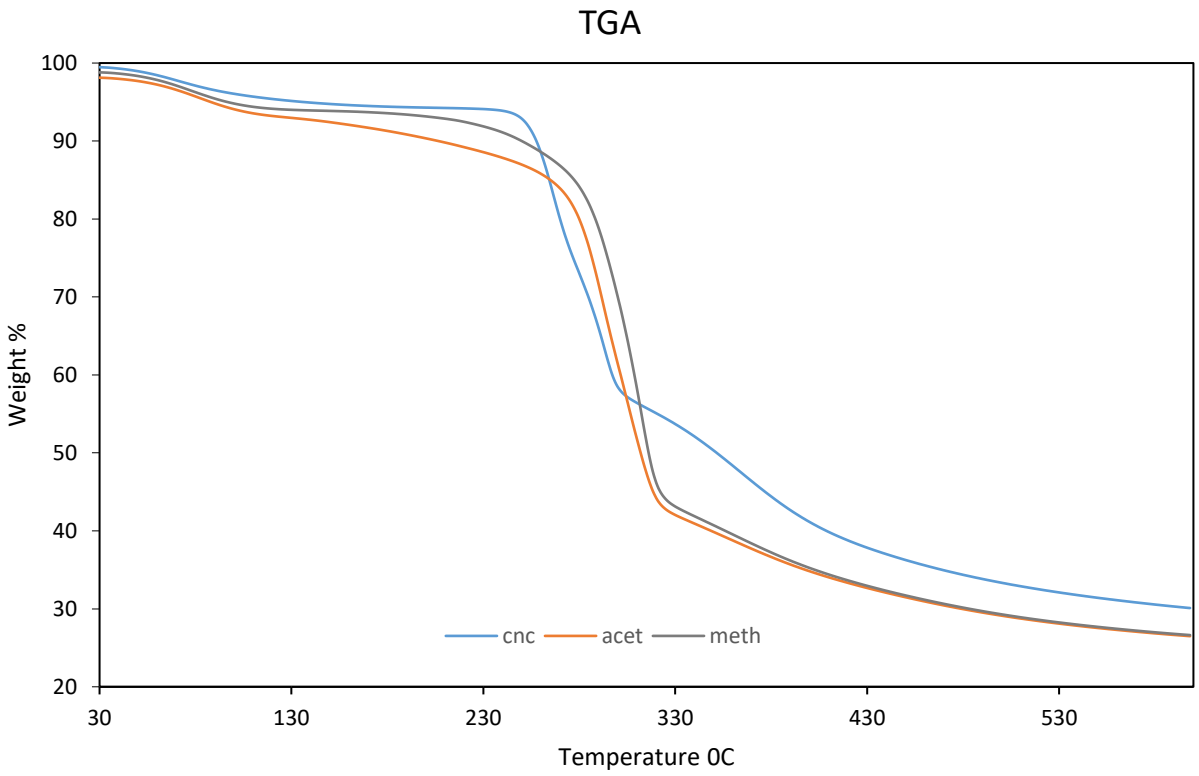

Figure 6.6 Thermogravimetric curves of pristine and modified cellulose nanocrystals.

Similar results were shown when different amount of acetyl groups was grafted on CNC, showing an increase in thermal stability as the amount of grafted groups increased [28, 39]. The early degradation of pristine CNC could also be attributed to have been catalysed by sulphate esters [40] which in the process of modification have been partly replaced by the modifying agents. Within the degradation temperature range, the thermal properties are tenable for processing especially up to 200^{0}C.

6.3.5 Vulcanization properties

The vulcanization properties of the various modified CNC were studied with the moving die rheometer. Samples were cured with sulphur curing package involving activators and accelerators at 150^0C for 30 minutes. Unlike the previous compounds, the modified compounds of cellulose acetate and cellulose methacrylate were subjected to vulcanization without addition of silanes. The scorch time (TS2), optimum curing time (T90), cure rate index (CRI), and the various torques were deduced from the vulcanization curve in Figure 6.7 and presented in table 6.4.

As it could be seen from the curves, the vulcanization kinetics of the CNC compounds were very similar. The scorch time for the acetate and methacrylate CNC was relatively the same and was short compared to silica compounds. In fact, without activators and accelerators, the scorch time of silica compounds could take longer. Silica is known to always absorb curatives and slowly releasing them, thereby taking a longer time for the vulcanization to start. As shown in table 6.4, it took CNC prepared compounds about half a scorch time of the silica compounds. When the crosslinking started, it proceeded almost at the same rate similarly for CNC compounds. The cure rate index for methacrylate was 28.57 min^{-1} while that of acetate was 29.67 min^{-1}. Despite having very similar kinetics, there was a remarkable difference in torque for both compounds. The methacrylate CNC compounds reached the highest torque M_H of 16.01 dNm compared to acetylated CNC at M_H - 12.62 dNm and silica compounds M_H - 11.78 dNm. The difference between the lowest and highest torque is an indication of the crosslinking density. In essence, the methacrylate CNC compounds achieved a higher crosslinking.

Parameter	S-TESPD	CNC-MET	CNC-ACET
TS2 (min)	9.30	4.35	4.53
T90 (min)	14.12	7.85	7.90
CRI (min-1)	20.75	28.57	29.67
ML (dNm)	1.30	1.93	1.57
MH (dNm)	13.08	16.01	12.62
ΔM (dNm)	11.78	14.08	11.05

Table 6.4 Vulcanization parameters of modified CNC (CNC-MET for methacrylate CNC and CNC-ACET for acetylated CNC) and silica compound (S-TESPD).

Achieving a high crosslinking density is subject to contributions from different factors. The macromolecular structures of methacrylate CNC have a double bond which is a desirable means to promote sulphur vulcanization.

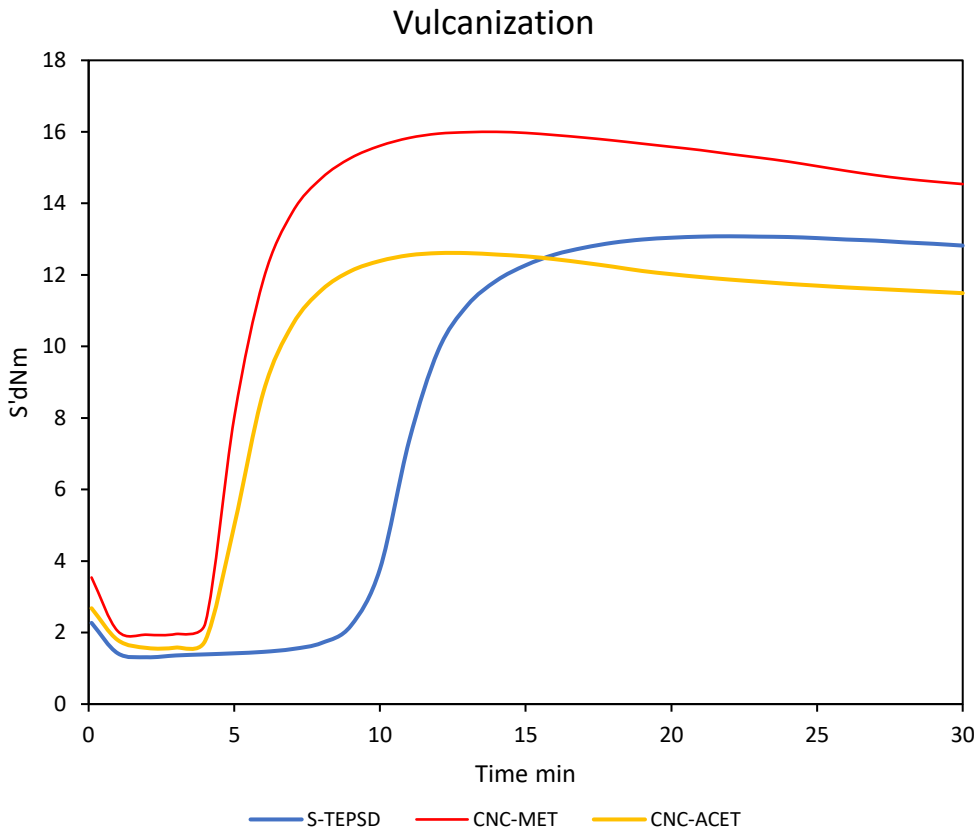

Figure 6.7 Vulcanization curve of silica compound (S-TESPD), methacrylate CNC (CNC-MET) and acetylated CNC (CNC-ACET).

In this scenario, the sulphur crosslinking does not only take place on the double bonds of the natural rubber chains, but it also extends to the double bond present on the filler because of the surface modification. Although it was expected that the crosslinking density should be higher; however, it was also considered that the grafting was low and only happening on the surface. The contributions to the crosslinking density were therefore few. This extent of functionalization is more of a trade-off, maintaining the structural and morphological integrity of the filler as against grafting more species which can compromise other useful properties. By comparison, the vulcanization properties of methacrylate CNC were superior to the reference silica, and similarly to acetylate CNC. The role acetyl groups played were more of enhancing dispersion within the matrix rather than contributing to the crosslinking process. There were reversions close to midway into the vulcanization for the CNC compounds. In fact, an optimum curing T_{90} where about 90% of the entire compounds were

cured was achieved very early for the CNC and reversions started early. Steep reversion was not experience for silica compounds because of their slow curing within the curing window. In essence, a reasonable part of the crosslinking network within the CNC compounds were lost afterwards and this goes a long way to compromise other properties of the compounds that would be determined afterwards. Curing for the modified CNC should therefore not exceed 15 minutes to avoid reversion and loss of part of the sulphur bridges. In general, the vulcanization kinetics of cellulose methacrylate were better when compared to the reference silica and acetylated CNC.

6.3.6 Dynamic mechanical analysis

Modified CNC compounds were subjected to dynamic mechanical analysis and results compared with silica compounds prepared with TESPD silanes as reference. Compounds were subjected to oscillatory deformations both in the unvulcanized and after vulcanization and results are presented in figure 6.8.

The viscoelastic properties of the green compounds showed cellulose methacrylate as rather having a remarkably different result. The storage modulus of this compound was reasonably high at low strain and this could be an indication of good dispersion as well as good filler-filler interaction. When the material was subjected to dynamic deformation, the strain dependent response of the methacrylate CNC compounds showed a steep drop in the storage modulus at about 35% strain. At this point, the filler networking was making unrecoverable losses. The hydrophobization of CNC with methacrylate group could give a clue to the ability of methacrylate enhancing easy dispersion within polymer matrixes. Although the grafting was considered moderately low considering the intensity of the FTIR peaks, it promoted efficient dispersion while maintaining good filler reinforcement.

In the unvulcanized compound, the storage modulus at low strains of methacrylate CNC was the highest followed by silica and that of acetylated CNC. The methacrylate modified CNC also came with high Payne effect which is attributed to lower filler-polymer interaction. Hydrophobization of the CNC with acetylated groups only promoted dispersion and filler-polymer interaction without good filler-filler networking. When the crude materials were vulcanized and subjected to dynamic deformation, the viscoelastic properties improved remarkably.

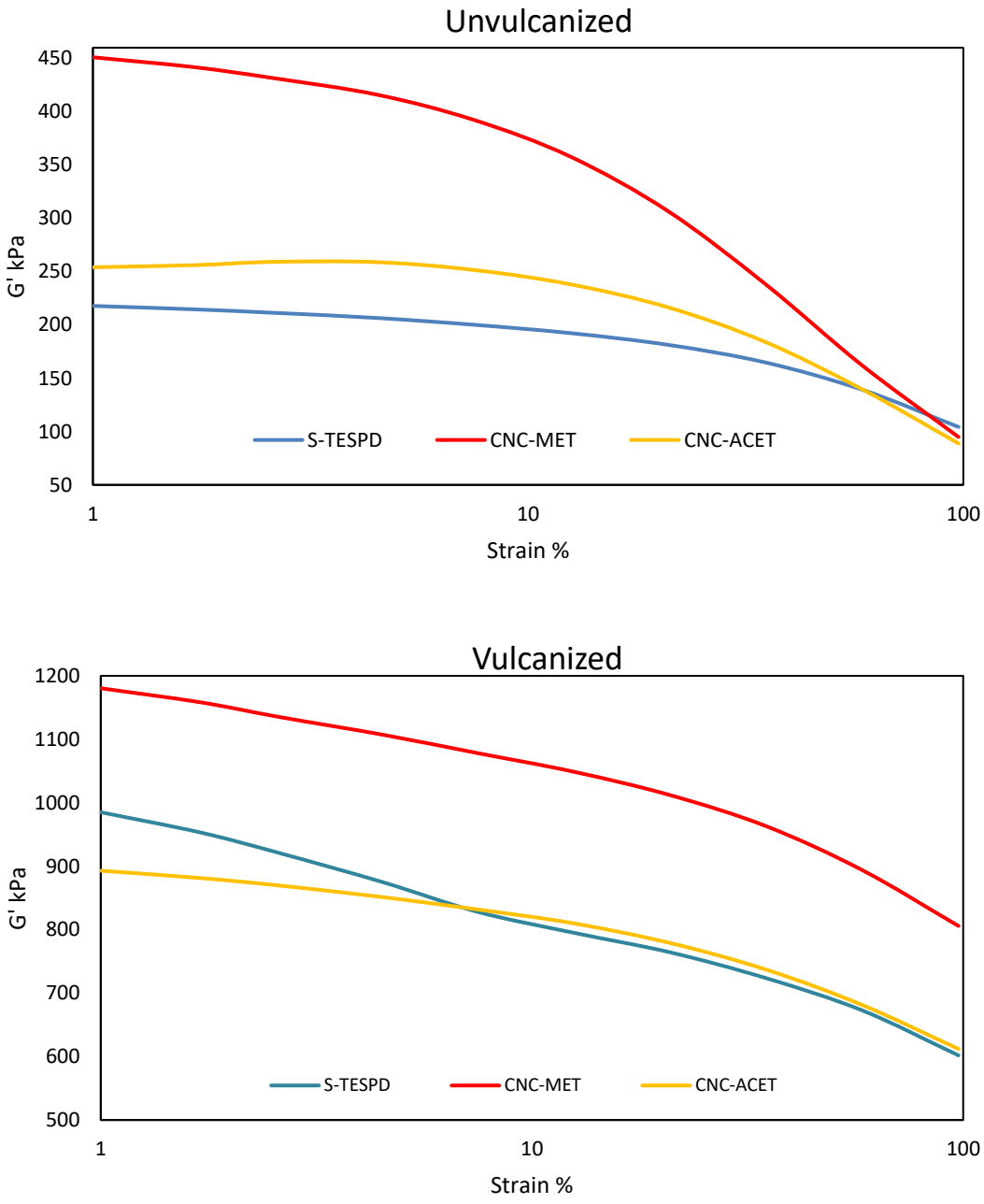

Figure 6.8 Storage modulus against strain of methacrylate CNC (CNC-MET), acetylated CNC (CNC-ACET) and silica compounds

In the vulcanized compound, the storage modulus of CNC compounds modified with methacrylate group were higher than the reference silica and acetylated CNC. In fact, even at 100% strain sweep, the storage modulus of the compound is nearly comparable to storage modulus of acetyl modified CNC at low strains. It is obvious that the viscoelastic properties improved owing to the increased crosslinking as provided by the double bond from the methacrylate group. The good dispersion,

filler-filler networking and filler-polymer interaction provides clue that the amount grafted may have been reasonably sufficient.

Payne effect	S-TESPD	CNC-MET	CNC-ACET
Unvulcanize	113.51	294.67	165.27
Vulcanize	383.14	374.57	280.8

Table 6.5 Payne effects of modified CNC and silica compounds.

The cellulose acetate CNC compound was also of interest. The reinforcement was low compared to the reference silica; however, the Payne effect was lower than all the other compounds. The behaviour of the cellulose acetate compound showed a rather high filler-polymer interaction which is later revealed in its tensile properties. In essence, grafting acetyl groups on CNC particles would greatly promote dispersion and this may come at the expense of filler-filler interaction that would maintain stronger reinforcement. In the SEM analysis, the structural integrity of the acetylated cellulose was maintained, and it is unclear why the reinforcement was lower than the reference silica.

The tangent delta of the various compounds also agrees with the results obtained from the storage modulus as presented in figure 6.9.

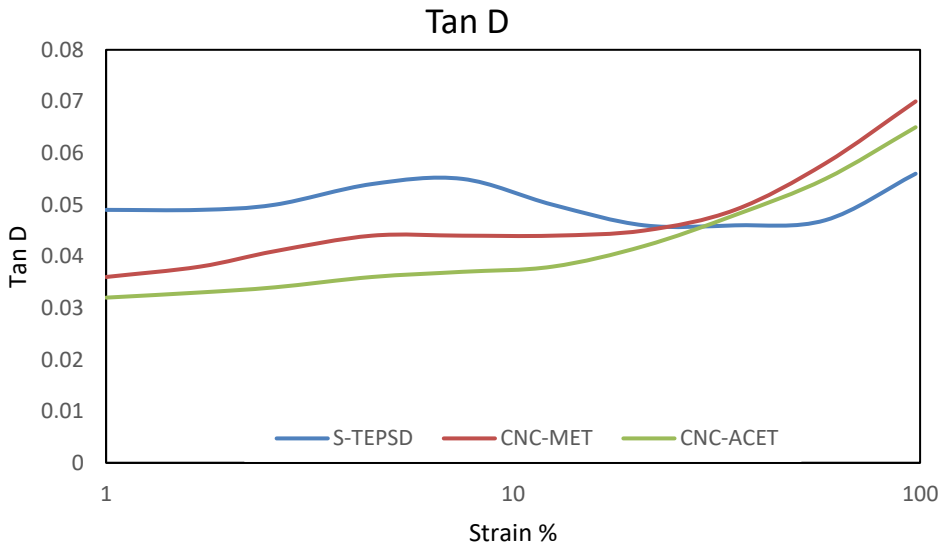

Figure 6.9. Tangent delta of cured silica compound (S-TESPD), methacrylate CNC (CNC-MET) and acetylated CNC (CNC-ACET).

At low strain, the tangent delta of silica compound was high and formed a plateau around 10% strain. That of cellulose acetate was lower than all the compounds. A lower tangent delta is desirable, and it is indicative of higher filler-polymer interactions which increases the elasticity of the material. However, at higher strain, the tangent delta increased for the CNC compounds while that of silica maintained a decreased before another increase. The difference in the behaviour of the tangent delta curves could be attributed to the particle morphology of CNC being different from spherical-like morphology of silica. In essence, during high deformations, there is debonding taking place at polymer-filler interphase. The filler network is expected to break, and reform and the behaviour of tangent delta curves is indicative that the silica network reformed better than CNC networks. The silica compound did not show a damping behaviour that reduced from lower strain up to the highest strain as seen with CNC. In this scenario, besides the good polymer-filler interactions, the filler morphology plays a crucial role to enhance the damping properties during cyclic deformations.

6.3.7 Tensile properties

The tensile properties of modified CNC were studied and compared with reference silica compound prepared with TESPD silanes. The elongation at break, tensile strength as well as 10 to 300% stress was deduced from the measurement and presented in table 6.6.

Property	S-TESPD	CNC-MET	CNC-ACET
Stress 10% [MPa]	0.58	0.47	0.43
Stress 50% [MPa]	2.00	1.79	1.25
Stress 100% [MPa]	4.32	3.67	2.33
Stress 300% [Mpa]	13.87	12.59	9.56
Elongation at break [%]	424.71	417.11	495.96
Tensile strenght [MPa]	19.21	19.35	22.85

Table 6.6 Tensile properties of modified CNC compounds compared with reference silica.

From the table above, the tensile properties of the reference silica and methacrylate CNC were very similar. From 10% strain to 300% strain, their results were very close up to the elongation at break. However, on the tensile strength, there were slight improvements over the reference silica compound. These comparable improvements in tensile properties were evident of good filler

dispersion and good filler-polymer interaction. For CNC compounds, the coprecipitation method is one of reliable means to disperse CNC effectively within a polymer matrix. This is necessary to have effective load transfer from matrix to filler during load bearing conditions. The synthesized cellulose acetate also came with interesting tensile properties. As explained earlier, it was evident that there was good dispersion and good filler-polymer interaction occasioned by the acetylated groups on the CNC surface. This eventually resulted to an increased elastic portion as against viscous portions within the polymeric composite. As seen on the table, the tensile strength of the acetylated CNC compound was higher than the reference silica, and subsequently the methacrylate CNC. The elongation at break of this compound was also reasonably higher and it is an indication of improved property requiring toughness. When compared to the reference material at 300% strain, the lower value may be attributed to the reduced filler-filler interaction. Even at this, the obtained tensile properties were seen to be good and interesting.

6.4 Conclusions

Silanes have been the most adopted means of modifying filler particles during composite preparation in the tire industry. Silica and cellulose nanocrystals have similar surface chemistry and studies on the modification of CNC have also incorporated the use of silanes for surface functionalization. Alternatively, green approaches by using enzymes as catalyst to graft moieties that can aid dispersion were employed in this chapter. Vinyl esters such as vinyl methacrylate and vinyl acetate were used as ester donors while lipase from *Aspergillus niger* was used as the catalyst. The reaction was conducted in dimethylsulphoxide (DMSO) for 24 hours and precipitated with ethanol at the end of the reaction. This procedure enabled the recovery of all the CNC that was used for the reaction. The reacting media such as the DMSO and other reagents were also recovered in a heterogeneous mixture having the unreacted vinyl esters on the surface which could be decanted and reuse. The success of the reaction was confirmed by FTIR and further characterization showed the preservation of the CNC morphology. Compounds with the functionalised CNC were prepared by coprecipitation and results were compared with a reference silica compound prepared with TESPD silanes. Results especially the vulcanization and the dynamic mechanical properties showed that the methacrylate CNC had a rather superior properties to the reference silica especially the storage modulus and vulcanization properties. The acetylated CNC showed better filler-polymer interactions which moderately affected the filler-filler interactions. However, the tensile properties of the methacrylate CNC were very similar to the reference silica with acetylate CNC having good

tensile properties especially the tensile strength which was higher than all. In this regard, it is evident that the concept of grafting moieties with double bond (methacrylate) on the surface of CNC with the intent to create a crosslinking on the CNC filler alongside the natural rubber yielded interesting results. More so, this means of modification could be a potential replacement of the sililation method of filler functionalization in the tire industry.

References

1. Habibi, Y., Lucia, L.A., Rojas, O.L. (2010) Cellulose nanocrystals: self-assembly and application. Chem rev., 110, 3479-3500.
2. Trache, D., Hussin, M.H., Haafiz M.K.M., Thakur, V.K. (2017) Recent progress in cellulose nanocrystals: sources and production. Nanoscale, 9: 1763-1786.
3. Samir, M.A., Alloin, F., Dufresne, A. (2005) Review of recent research into cellulosic whiskers, their properties and their applications in nanocomposites. Biomacromolecules, 6: 612-626
4. Eyley, S., Thielemans, W. (2014) Surface modification of cellulose nanocrystals. Nanoscale, 6: 7764-7779.
5. Moon, R.J., Martini, A., Nairn, J., Simonsen, J., Youngblood, J. (2011) Cellulose nanomaterials review: structure, properties and nanocomposites. Chem soc rev, 40:3941-3994.
6. Elazzouzi-Hafraouti, S., Nishiyama, Y., Putaux, J.L., Heux, L., Dubreuil, F., Rochas, C. (2008) The shape and size distribution of crystalline nanoparticles prepared by acid hydrolysis of native cellulose. Biomacromolecules, 9: 57-65.
7. Oksman K, Aitomaki Y, Mathew AP, Siqueira G, Zhou Q, Butylina S, Tanpichai S, Zhou X, Hooshmand S. Review of the recent developments in cellulose nanocomposite processing. Composites: Part A 2016, 83; 2-18.
8. Mariano M, El Kissi N, Dufresne A. Cellulose nanocrystals and related nanocomposites: review of some properties and challenges. J. Polym Sci Part B: Polym Phys 2014;52: 791-806.
9. Klemm, D., Kramer, F., Moritz, S., Lindström, T., Ankerfors, M., Gray, D., Doris, A. (2015) Nanocelluloses: a new family of nature-based materials. Angew Chem Int Ed, 50:5438-5466.
10. Jorfi, M., Foster EJ. (2015) Recent advances in nanocellulose for biomedical applications. J Appl Polym Sci, 132, 41719/1-19.
11. Saini, S., Belgacem, N., Mendes, J., Elegir, G., Bras, J. (2015) Contact antimicrobial surface obtained by chemical grafting of microfibrillated cellulose in aqueous solution limiting antibiotic release. ACS Appl Mater Interfaces, 7:18076-18085.
12. Abdelmouleh, M., Boufi, S., Belgacem, M.N., Dufresne, A., Gandini, A. (2005) Modification of cellulose fibers with functionalized silanes: effect of the fiber treatment on the mechanical performances of cellulose-thermoset composites. J Appl Polym Sci, 98:974-84.
13. Rol, F., Belgacem, M.N., Gandini, A., Bras, J. (2019) Recent progress in surface-modified cellulose nanofibrils. Prog. Poly. Sc., 88:241-264.

14. Agostinho, F., and Ortega, E. (2013). “Energetic-environmental assessment of a scenario for Brazilian cellulosic ethanol,” J. Cleaner Prodn. 47, 474-489.
15. Meyer, M. A., and Priess, J. A. (2014). “Indicators of bioenergy-related certification schemes - An analysis of the quality and comprehensiveness for assessing local/regional environmental impacts,” Biomass Bioenergy 65, 151-169.
16. Gibberd, J. (2015). “Measuring capability for sustainability: The Built Environment Sustainability Tool (BEST),” Building Res. Infor. 43(1), 49-61.
17. Poveda, C. A., and Lipsett, M. G. (2014). “An integrated approach for sustainability assessment: The Wa-Pa-Su project sustainability rating system,” Intl. J. Sustain. Devel. World Ecol. 21(1), 85-98.
18. Hubbe, M.A., Rojas, O.J., Lucia, L.A. (2015) Green modification of surface characteristics of cellulosic materials at the molecular or nano scale: A review. Bioresources, 10: 6095-6206.
19. Gandhi, N.E., Patil, N.S., Sawant, S.B., Joshi, J.B., Wangikar, P.P., Mukesh, D. (2000) Lipase-catalyzed esterification. Catalysis review-Sci. Eng, 42: 439-480.
20. Yang, K. and Wang, Y. (2003). Lipase-catalyzed cellulose acetylation in aqueous and organic media. Biotechnology prog; 19: 1664-1671.
21. Yang, K. and Wang, Y. (2004) Lipase-catalyzed transesterification in aqueous medium under thermodynamic and kinetic control using carboxymethyl cellulose acetylation as model reaction. Enzyme and microbiology Tech. 35: 223-231.
22. Sereti, V., Stamatis, H., Koukios, F., Kolisis, F.N. (1998) Enzymatic acylation of cellulose acetate in organic media. J. Biotech. 66: 219-223.
23. Xie, J., Hsieh, Y. (2001) Enzyme-Catalyzed Transesterification of Vinyl Esters on Cellulose Solids. Journal of Polymer Science: Part A: Polymer Chemistry, Vol. 39, 1931-1939.
24. Bozic, M., Vivod, V., Kavcic, S., Leitgeb, M., Kokol, V. (2015) New findings about lipase acetylation of nanofibrilated cellulose using acetic anhydride as acyl donor. Carbohydrate polym, 125: 340-351.
25. Gan, L., Liao, J., Lin, N., Hu, C., Wang, H., Huang, J. (2017) Focus on gradientwise control of the surface acetylation of cellulose nanocrystals to optimize mechanical reinforcement for hydrophobic polyester-based nanocomposites. ACS Omega, 2, 4725−4736.

26. Benjamin Dhuiège, B., Pecastaings, G., Sèbe, G. (2019) Sustainable approach for the direct functionalization of cellulose nanocrystals dispersed in water by transesterification of vinyl acetate. ACS Sustainable Chem. Eng., 7, 187−196.
27. Çetin, N.S., Philippe Tingaut, P., Özmen, N., Henry, N., Harper, D., Mark Dadmun, M., Sebe, G. (2009) Acetylation of cellulose nanowhiskers with vinyl acetate under moderate conditions. Macromol. Biosci., 9, 997-1003.
28. Li, W., Cai, G., Zhang, P. (2019) A simple and rapid Fourier transform infrared method for the determination of the degree of acetyl substitution of cellulose nanocrystals. J Mater Sci., 54,8047-8056.
29. Frisoni, G., Baiardo, M., Scandola, M., Lednicka, D., Cnockaert,´ M.C., Mergaert, J., Swings, J. (2001) Natural cellulose fibers: heterogeneous acetylation kinetics and biodegradation behavior. Biomacromolecules, 2, 476−482.
30. Zini, E., Scandola, M., Gatenholm, P. (2003) Heterogeneous Acylation of Flax Fibers. Reaction Kinetics and Surface Properties. Biomacromolecules, 4, 821−827.
31. Gong, J., Li, J., Xu, J., Xiang, Z., Mo, L. (2017) Research on cellulose nanocrystals produced from cellulose sources with various polymorphs. RSC Adv., 7, 33486-33493.
32. Cheng, G., Varanasi, P., Li, C., Liu, H., Melnichenko, Y.B., Simmons, B.A, Kent, M.S, Singh, S. (2011) "Transition of Cellulose Crystalline Structure and Surface Morphology of Biomass as a Function of Ionic Liquid Pretreatment and Its Relation to Enzymatic Hydrolysis. Biomacromolecules, 12, 933-941.
33. Schroeder, L.R., Gentile, V.M., Atalla, R.H. (1986) Nondegradative preparation of amorphous cellulose. J Wood Chem Tech, 6:1-14.
34. Ju, X., Bowden, M., Brown, E.E., Zhang, X. (2015) An improved X-ray diffraction method for cellulose crystallinity measurement. Carbohydrate Polymers, 123, 476-481.
35. Rongpipi, S., Ye, D., Gomez, E.D, Gomez, E.W. (2019) Progress and opportunities in the characterization of cellulose - An important regulator of cell wall growth and mechanics. Front. Plant Sci., 9:1894. doi: 10.3389/fpls.2018.01894
36. Rambo, M.K.D., Ferreira, M.M.C. (2015) Determination of cellulose crystallinity of banana residues using near infrared spectroscopy and multivariate analysis. J. Braz. Chem. Soc., Vol. 26, No. 7, 1491-1499,

37. Park, S., Baker, J.O., Himmel, M.E., Parilla, P.A., Johnson, D.K. (2010) Cellulose crystallinity index: measurement techniques and their impact on interpreting cellulase performance. Biotechnology for Biofuels, 3, 10.
38. Dong, F., Yan, M., Jin, C., Li, S. (2017) Characterization of type-II acetylated cellulose nanocrystals with various degree of substitution and its compatibility in PLA films. Polymers, 9, 346.
39. Zhao, J., Zhao, Y., Wang, Z., Peng, Z. (2016) Effect of polymorphs of cellulose nanocrystal on the thermal properties of poly(lactic acid)/ cellulose nanocrystals composites. Eur. Phys. J. E., 39, 118.
40. Roman, M., Winter, W.T. (2004) Effect of sulphate groups from sulphuric acid hydrolysis on the thermal degradation behavior of bacterial cellulose. Biomacromolecules, 5, 1671-1677.

Chapter 7

General conclusions

This research project has been devoted to exploring the possible use of lightweight polysaccharides as fillers in elastomeric compounds. The intention is to see if they could be used to possibly replace convention fillers that are used in the tire industries. In the tire industry, carbon black and silica are the conventional fillers. In fact, carbon black which is derived from petroleum sources has its attendant environmental concerns and this is making industrialist to find alternative fillers. Silica was subsequently researched as one of the alternatives and is presently used to partially replace carbon black. Silica is known to have some good properties over carbon black. However, the production process of the highly dispersible silica used in the tire industry comes with reasonably large chemical waste. Despite the good properties that could be derived from these fillers, the end life of the tire compound is another challenge that awaits in the future as they are not bio derived. Going back to nature to see how bio derived materials can be used to replace the conventional fillers has been the current drive for this work.

The fillers that were used in this project were cellulose nanocrystals and alpha 1,3 glucan. Their surface chemistry is like that of silica fillers having abundant surface hydroxyl groups. These bio fillers are hydrophilic and not compactible with hydrophobic polymer matrix such as natural rubber. In this regard, the fillers were modified to be compatible with the polymeric matrix. To achieve this modification, two silanes were employed: Bis(triethoxysilylpropyl)disulfide (TESPD) and 3-aminopropyltriethoxysilane (APS) silanes being aliphatic silanes and 2,2-dimethoxy-1-thia-2-silacyclopentane (SID) and n-n-butyl-aza-2,2-dimethoxysilacyclopentane (SIB) being cyclic silanes. All the compounds were compared with silica compounds as reference. The results obtained with these fillers showed that the APS silanes promote very fast vulcanization and increases the crosslinking density. With this silane, a higher storage modulus was achieved, and properties were better than the reference silica compounds. The drawback that was experience with APS is the fact that large amount of the silane affects the tensile properties. The reaction mechanism observed for TESPD silanized compounds reveals that the storage modulus of the compounds with this silane may

not be comparable to that of APS but the tensile properties were remarkably higher. Deciding on which silanes to be used would therefore connect with the expected properties that is of interest.

When the cyclic silanes were explored, their reactive nature made the vulcanization to be fast. The reinforcement of the various compounds was very interesting. However, it was observed that at low silane loading between 2-5%, the properties remain fairly the same even when the silane amounts were increased up to 12%. In fact, the cyclic silanes amount exceeding 5% made the material brittle and resulted in very inferior tensile properties. It is therefore advisable to prepare the polysaccharides filler with very low amount of cyclic silanes.

The modifications with silanes were explored as it is heavily used in the tire industry. Alternatively, a green enzymatic modification using lipases as catalyst was also investigated. The procedure developed in this work was simplified with the possibility of recovering all the filler used in the reaction and the reuse of other reacting species. The concept in this modification was to graft moieties that can serve to hydrophobized the surface and subsequently promote a direct crosslinking between the filler and rubber. The cellulose nanocrystal was the filler for this modification and acetyl and methacrylate groups were grafted on the surface. When compounds were prepared with the modified CNC, the properties they conferred on the composites were very interesting. In fact, they were better than the reference silica. The results obtained in this process are very promising especially when the future of the tire industry is considered.

Much attention was given to cellulose nanocrystals compared to alpha 1,3 glucan. Although glucan is a new entrant into the biofiller world for the tire industry, it is still being studied to ascertain their suitability. The compounds made with glucan using silanes showed that some aspects of the properties are lower that the reference silica. In terms of the green compounds and vulcanization properties, it was relatively better than silica compound. But when the glucan compounds were vulcanized, the reinforcements and tensile properties were observed to be lower than silica compounds. It is obvious that more treatment, processing methods and the use of vast alternative modification strategy is needed to prepare glucan for improved properties and possible use in tire compounds.

It is evident that the fillers that were considered are promising and the results from the characterizations have shown their suitability. However, the decade long tire industry has been using fillers that have different morphology and also different from newly explored fillers, especially

the cellulose nanocrystals. For example, CNC morphology is rod-like, and the reinforcing pattern is expected to be different from that of the conventional fillers. Some of the concept developed and embedded in the characterization models to describe the interactions of fillers in composite may not necessarily apply to fillers such as CNC. It is observed that CNC may form larger structural cavities that can exclude large polymeric matrixes in the form of occluded rubber, and this can lead to higher strain amplification and higher Payne effect. Here the Payne effect may not necessarily be a result of poor dispersion but the structural formations and some of these considerations should be considered when developing future models. In essence, some characterizations to ascertain the mechanical properties of CNC reinforced compounds may not give the actual or detail mechanical response of the compounds during deformations. While the results obtained with these bio fillers are promising and continued research is important, the characterization models needed to understand the interactions and reinforcement pattern need to be revisited specifically for these bio fillers.